VERIFYING THE DECLARED ORIGIN OF TIMBER USING STABLE ISOTOPE RATIO AND MULTI-ELEMENT ANALYSES

GARETH OWAIN REES

MSc by Research

University of York

Chemistry

January 2015

Abstract

Verifying the declared origin of timber using stable isotope ratio and multi-element analyses

The FLEGT (Forest Law Enforcement Governance and Trade) regulations were introduced in 2003 with the intention of reversing the rate of destruction of the world's forests. One of the European Union's aims is to halt the import of illegally acquired and endangered timber. The timber trade law (regulation (EU) 995/2010) stipulates that importers of tropical timber must be able to identify the origin of timber used in their products, and from the 3rd March 2013, it is a criminal offence to sell endangered timber in the European Union without a FLEGT licence. There are few analytical methods available to determine the declared origin of timber. The current procedure involves checking of shipping documents and visual checks of common timber species for origin identification.

In this project, one hundred timber core samples of Sapele *(Entandrophragma)*, Rosewood *(Dalbergia)* and Ebony (*Diospyros*) trees were taken from across West Africa and Madagascar. The δ^2H, $\delta^{13}C$, and $\delta^{18}O$ isotopes of the extracted cellulose were determined by using an elemental analyser coupled to an isotope ratio mass spectrometer (EA-IRMS). The study revealed that δ^2H and $\delta^{18}O$ of cellulose showed no correlation with δ^2H and $\delta^{18}O$ of precipitation water, suggesting the leaf-to-air-vapour pressure difference (VPD), as well as alternative ground water sources may influence the isotopes laid down in cellulose of tropical timber. Additionally, multi-element profiles of the timber samples were determined by inductively coupled plasma mass spectrometry (ICP-MS), to assess the potential for geographical origin discrimination based on the combined profile of stable isotope ratios and multi-element concentrations. Using the multivariate statistical technique of canonical discriminant analysis (CDA), data were processed enabling a cross validation rate of 86.6%.

Twelve elemental variables were selected by the CDA for the multivariate analysis (Mo, Zn, Ca, As, $\delta^{13}C$, $\delta^{18}O$, Sb, Mn, Pb, Cu, La, Ba), which provided maximum discrimination between the timber samples originating from Ghana, Cameroon, The Congo, The Democratic Republic of Congo (DRC), and Madagascar. Hence, the combination of the methodologies of stable isotope ratio and trace element analysis offers an effective approach to verifying the declared origin of timber.

List of contents

ABSTRACT 2

LIST OF CONTENTS 3

LIST OF TABLES 7

LIST OF FIGURES 9

ACKNOWLEDGEMENTS 13

DECLARATION 14

Chapter 1 – Introduction 15

1.1 An overview of Timber production 16
- 1.1.1 Impacts of deforestation 17
  - 1.1.1.1 Trace elements and nutrients 17
  - 1.1.1.2 Microbial biodiversity 18
- 1.1.2 Forest management 19
  - 1.1.2.1 Conventional practices 19
  - 1.1.2.2 New and emerging practices 21
- 1.1.3 Worldwide production areas 24
  - 1.1.3.1 Cameroon 24
  - 1.1.3.2 The Democratic Republic of Congo 25
  - 1.1.3.3 Ghana 25
  - 1.1.3.4 Republic of Congo 25
  - 1.1.3.5 Madagascar 25
- 1.1.4 Timber Morphology 25
  - 1.1.4.1 Cellulose and hemicellulose 27
  - 1.1.4.2 Lignin 28
- 1.1.5 Wood biosynthesis 29
  - 1.1.5.1 Xylem 30
  - 1.1.5.2 Phloem 31
- 1.1.6 Mineral nutrition in trees 33
  - 1.1.6.1 Uptake of minerals by trees 33
  - 1.1.6.2 Geochemical inputs to soil and water 36

1.2 An overview of illegal logging and controls 37
- 1.2.1 Physical, biological and chemical impacts 37
  - 1.2.1.1 Erosion and hydrological feedback loops 37
  - 1.2.1.2 Forest fires 38
  - 1.2.1.3 Animal Biodiversity 38
- 1.2.2 Endangered timber species 40
  - 1.2.2.1 Dalbergia 40
  - 1.2.2.2 Diospyros 40
  - 1.2.2.3 Entandrophragma 41
- 1.2.3 Law enforcement and regulations to combat illegal logging 42
  - 1.2.3.1 EU and FLEGT 42
  - 1.2.3.2 Lacey Act 42

1.2.3.3 CITES regulations 42
1.2.3.4 The International Tropical Timber Organisation (ITTO) 43
1.2.3.5 Forest Stewardship Council 43
1.2.3.6 INTERPOL 43

1.3 Elemental analysis methods used to determine the provenance of timber 45
1.3.1 Stable isotopes 45
1.3.1.1 Introduction to stable isotopes and stable isotope ratio mass spectrometry 45
1.3.1.1.1 Stable isotope notation 46
1.3.1.1.2 Stable isotope standards 46
1.3.1.2 Isotope effects 47
1.3.1.2.1 Equilibrium fractionation 47
1.3.1.2.2 Kinetic fractionation 48
1.3.1.3 Applications of carbon, oxygen and hydrogen stable isotope ratio analysis 50
1.3.1.3.1 Carbon isotopes 51
1.3.1.3.1.1 Carbon dioxide fixation in plants 53
1.3.1.3.2 Hydrogen and oxygen isotopes 56
1.3.1.3.2.1 Hydrogen 56
1.3.1.3.2.2 Oxygen 57
1.3.1.3.2.3 Hydrogen and oxygen isotope fractionation 57
1.3.1.3.3 The global meteoric water line 59
1.3.1.3.4 Hydrogen and oxygen isotope fractionation in plants 60

1.4 Analysis techniques 61
1.4.1 Principles of stable isotope ratio mass spectrometry 61
1.4.2 Bulk stable isotope analysis 63
1.4.2.1 Flash combustion element analysis 63
1.4.2.2 High temperature pyrolysis elemental analysis 64
1.4.3 Measurement of trace elements 66
1.4.3.1 Microwave acid digestion 66
1.4.3.2 Principles of inductively coupled plasma mass spectrometry (ICP-MS) 68

1.5 Research objectives 70

Chapter 2 - Multi-element ICP-MS analysis of timber samples 71

2.1 Introduction 71
2.1.1 Trace elements in timber 72
2.2 Multi element concentrations in timber 74
2.2.1 Limits of detection and quantification 75
2.2.2 Instrument stability 76
2.2.3 Quality controls 77

2.3 Introduction to canonical discriminant analysis 78

2.4 Results of the multivariate analysis of timber samples 79
2.4.1 Discussion of the multivariate analysis 82
2.4.2 Further multivariate analysis of timber samples 84
2.4.3 Discussion of the 2nd multivariate analysis 86

2.5 Conclusions 88

Chapter 3 - Stable isotope ratio analysis of timber samples 89

3.1 Introduction 89

3.2 Stable isotope of carbon ($^{13}C/^{12}C$ ratio) 90
3.2.1 Quality controls for the carbon stable isotope ratio analysis 90
3.2.2 Carbon isotope composition of timber 94
3.2.2.1 Discussion of the carbon isotope results 95

3.3 Stable isotope of oxygen ($^{18}O/^{16}O$ ratio) 101
3.3.1 Quality controls for the oxygen stable isotope ratio analysis 101
3.3.2 Oxygen isotope composition of timber 105
3.3.2.1 Discussion of the oxygen isotope results 108

3.4 Stable isotope of hydrogen ($^{2}H/^{1}H$ ratio) 111
3.4.1 Quality controls for the hydrogen stable isotope ratio analysis 111
3.4.2 Hydrogen isotope composition of timber 115
3.4.2.1 Discussion of the hydrogen isotope results 118

Chapter 4 – Identification of timber origin 121

4.1 Introduction 121

4.2 Evaluation of the stable isotope ratio data 121

4.3 Evaluation of the multi element data 122

4.4 Evaluation of the combined stable isotope ratio and trace element data 123

4.5 Evaluation of inter and intra-site variation of stable isotopes and trace elements within the same species 125

4.6 Conclusions 129

Chapter 5 – Overall summary and future work 131

Chapter 6 – Experimental 134

6.1 Sources of timber samples 134
6.1.1 Collection of timber samples

6.2 Preparation of timber samples 135
6.2.1 Preparation of wood in house reference material 135
6.2.2 Pulverisation of timber samples by ball milling 136

6.3 Isotope ratio analysis 137
6.3.1 Preparation of timber samples for IRMS analysis 137
6.3.2 Selection of stable isotope standards and reference materials 138
6.3.2.1 Materials with known carbon isotopic compositions 139
6.3.2.2 Materials with known oxygen isotopic compositions 139
6.3.2.3 Materials with known hydrogen isotopic compositions 139

6.3.3 Measurement by IRMS 140
6.3.3.1 $\delta^{13}C$ analysis 140
6.3.3.2 $\delta^{2}H$ and $\delta^{18}O$ analysis 141
6.3.4 Corrections applied to the instrumental result data 141
6.3.4.1 Correction for drift 141
6.3.4.2 Correction for delta linearity 142
6.3.4.3 H_3^+ correction 142

6.4 Multi-element analysis 143
6.4.1 Preparation of timber samples for acid digestion 143
6.4.2 Selection of multi-element standards and reference materials 143
6.4.3 Measurement by ICP-MS 144
6.4.3.1 Quality control acceptance criteria 145

APPENDICES 146

LIST OF ABBREVIATIONS AND UNITS 156

LIST OF REFERENCES 158

List of tables

Table 1.1 Contents of the main components, % of dry wood.

Table 1.2 Species count within worldwide rainforests.

Table 1.3 Summary of threat classifications for timber species of analysed.

Table 1.4 Relative abundance of the isotopes most commonly determined using IRMS.

Table 1.5 List of certified reference materials issued by the IAEA, Vienna, Austria.

Table 2.1 Bioavailability of trace elements under different soil redox conditions. Taken from Pendias, (2004).

Table 2.2 Operation mode of the ICP-MS octopole reaction system (ORS) for the respective trace elements.

Table 2.3 Quality control results of the trace element analysis.

Table 3.1 Compilation of JRC sucrose average $\delta^{13}C$ ‰ values from the analytical batches.

Table 3.2 Compilation of IAEA CH3 cellulose average $\delta^{13}C$ ‰ values from the analytical batches.

Table 3.3 Compilation of wood in house reference material (WIHRM) average $\delta^{13}C$ ‰ values from the analytical batches.

Table 3.4 Mean $\delta^{13}C$ values, standard deviation, max and minimum $\delta^{13}C$ values for timber cellulose classified by country of origin.

Table 3.5 West African meteorological data taken from: http://www.climatemps.com/.

Table 3.6 Compilation of IAEA CH3 cellulose average $\delta^{18}O$ ‰ values from the analytical batches.

Table 3.7 Compilation of wood in house reference material (WIHRM) average $\delta^{18}O$ ‰ values from the analytical batches.

Table 3.8 Mean $\delta^{18}O$ values, standard deviation, max and minimum $\delta^{18}O$ values for timber cellulose classified by country of origin.

Table 3.9 Performance of IAEA CH3 cellulose mean $\delta^{2}H$ values measured as part of analytical batches. (Assigned value was -41.73‰).

Table 3.10 Compilation of WIHRM mean $\delta^{2}H$ ‰ values from the analytical batches. (Assigned value for WIHRM cellulose was -77.1‰).

Table 3.11 Mean $\delta^{18}O$ values, standard deviation, max and minimum $\delta^{2}H$ values for timber cellulose classified by country of origin.

Table 6.1 Sample digestion parameters for timber samples.

Table 6.2 List of elemental standards used in the ICP-MS analysis.

List of figures

Fig. 1.1 Environmental disruption following deforestation.

Fig. 1.2 Ecological effects of timber deforestation upon forest microflora.

Fig. 1.3 Layers of a rain forest.

Fig. 1.4 Application of *Faidheria* fertilizer trees to aid crop production in Malawi.

Fig. 1.5 Worldwide forest areas.

Fig. 1.6 Diagram of plant cell wall showing the arrangement of cellulose microfibrils, hemicellulose and pectin.

Fig. 1.7 Structure of cellulose.

Fig. 1.8 Common forms of monomers found in hemicellulose.

Fig. 1.9 Structure of p-hydroxy cinnomyl alcohol unit forming lignin.

Fig. 1.10 Cross section view of wood components.

Fig. 1.11 Cross section of xylem cells.

Fig. 1.12 Mechanism of photosynthate translocation with xylem and phloem pathways.

Fig. 1.13 The movement of mineral elements from soil to the root surface. ① Soil volume by root volume. ② Mass flow of nutrients along the water potential gradient (driven by transpiration). ③ Diffusion: nutrient transport along the concentration gradient.

Fig. 1.14 The influence of soil pH on the availability on a selection of essential plant elements.

Fig. 1.15 Leibigs law of the minimum. Idealised relationship between nutrient content of a plant and growth yield.

Fig. 1.16 The influence of physical factors upon the formation of soil.

Fig. 1.17 Hydrological feedback loops before and after deforestation.

Fig. 1.18 Ecological effects of timber deforestation upon forest animal populations.

Fig. 1.19 Potential energy curve for the interaction of two atoms in a liquid or solid state.

Fig. 1.20 Variation of $\delta^{13}C$ isotope in carbon sources.

Fig. 1.21 Diagram showing a representation of the Calvin cycle, adapted to illustrate the formation of one glucose molecule.

Fig. 1.22 Simplified schematic of the relationship between carbon isotope composition ($\delta^{13}C$) and stomatal conductance; (a) high stomatal conductance, low discrimination; and (b) low stomatal conductance, high discrimination.

Fig. 1.23 Variation of $\delta^{2}H$ isotope in hydrogen sources.

Fig. 1.24 $\delta^{18}O$ isotope ranges of oxygen pools.

Fig. 1.25 Global variation of $\delta^{2}H$ in precipitation.

Fig. 1.26 Fractionation of $\delta^{2}H$ and $\delta^{18}O$ isotopes during evaporation and precipitation processes

Fig. 1.27 Global meteoric water line

Fig. 1.28 Isotopic composition of C, O and H pools in the carbon and water cycles.

Fig. 1.29 Schematic of an isotope ratio mass spectrometer.

Fig. 1.30 Configuration of the elemental analyser IRMS system in flash combustion mode.

Fig. 1.31 High temperature conversion during pyrolysis.

Fig. 1.32 Configuration of the elemental analyser IRMS system in high temperature pyrolysis mode.

Fig. 1.33 Cavity type microwave digestion system.

Fig. 1.34 Schematic of a typical ICP-MS system.

Fig. 1.35 ICP-MS plasma torch based on the Fassel design.

Fig. 1.36 Representation of ICP-MS processes following sample introduction.

Fig. 2.1 African surficial lithology and timber sampling locations. Taken from the United States geological survey. http://rmgsc.cr.usgs.gov/ecosystems/africa.shtml.

Fig. 2.2 Cross plot of all countries timber multi element data separated by two discriminant functions calculated from the step-wise canonical discriminant analysis.

Fig. 2.3 Interval plots of trace elements selected by the canonical discriminant analysis. The mean values for each country are represented by solid circles, and the error bars represent the 95% confidence interval.

Fig 2.4 Cross plot of all countries timber multi element data (minus Congolese) separated by two discriminant functions calculated from the step-wise canonical discriminant analysis.

Fig 2.5 Interval plots of trace elements selected by the canonical discriminant analysis. The mean values for each country are represented by solid circles, and the error bars represent the 95% confidence interval.

Fig. 3.1 Mean $\delta^{13}C$ values measured in JRC sucrose QC material across analytical batches. (Assigned value for sucrose from inter-laboratory comparison was -11.30‰).

Fig. 3.2 Mean $\delta^{13}C$ values measured in IAEA CH3 cellulose across analytical batches. (Assigned value for sucrose from inter-laboratory comparison was -24.72‰, IAEA, Vienna).

Fig. 3.3 Performance of mean $\delta^{13}C$ values measured in WIHRM cellulose with analytical batches. (Assigned value for WIHRM cellulose was -26.25‰).

Fig. 3.4 Interval plot of timber cellulose $\delta^{13}C$ values classified by country of origin. Mean values for each country are represented by solid circles, the error bars representing the 95% confidence interval.

Fig. 3.5 Comparison between mean $\delta^{13}C$ values in tree cellulose and the mean annual humidity in West Africa and Madagascar.

Fig. 3.6 Koppen-Geiger classification map (Af. represents tropical rainforest climate). Taken from Nature, 487, 358–361 (19 July 2012).

Fig. 3.7 Aquifer potential of continental Africa. Taken from: http://www.bgs.ac.uk/research/groundwater/international/africanGroundwater/maps.html.

Fig. 3.8 Comparison between mean $\delta^{13}C$ values in cellulose and the mean annual wind speed in West Africa and Madagascar.

Fig. 3.9 Performance of mean $\delta^{18}O$ values measured in IAEA CH3 cellulose across analytical batches. (Assigned value for cellulose was -31.68.‰, Loader *et al.*, 1999).

Fig. 3.10 Performance of mean $\delta^{18}O$ values measured in WIHRM cellulose with analytical batches. (Assigned value for WIHRM cellulose was 26.43‰).

Fig. 3.11 Interval plot of timber cellulose $\delta^{18}O$ values classified by country of origin. Mean values for each country are represented by solid circles, the error bars representing the 95% confidence interval.

Fig. 3.12 Comparison between the mean $\delta^{18}O$ values of timber cellulose and mean country level annual temperature.

Fig. 3.13 Comparison between the mean $\delta^{18}O$ values of timber cellulose and mean annual rainfall in West Africa and Madagascar.

Fig. 3.14 Comparison between mean $\delta^{18}O$ of cellulose and altitude of the sampling locations for the respective countries.

Fig. 3.15 Performance of IAEA CH3 cellulose measured as part of analytical batches.

Fig. 3.16 Performance of WIHRM cellulose measured as part of analytical batches.

Fig. 3.17 Interval plot of timber cellulose $\delta^{2}H$ values classified by country of origin. Mean values for each country are represented by solid circles, the error bars representing the 95% confidence interval.

Fig. 3.18 Mean values for $\delta^{18}O$ and $\delta^{2}H$ calculated from precipitation (MWL) and measured in cellulose.

Fig. 4.1 Cross plot of timber cellulose stable isotope data for all countries, separated by two discriminant functions calculated from the step-wise canonical discriminant analysis.

Fig. 4.2 Cross plot of timber multi element data and stable isotope data for all countries, separated by two discriminant functions calculated from the step-wise canonical discriminant analysis.

Fig. 4.3 Comparison of inter and intra-site isotopic variation of $\delta^{13}C$, $\delta^{2}H$ and $\delta^{18}O$ in timber samples of *Entandrophragma cylindricum* at sampling locations in Eastern and Western Cameroon.

Fig. 4.4 Comparison of inter and intra-site variation of B, Ti, Mn, Cu, Zn and La trace element concentrations in timber samples of *Entandrophragma cylindricum* at sampling locations in Eastern and Western Cameroon.

Fig. 4.5 Comparison of inter and intra-site variation of Na, Al, Fe, Rb, and Sr trace element concentrations in timber samples of *Entandrophragma cylindricum* at sampling locations in Eastern and Western Cameroon.

Fig. 4.6 Comparison of inter and intra-site variation of Li, V, Cr, Co, Y, Sb, La, and Nd trace element concentrations in timber samples of E*ntandrophragma cylindricum* at sampling locations in Eastern and Western Cameroon.

Fig. 4.7 Comparison of inter and intra-site variation of Mg, K, and Ca trace element concentrations in timber samples of *Entandrophragma cylindricum* at sampling locations in Eastern and Western Cameroon.

Fig. 6.1 West African and Madagascan sampling locations.

Fig. 6.2 Increment borer. Taken from: Forestry-suppliers.com

Fig. 6.3 Retsch centrifugal mill. Photo taken at FERA, Sand Hutton. UK.

Fig. 6.5 Retsch ball mill, MM400. Taken from www.coleparmer.co.uk

Fig. 6.4 Madagascan Ebony core. Photo taken at FERA, Sand Hutton. UK.

Fig. 6.6 The protocol for purification of cellulose from microsamples of plant cell wall material using acetic acid : nitric acid for simultaneous delignification and removal of non-cellulose polysaccharides. Adapted from Brendel *et al.* (2000).

Acknowledgements

Foremost, I would like to thank Paul Wheeler at Isoprime for his support and funding the MSc research degree. Without the financial support from Isoprime, funding the MSc would have been difficult. I am also thankful to the staff at Isoprime for their provision of advanced training which enhanced my research.

I certainly could not have undertaken this research without authentic samples to analyse. I am thankful to Stuart Cable and Noel McGough at Kew Garden, and Bernd Dagen and Henri Bouda at the International tropical timber organisation (ITTO) for arranging collection and shipping of authentic timber samples from Madagascar and West Africa.

I would like to thank Dr Markus Boner and Micha Horacek for their advice and technical expertise in the field of timber authenticity.

I thank Dr Simon Kelly at the University of East Anglia for his inspiration and encouraging me to undertake the MSc in the first place. Simon was always available to answer questions and offer his expertise in the field of authenticity and isotope ratio mass spectrometry.

I would like to thank Professor Brendan Keely at the University of York. Proffesor Keely was aware I was undertaking my research away from the University and ensured sure I received the right level of support and guidance with my studies.

Additionally, I would like to thank FERA and my team leader Dr James Donarski for offering academic support and allowing me the flexibility to adapt the research degree around my full time work commitments. Furthermore, I thank fellow members of my team Nicola Brereton, Malcolm Baxter, Katharina Heinrich, Celine Pye, and Leticia Geitero for their administrative and technical support during my studies.

Not forgetting the staff of the University of York chemistry graduate office to whom I am grateful for their administrative support and guidance while I undertook my studies.

Declaration

I hereby declare that the work herein submitted for the MSc degree at the University of York, United Kingdom is the result of my own investigation, except where reference is made to the published literature. I also declare that the material submitted in this thesis has not been accepted for any other degree and is not being concurrently submitted for any other degree.

Chapter 1 – Introduction

This introductory chapter will cover the many aspects of timber production and how this influences the wider environment and biodiversity of tropical timber exporting nations. Regulations covering the protection of timber species in these countries will also be discussed, as well as the providing the justification for the analysis techniques applied in this thesis. Objectives for the research are also listed at the end of this chapter.

Trees are known to have existed for at least 370 million years (Petit & Hampe, 2006) and support diverse ecosystems including invertebrates, lichens, algae, and fungi among others. Their ability to trap carbon dioxide from the atmosphere and in turn release oxygen means they play a vital role in sustaining life on earth. Tropical rainforests are reported to contain up to 90% of the worlds described species (State of the Environment and Policy Retrospective; 1972–2002). Timber is one of the oldest and most versatile building materials known to man, and because of this, there has been a tendency to overexploit this precious natural resource throughout the centuries. Current demand and the increasingly globalised economy have intensified overexploitation to unprecedented levels (Laurance, 1999). The scale of the destruction of ancient forest not only presents a serious threat to the ecosystem, it also threatens the existence of the 1.6 billion poorest peoples of the world through loss of livelihood and desertification (The International Conservation Budget, 2011). Deforestation accounts for up to a third of anthropogenic greenhouse gas emissions and is a significant contributor to climate change (Fearnside & Laurance, 2004).

Concern about climate change and political desires to reduce dependency on fossil fuels, (coupled with the increased focus on CO_2 emission targets) have increased the focus of investment on alternative means of energy production – an unfortunate consequence of which is the environmental impact of deforestation. Timber is classed as a renewable material, and therefore is considered carbon neutral when disregarding factors such as transportation and subsequent loss of biomass from native forests. Not only does mislabelling or lack of traceability associated with timber pose a threat to the

environment where felling takes place, but there is also an increasing possibility of the introduction of fungal plant pathogens and invasive species into importing countries (Begoude *et al*., 2011).

The advance of globalisation and the steady increase in the supply chain of plant derived products places great demands on the scientific community to develop analytical techniques which can answer the question of provenance of traded goods. Governments, business and consumers now expect to see evidence that timber is sourced ethically, and that robust procedures can be called upon to verify authenticity claims.

1.1 An overview of timber production

Global sales of tropical timber are reported to be worth an estimated $30 -100 billion annually, with up to 30% harvested illegally and projected trade to increase with the growth of the world economy (United Nations Office on Drugs and Crime, 2013). Harvesting tropical timber requires little investment, hence it is an attractive option for poor countries. The growth of developing world export-led economies, such as Brazil, Russia, India and China, and the requirement for many governments to increase the production of agriculture and biofuels, represent increasing pressures that look unlikely to reverse in the foreseeable future. A total of 40% of global illegal timber is ultimately exported to countries in the G8, mostly in the form of processed goods, with China responsible for importing 25% of global illegal raw timber supply (Global Timber, 2006). The processing of timber into finished products before export to Europe and the USA further complicates the challenge of identifying the species and provenance of wood, and it is possible that steps such as seasoning and heat treatment may complicate the extraction of DNA which would otherwise assist with species identification (Rachmayanti *et al*., 2009).

1.1.1 Impacts of deforestation

1.1.1.1 Trace elements and nutrients

While slash and burn practices release much of the plant soluble nutrients back into the soil, the imbalance brought about through forest clearing means that nutrient recycling processes are significantly disrupted. Studies have shown deforestation increases surface water runoff, consequently resulting in a net loss of soil nutrients and trace elements through leaching processes to surrounding rivers and streams (Fig. 1.1). Phosphorus and silicon are both geologically derived, being produced through mechanical weathering of the underlying rocks. An increase in the dissolved concentrations of many elements can largely be attributed to deforestation and an interruption of the floral bio-assimilation by which they would otherwise be sequestered. The deep roots of trees have the ability to trap and utilise trace elements, many of which can otherwise be toxic to mammalian and aquatic life at high concentrations. Deforestation disturbs the buffering capacity for many toxic elements, allowing them to be leached and transported by water runoff into nearby aquifers and lakes (Lombardozzi *et al*., 2003).

A study in Southern Yucatan, Mexico showed that the bio available soil phosphorus concentration decreased 44% over a period of three growing seasons following forest clearance to make way for agricultural practices. The declining trend indicated that crop yields will continue to fall until it is uneconomically viable for the farmer to sustain crops (Lawrence *et al*., 2007).

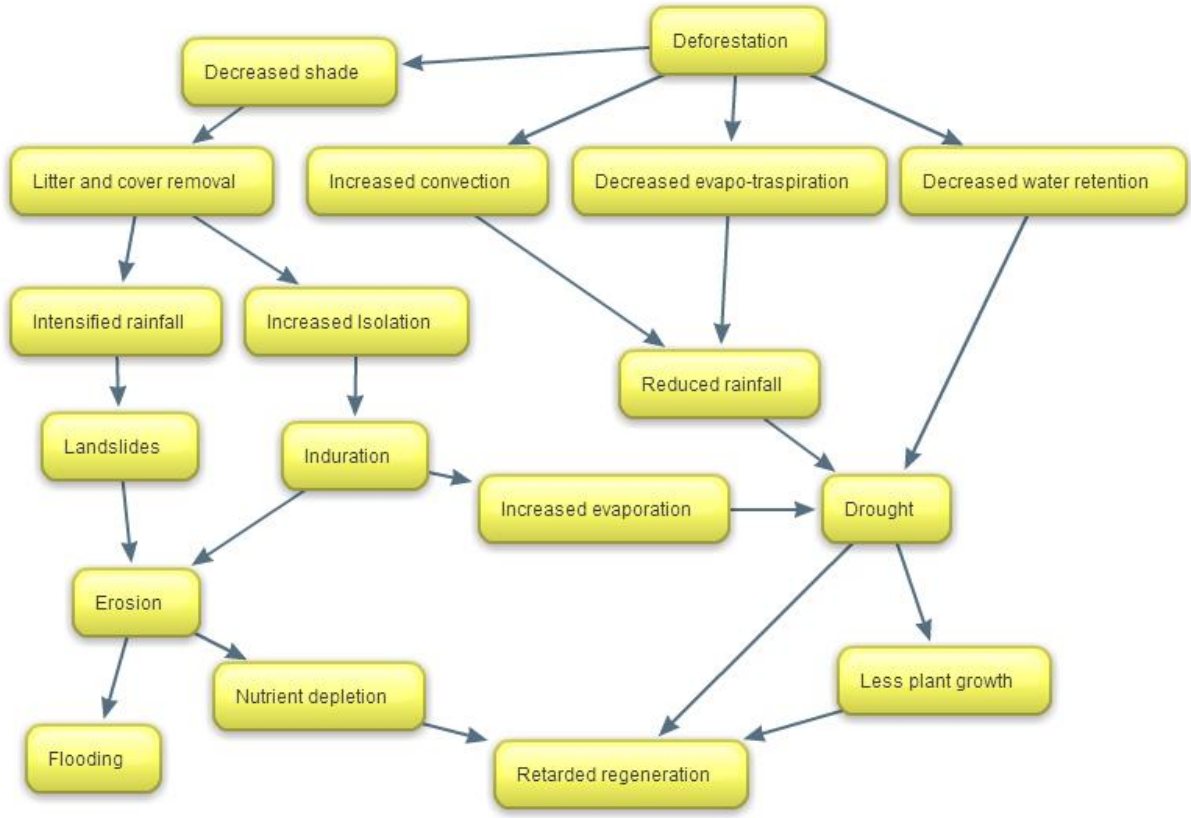

Fig. 1.1 Environmental disruption following deforestation. Adapted from Goodland & Irwin (1974).

Crowther *et al*. (2014) showed that %C, %N, pH, and soil moisture correlated with soil type, thus changes in soil pH can adversely affect chemical weathering of the underlying geology, resulting in a change to the rate and type of trace elements which will be released into the soil (Olander *et al*., 2005).

1.1.1.2 Microbial biodiversity

Microbial populations were studied in a field exercise to assess the impact of logging on the forest microflora populations (Amali *et al*., 2013). Soil samples were selected randomly within 100 m quadrants and at a depth of approximately 1.5 cm. Serial dilution and plate count analysis revealed all populations of microflora were shown to decrease in the deforested area compared to the forested area (Fig. 1.2).

Another study applied high throughput DNA sequencing to study the difference in microbial diversity between paired sites consisting of natural forest, adjacent to a previously forested old-field grassland deforested area. Results showed a variable response with vegetation type, and soil texture having significant influence on the susceptibility of fungal biomass to land use change. Fine textured soils were shown to have an increased buffering capacity when compared to sandy soils, the latter dramatically altering below ground populations upon forest removal (Crowther *et al*., 2014).

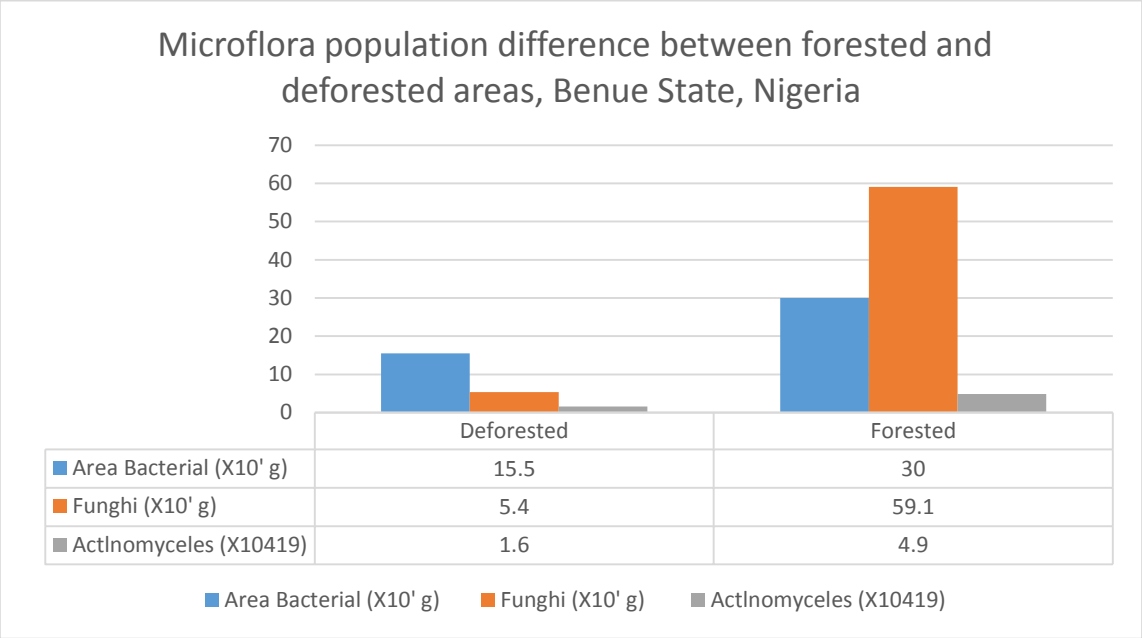

Fig. 1.2 Ecological effects of timber deforestation upon forest microflora. Adapted from Amali *et al*. (2013).

1.1.2 Forest Management

1.1.2.1 Conventional practices

Two primary motivating factors drive current forest management practices: the economic benefit of increased production yields and ecological considerations such as species recovery or carbon dioxide sequestration, where atmospheric CO_2 is captured and stored for a period of time (Sedjo & Sohngen, 2012). Preservation criteria such as clearing a limited number of trees will sometimes be applied in order to prevent the spread of disease or to limit the vulnerability of the forest to wild fires (Sizer *et*

al., 2000). Conservation practices, such as sustainable forest management, aim to maximise timber yields over a number of generations, with the intention of preserving the physical and social environment for the benefit of local communities and biodiversity.

1) The environmental security associated with the planting of huge numbers of fast growing trees has been suggested as a way of mitigating the effects of climate change. Trees are excellent sequesters of CO_2 and offer an effective method of carbon capture if planted in large enough numbers and managed effectively (Sedjo & Sohngen, 2012).
2) Species of timber known as primary timbers are an essential part of forestry economic security. These generally come from slow-growing, aesthetically appealing hardwoods which have considerable natural resistance to biological attack, moisture, movement and distortion. As a result, primary timbers are highly sought after which makes them expensive and in short supply. Secondary timbers are usually prevalent in plantations where there is dominant monoculture of mainly fast-grown species with low natural durability, such as *Pinus sylvestris* grown in the plantations of northern Europe. Rising costs and diminishing supplies of primary timbers mean the importance of secondary timber is rapidly increasing (Kanel & Shrestha, 2001). With appropriate seasoning and preservative treatment, the physical properties and durability of secondary timber can be improved greatly. However, plantations of timber monocultures (secondary timber) are shown not sustain the same levels of biodiversity as the original trees (Bajracharya, 1983).

Plantations rarely contain trees older than 60 years. Hence, they do not contain the same type of enriched soil and wildlife as exists in an old growth forest ecosystem. Regular cultivation means that decaying timber (an important part of a natural forest) does not get a chance to assimilate into the ecosystem. The dominance of timber monocultures and the subsequent lack of genetic diversity within the forest have the effects of reducing the rate of insect and fungal genetic mutations taking place. This much needed evolutionary process is essential in order for species to survive (Paula *et al*., 2014).

A technique known as clearcutting or clearfelling is often applied by the logging industry to promote favourable types of forest ecosystem (Kanel & Shrestha, 2001). Standard clearcut is the most commonly applied, where all of the canopy is removed regardless of commercial viability. Patch and strip clearcuts are typically applied where only a limited number of stems are to be removed, reducing the impact of mass felling upon the forest, or where windthrow (trees being uprooted or snapping) is a major threat to the timber harvest (Pojar,1991).

1.1.2.2 New and emerging practices

Forest farming (agroforestry) is a form of sustainable agriculture which is gaining momentum in temperate areas of the world such as North America and Europe. However, the complexities of integrating crops with trees in one system coupled with the uncertainty of economic returns means the technique is still in its infancy (Jacobson, 2013). One type of agroforestry employs partial clearing and partial preservation of established forest, allowing for the simultaneous development of productive agriculture such as non-forest crops and/or livestock in a level of the forest called the understorey (Fig. 1.3). The tallest trees tend to make up the majority of forest canopy, blocking out sunlight and preventing wind from entering the forest floor, shrub layers and understory. The lack of penetration of sunlight below the canopy causes environmental conditions to be significantly different in this region, resulting in a dark, damp and humid environment, favourable for many types of microflora and fauna.

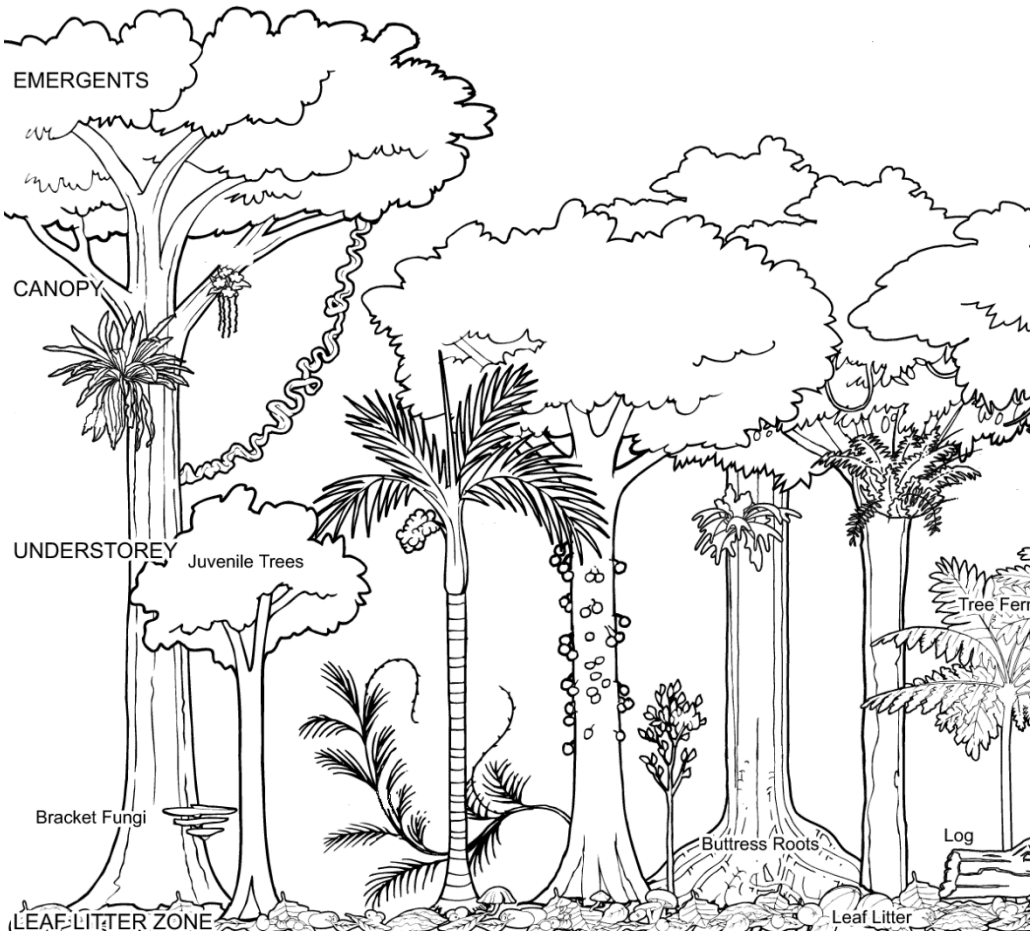

Fig. 1.3 Layers of a rain forest. Adapted from http://mrsgebauer.com/rainforestweb/WebQuest.htm

The majority of forest biodiversity occurs in the understory, at the level between forest floor and head height. Here, the predominant flora support a range of microorganisms and insect life which provide essential elements and nutrients to the surrounding canopy, emergent layer, and forest floor components of the forest. Partial clearing of the forest canopy is crucial in agroforestry and allows for increased uptake of solar radiation by photosynthetic fixation within the flora in the understory (Ghuman, & Lal, 1987). Agroforestry has proved successful in conserving natural forests, through restoration of aquifers and increased biodiversity, whilst allowing farmers to grow high value speciality crops such as coffee, herbs and vines (Muschler, 2001). Further agroforestry techniques involve the interspersed planting of leguminosae fertilizer trees amongst crops.

Fig. 1.4 Application of *Faidheria* fertilizer trees to aid crop production in Malawi. Taken from the world agroforestry centre.

1.1.3 Worldwide production areas

The majority of the world's forests are situated within the northern hemisphere countries of Northern America, Canada and the Russian Federation. Rainforests are prevalent in the tropics, encompassing areas such as Central America, Brazil, the Congo river basin, Madagascar and South East Asia (Fig. 1.5). The countries outlined below are all undergoing significant illegal logging and form the basis for the sampling strategy on which this study was based. A higher resolution map of the timber exporting countries outlined below is shown in Fig. 6.1.

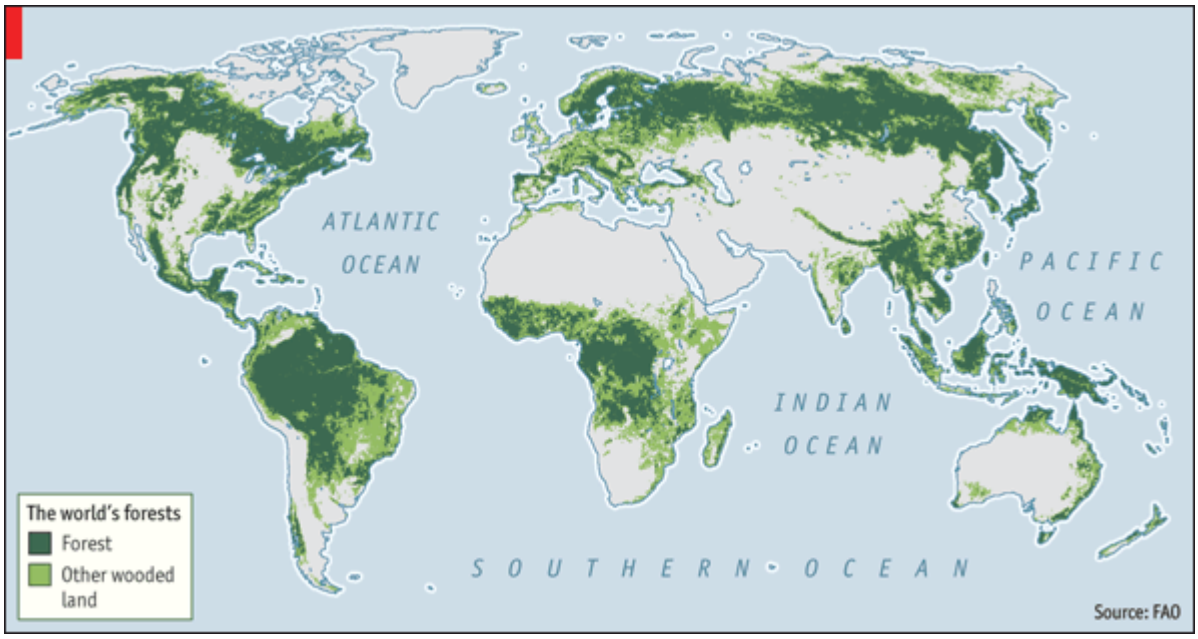

Fig. 1.5 Worldwide forest areas. Taken from the Economist, (2010). Available at: http://www.economist.com/node/17062713.

1.1.3.1 Cameroon

Cameroon has over 20 million hectares of tropical forest, most of which has been permanently allocated for industrial logging and conservation. Forestry contributes over 5% to the GDP of the country with the majority of exports reaching EU markets (Van Solinge, 2008).

1.1.3.2 The Democratic Republic of Congo

The Democratic Republic of Congo (DRC) has the largest tropical rainforest in the Congo basin, covering an area of 145 million hectares. The majority of DRC timber is exported to the EU (Debroux, 2007).

1.1.3.3 Ghana

Ghana has natural forest reserves of over 2.6 million hectares. The country has a reputation for applying technology in the processing of its timber, with forestry accounting for a quarter of the country's gross domestic product (Marfo *et al*., 2014).

1.1.3.4 Republic of Congo

Forest in the Republic of Congo covers over 65% of the country and logging is the second most important export after crude oil. The majority of Congolese timber is exported to the EU and China. Cameroon, Ghana and the Republic of Congo are currently in the process of implementing voluntary partnership agreements with the European Union, while the Democratic Republic of Congo is in negotiation to reach an agreement (Dooley & Ozinga, 201l).

1.1.3.5 Madagascar

Madagascar has over 12000 hectares of forest cover making up 21.6% of the total surface area of the island. Since 2009, the Madagascan government has removed restrictions aimed at protecting the islands natural forests from destruction. Most illegally sourced Madagascan timber is exported to China for processing into finished products (Butler, 2005).

1.1.4 Timber morphology

The chemical structure of wood cells varies with tree species, growth phase and even between the differing components of a tree such as branches and roots (Leisola *et al*., 2012). Wood typically contains 50% carbon, 42% oxygen, 6% hydrogen, 1% nitrogen, and 1% trace elements such as calcium and potassium (Rowell, 1984). These elements are the building blocks of four essential plant

components: Polysaccharides (cellulose and hemicelluloses), lignin and other soluble (flavonoids, terpenoids) and non-soluble compounds (pectins and cell wall proteins). Cellulose typically constitutes 40%-50% of wood with hemicelluloses and lignin providing 25% and 25% - 35% of the dry weight respectively (Plomion *et al*., 2001). Celluloses and lignins are important plant components, providing useful energy stores and imparting strength within plants. Fig. 1.6 shows the arrangement of the various celluloses and pectin within a plant cell wall.

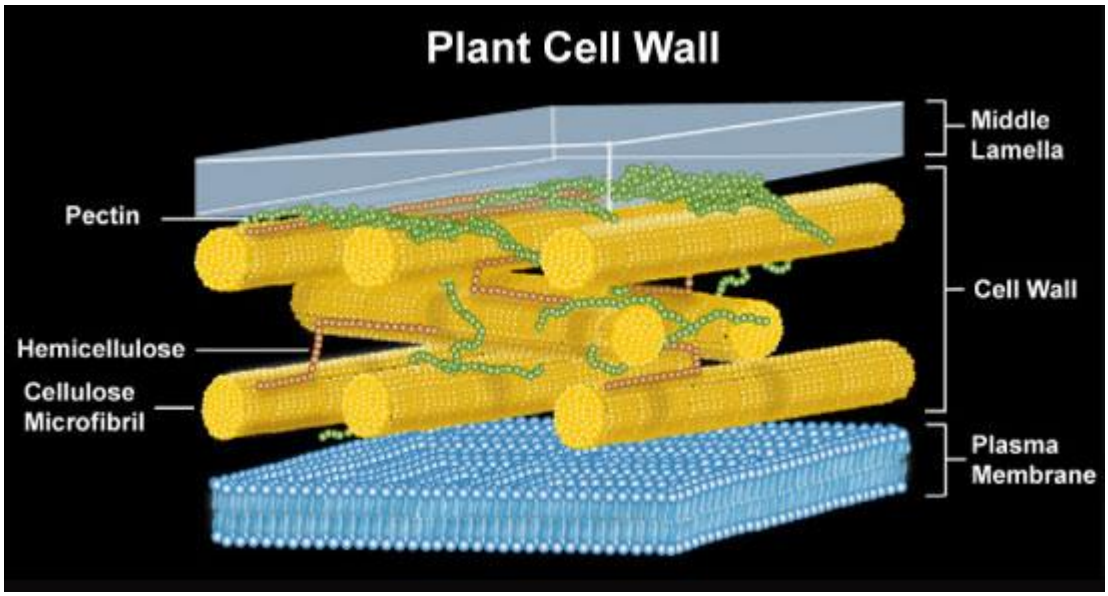

Fig. 1.6 Diagram of plant cell wall showing the arrangement of cellulose microfibrils, hemicellulose and pectin. Taken from http://www.sigmaaldrich.com/life-science/metabolomics/enzyme-explorer/analytical-enzymes/enzymes-for-aer.html

Softwoods and hardwoods are named as such due to cellular structure of the wood rather than the overall density. Hardwoods and softwoods are classified as angiosperms and gymnosperms respectively, the names referring to the covered and uncovered seeds which are released from the trees. The main difference between soft and hardwoods is the presence of vessels (tracheids) in the xylem of hardwoods. Tracheids are elongated cells, up to 80 µm wide with secondary lignified cell walls, which allow for conductance of water and solutes throughout the tree. They also have the important function of providing strength while allowing for the expansion of unlignified cellulose during cell growth (Map of life.org, 2009).

1.1.4.1 Cellulose and hemicellulose

Celluloses typically provide up to 75% of the dry weight of wood and plant material, and are important in the formation of plant cell walls, making them the most abundant organic polysaacharides on Earth (Klemm *et al*., 2005). A high degree of polymerisation is achieved from a repeating unbranched chain of D-glucose units, up to 15000 in length, formed by condensation of β1-4 glycosydic bonds (Crawford, 1981). Cellulose has a tendency to form a large number of inter and intra molecular hydrogen bonds at its hydroxyl groups, resulting in the formation of cellulose micro fibrils imparting a stiff crystalline structure which gives support to cell walls and provides resistance to hydrolysis along the length of the polymer (Sjöström, 1993; Ha, 1998).

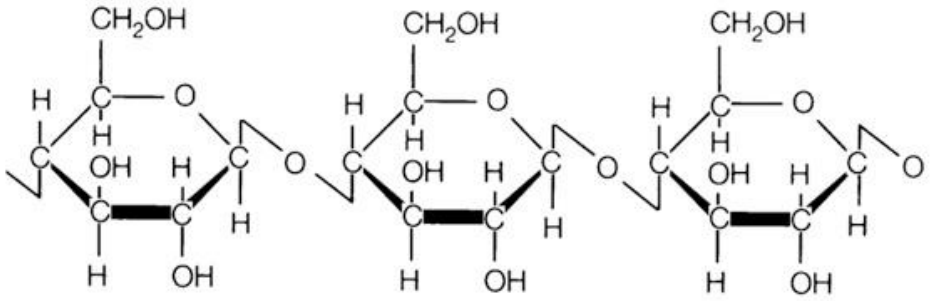

Fig. 1.7 Structure of cellulose. Taken from; https://www.omegafields.com/blog/tag/equine-disorders/.

Hemicelluloses differ slightly in that they typically have shorter chain lengths of up to 3000 linked sugar units; hence they have a lower molecular weight than cellulose. Unlike cellulose, hemicellulose contains hetropolymers consisting of repeating branched and unbranched chains of sugar monomers. Because of this, hemicellulose polymers can take the form of a number of amorphous structures, resulting in differing wood material properties. There is also considerable variation in the makeup of hemicellulose between the stem, roots, bark and branches within a single tree, as well as in the structure and composition of hemicelluloses between species of timber (Table 1.1), especially hardwood and softwood trees (Sjöström, 1993). The combination of cellulose and hemicellulose is called holocellulose.

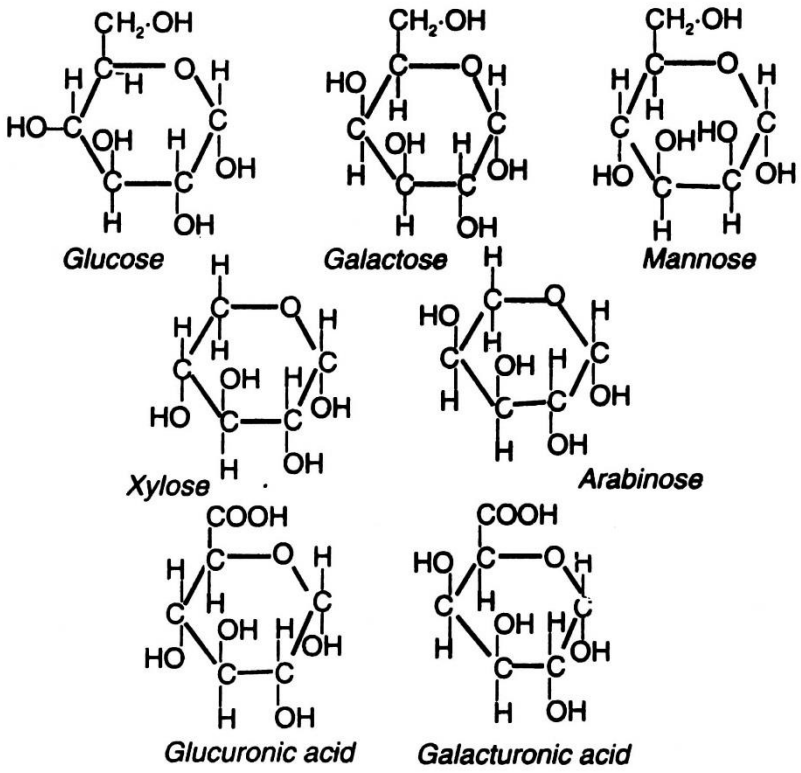

Fig. 1.8 Common forms of monomers found in hemicellulose. Taken from; http://www.eplantscience.com/index/biotechnology/biotechnology_and_environment/biomass_a_renewable_source_of_energy/biotech_biomass_composition_of_biomass.php.

Table 1.1. Contents of the main components, percentage of dry wood. Adapted from Sjöström (1993).

	Cellulose	Glucomannan	Xylan	Other polysaccharides	Lignin
Softwood	33-42	14-20	5-11	3-9	27-32
Hardwood	38-51	1-4	14-30	2-4	21-31

1.1.4.2 Lignin

Lignin is the second most abundant biological material on earth and is distributed throughout the secondary cell wall of plants, with the highest concentration in the middle lamella (Leisola *et al*., 2012). It is highly complex amorphous molecule mainly consisting units of aromatic polymers of phenyl propane. Polymers of lignin are extremely stable and resistant to microbial decay, therefore offering a high degree of protection for plant cell walls (Vanholme *et al*., 2010). Wood lignin

polymers typically consist of three building blocks; guaiacyl, syringyl, and *p*- hydroxymethyl moieties, although different aromatic type variations exist in other wood species (Sjöström, 1993). It is an integral part of the secondary cell wall of plants, and is formed by the de-hydrogenation of p-hydroxy-cinnamyl alcohols (Fig. 1.9) namely p-coumaryl (I), coniferyl (II), and sinapyl (III) alcohols. Coniferyl alcohols (II) are the main reaction ingredients for lignin formation in gymnosperms, with a mixture of coniferyl (II) and sinapyl (III) alcohols making up the main precursors of lignin in angiosperms (Kärkönen & Koutaniemi, 2010).

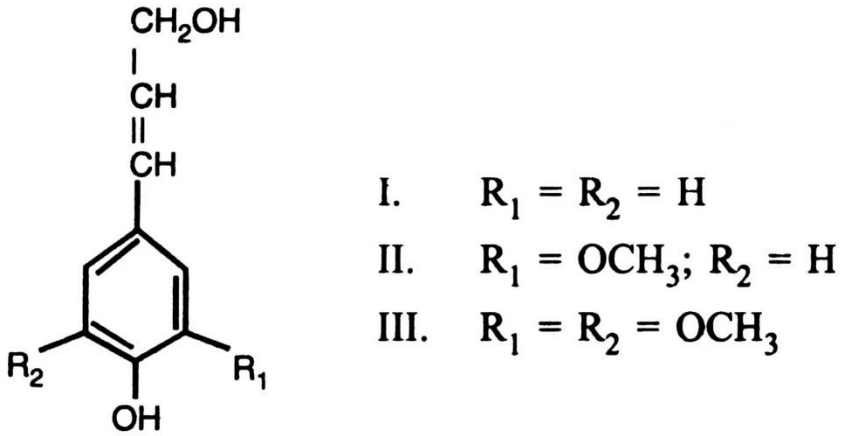

Fig. 1.9 Structure of p-hydroxy cinnomyl alcohol unit forming lignin. Taken from http://www.eplantscience.com/index/biotechnology/biotechnology_and_environment/biomass_a_renewable_source_of_energy/biotech_biomass_composition_of_biomass.php.

1.1.5 Wood biosynthesis

Wood forms from the cumulative activity of the vascular cambium (Li *et al*., 2010). The growth of trees is driven by a number of complex biological processes, many of which are not yet fully understood. Xylogenesis, the process of cell differentiation, is influenced by exogenous (sensitivity to light and temperature) and endogenous (hormone response) processes, driven by the expression of a number of genes, responsible for cell origination, differentiation, and death associated with the formation of heartwood (Plomion *et al*., 2001). The annual loss of leaves and subsequent ceasing of photosynthesis associated with trees growing in temperate areas, leads to the formation of distinct annual growth rings present in the hardwood and sapwood.

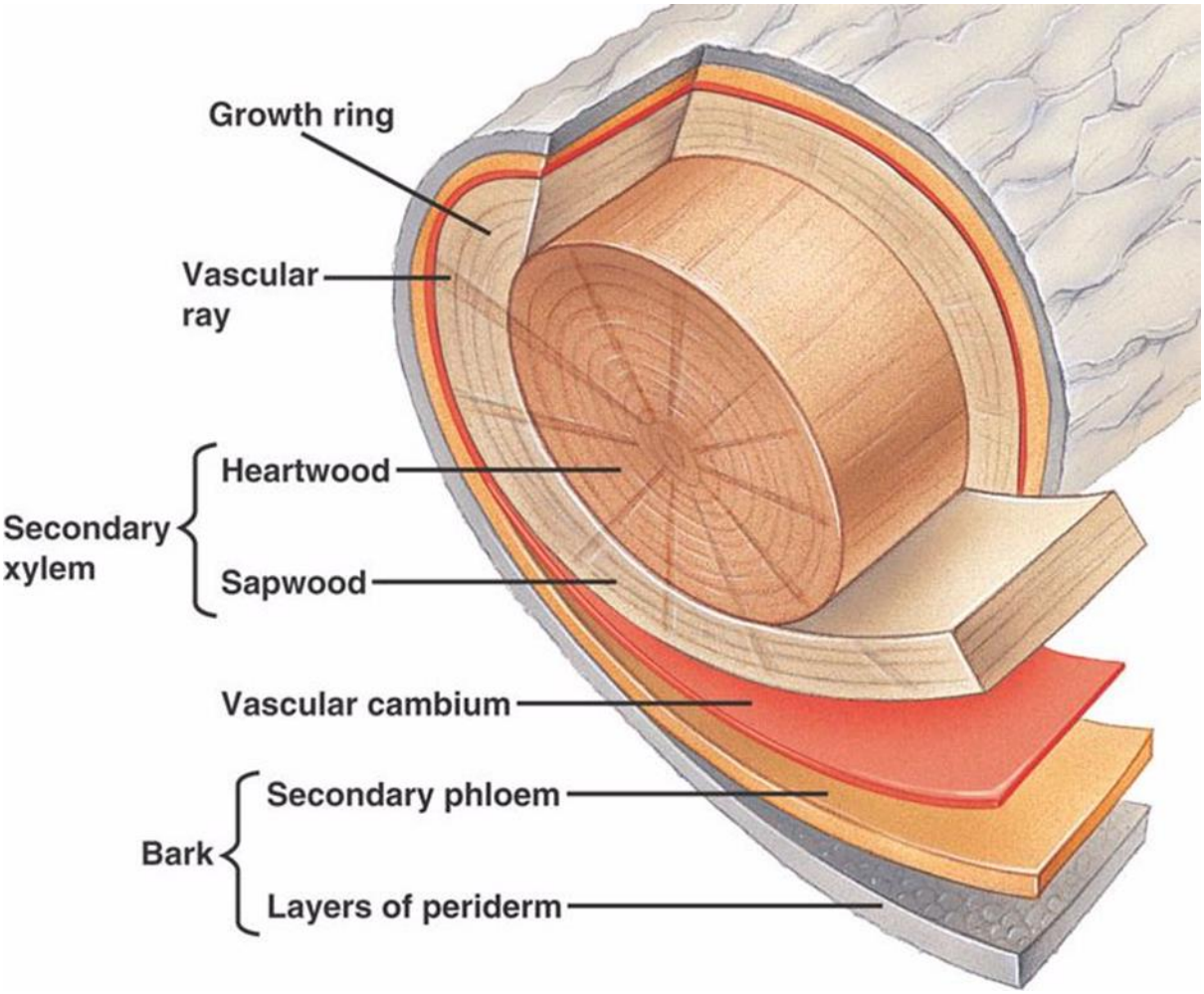

Fig. 1.10 Cross section view of wood components. Taken from http://learningtoworkthewood.blogspot.co.uk/.

1.1.5.1 Xylem

Primary and secondary xylems are types of conduction tissue located between the cambium layer and the centre of the tree. The function of both is the transportation and distribution of water and solutes (xylem sap) from roots to elsewhere higher up within the tree (Marschner, 1983). The primary and secondary xylem is formed during primary and secondary growth stages from the vascular cambium. Secondary xylem is formed through a process called xylogensis in which specific plant genes initiate a programmed cell death (PCD) leading to the formation of tracheids (Demura & Fukuda, 2007). A number of pits along the length of each tracheid allow for the lateral distribution of water and nutrients to specific tree components. In angiosperms such as tropical hardwoods, water and solutes are transported through vessel elements. These originate from the vascular cambium and continue to

form in the secondary xylem, becoming reinforced with lignin over time, finally resulting in the formation of heartwood in the inner tree.

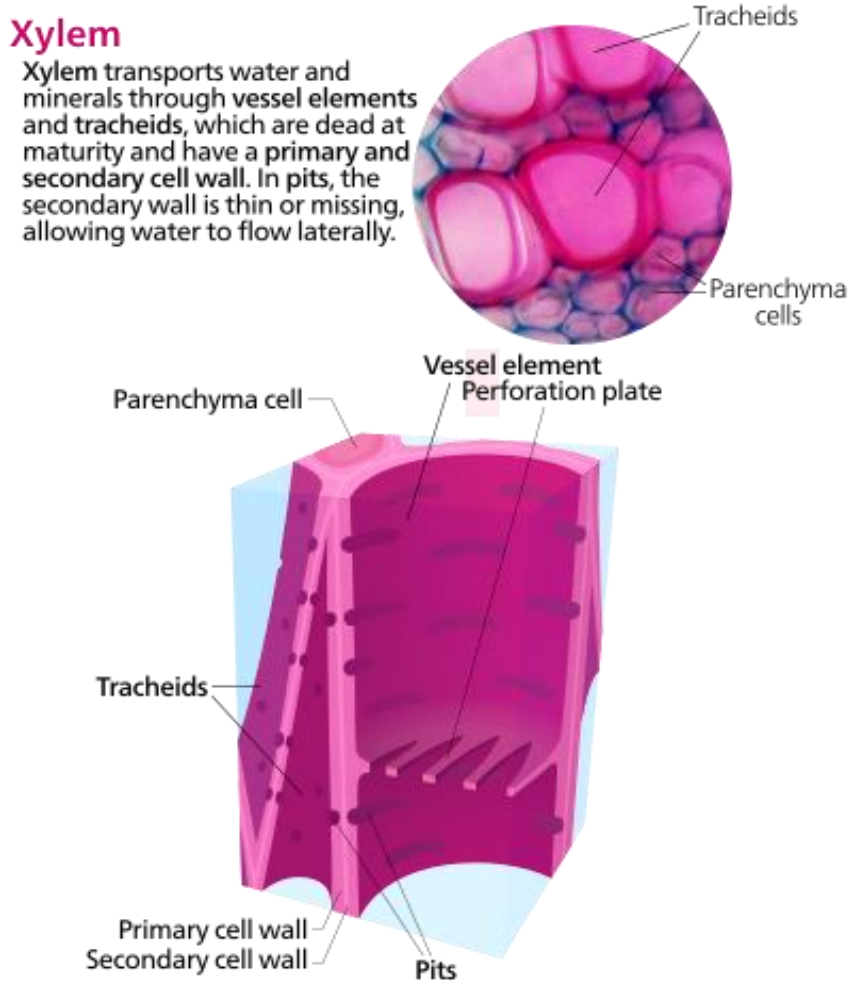

Fig. 1.11 Cross section of xylem cells. Taken from Biology - Campbell & Reece 8th edition (p751).

1.1.5.2 Phloem

The phloem is responsible for the translocation of water and nutrients (phloem sap) throughout the tree (Khan, 2001). Photosynthesis produces carbohydrates which must be transported to areas of the tree for growth, storage and respiration. The phloem aids this process by use of a solute concentration gradient; at photosynthetic specific tissues, sugars are loaded from the leaf cells, first into the companion cells and then into the phloem, in turn increasing the solute concentration. This has the effect of drawing water (through osmosis) from xylem, increasing turgor pressure (Campbell *et al*.,

2008). Isosolutes are then forced along channels within the phloem (called sieve tubes) until the solute reaches areas of low solute concentration, hence growing or damaged parts of the tree tend to receive an elevated concentration of carbohydrates (Münch, 1930; Raven *et al*., 1992). Once the isosolute reaches an area of low solute concentration (low turgor pressure), osmotic pressure increases in the companion and sink cells (Fig. 1.12), initiating the passive diffusion of isotonic carbohydrates out of the phloem until a low osmotic pressure and the reverse osmosis of water back into the xylem occurs (Ryan & Shinichi, 2014). Unlike the xylem where tracheids and vessel elements only transport water and nutrients in one an upward direction, the phloem utilises a bi-directional flow, allowing the distribution of photosynthates and hormones within the tree.

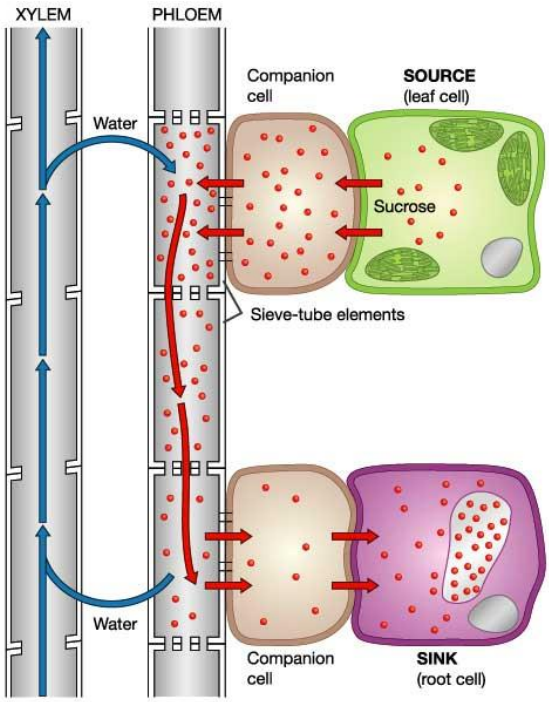

Fig. 1.12 Mechanism of photosynthate translocation with xylem and phloem pathways. Taken from http://www.uic.edu/classes/bios/bios100/lectf03am/translocation.jpg.

1.1.6 Mineral nutrition in trees

There are fourteen known essential elements needed in the metabolism of plants and trees classified as primary micro and macronutrients. Primary macronutrients include nitrogen (N), phosphorus (P) and potassium (K). Secondary macronutrients include calcium (Ca), sulphur (S) and magnesium (Mg). Micronutrients include boron (B), chlorine (Cl), manganese (Mn), iron (Fe), zinc (Zn), copper (Cu), molybdenum (Mo), and nickel (Ni) (Barker & Pilbeam, 2007). Trace element concentrations of plants and trees largely reflect the bioavailability of water soluble nutrients derived from lithology and anthropogenic activity (Baes & McLaughin, 1984). Additionally, in undisturbed forests, many trace elements are released by bacteria feeding on decaying biomass, providing recycled nutrients for plants and trees in the surrounding environment. Multi element analysis using ICP-MS can quantify many of these essential nutrients, with the potential for revealing detailed information on the multi element concentrations of a given location. For the purposes of determining provenance, analysis of trace elements offers complementary approach when combined with stable isotopes.

1.1.6.1 Uptake of minerals by trees

Trace elements in trees are almost entirely derived from the soil via absorption through roots, with a small, select number of nutrients able to be assimilated through leaves (Whitehead, 2000). The assimilation rates of trace elements are influenced by both soil and plant processes. The concentration of ions that come into contact with a tree root depends partly upon the growth of the root itself, but mainly upon the rate of mobilisation of the ion at the root surface, as most interaction between root and ion is driven by mass flow and diffusion processes (Fig. 1.13). Mass flow occurs when water and soluble ions move towards a root as a result of transpiration, and for some ions such as Ca^{2+} and Mg^{2+}, the concentration in the soil is sufficiently high enough to satisfy the tree's needs. Indeed, mass flow may even produce an oversupply of select elements at tree roots, leading to bioaccumulation (Jungk and Claassen, 1997; Whitehead, 2000). Diffusion occurs when an ion moves randomly in a solution from high to low concentration, the process often occurring when a trees demand for a trace element is greater than what can be absorbed through mass flow alone. Soil pH (Fig. 1.13), humidity, porosity,

clay type and humic complex all influence the bioavailability of trace elements. The cation and anion exchange capacity (CEC, AEC) of the soil is also critically important, heavily influenced by the surface area of the soil particles (Kim & Thornton, 1993; Barber, 1995; Pendias, 2004).

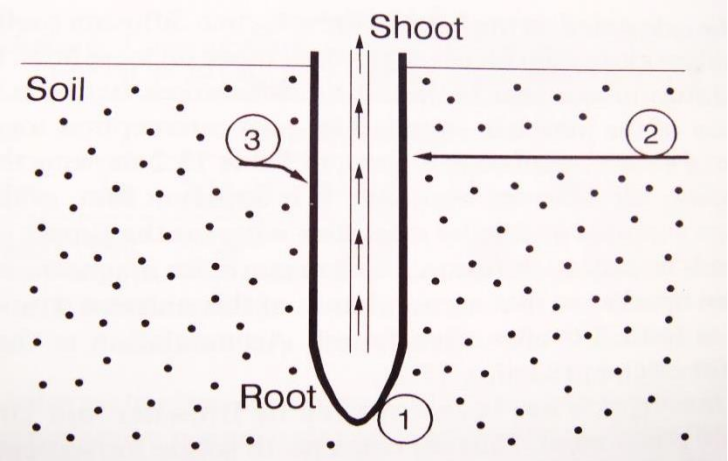

Fig. 1.13 The movement of mineral elements from soil to the root surface. ① Soil volume displaced by root volume. ② Mass flow of nutrients along the water potential gradient (driven by transpiration). ③ Diffusion: nutrient transport along the concentration gradient. • = Available nutrients. Taken from Marschner (1995).

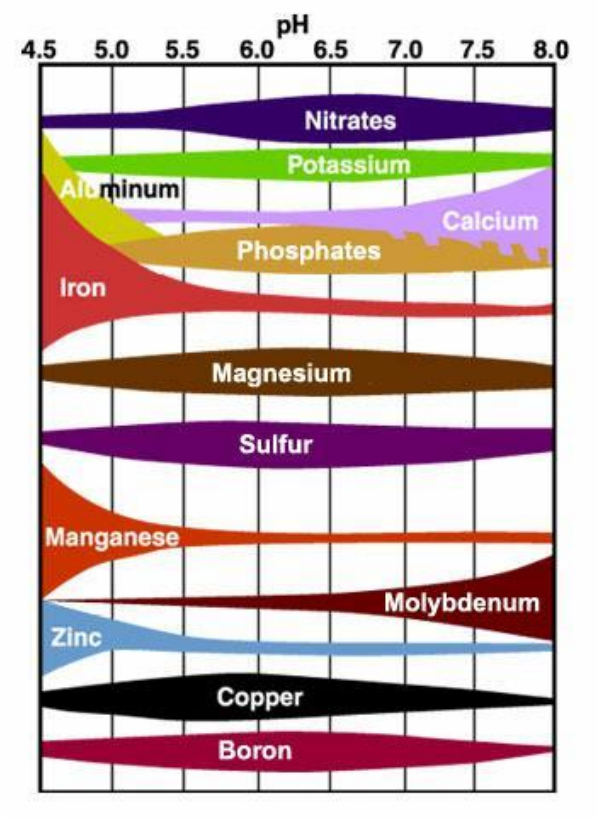

Fig. 1.14 The influence of soil pH on the availability on a selection of essential plant elements. Taken from: http://www.swac.umn.edu/classes/soil2125/img/8phgrph.jpg

Liebig's law of the minimum (Fig. 1.15) states "availability of the most abundant nutrient in the soil is only as good as the availability of the least abundant nutrient in the soil". Therefore, if bioavailability of an element is affected after forest clearing, the growth of any remaining trees can still be restricted. The critical concentration of a nutrient in plant tissue is defined as slightly less than that needed for maximum growth when all other nutrients are in adequate supply (Barber, 1995).

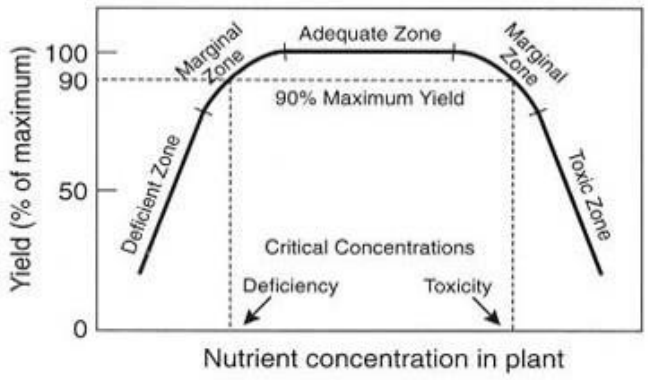

Fig. 1.15 Leibigs law of the minimum. Idealised relationship between nutrient content of a plant and growth yield. Taken from http://www.sesl.com.au/fertileminds/200801/Interpreting.php

1.1.6.2 Geochemical inputs to soil and water

Soil is formed through mechanical weathering of underlying rock formations. Formation involves meteorological and climatic processes such as freeze thawing, wind exposure, extremes of temperature and pressure resulting in parent material rock degrading into smaller pieces over time (Fig. 1.16). Fine parent rock undergoes chemical weathering and acid breakdown into smaller units of sand/quartz, silt, silica, mineral and nutrients, aluminium and iron oxides, cations and anions. Mineral nutrients will combine with silica to form two or three layer clays, commonly found in temperate and tropical top soils respectively.

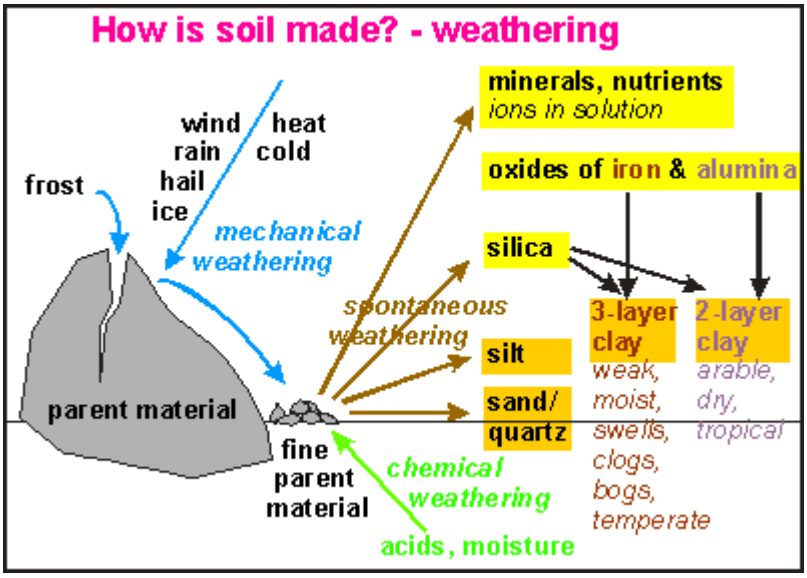

Fig. 1.16 The influence of physical factors upon the formation of soil. Taken from Anthoni, (2000). Available at: http://www.seafriends.org.nz/enviro/soil/geosoil.htm.

1.2 An overview of illegal logging and controls

Much of the tropical timber imported into BRIC's countries (Brazil, Russia, India, and China) undergoes processing and manufacture into finished products which are subsequently exported to the USA, EU, Canada, and Australasia. Many developing countries have little economic incentive, or legal controls to ensure imports of raw materials are ethically sourced. Illegal activities include cultivating trees from unauthorised areas, taking more timber than is permitted and cultivating trees deemed to be too small for harvesting. Developing country exporters will often resort to laundering timber to cover up the origin. Combining illegally and legally sourced consignments, or providing false documentation are some of the methods used to overcome export laws (Timber, 2006).

1.2.1 Physical, biological and chemical impacts of illegal logging

1.2.1.1 Erosion and hydrological feedback loops

Following forest clearing, the agricultural vegetation which replaces the original forest has a lower biomass, and therefore fewer leaves and roots are available for water uptake. During heavy rainfall, the reduced phytological demand for water leads to increasing water runoff, in turn reducing the

volume of moisture available for evaporation and formation of essential forest cloud cover (Fig. 1.17). Water runoff also decreases soil percolation, infiltration and interflow resulting in drying of the forest top soil (Jacobs & Bruin, 1992). Opening up of the forest canopy increases the penetration of sunlight to the forest floor and therefore an increase of temperature is observed. Once the wind insulating ability of the forest has been compromised, dehydrated top soil particles are carried away, initiating the process of land erosion and desertification (Hudson, 1995).

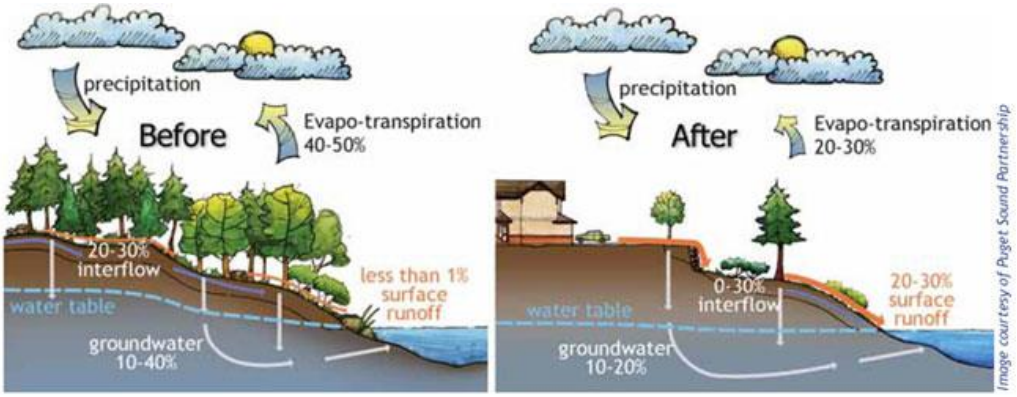

Fig. 1.17 Hydrological feedback loops before and after deforestation. Taken from: https://www.teachengineering.org/view_activity.php?url=collection/usf_/activities/usf_stormwater/usf_stormwater_lesson01_activity1.xml

1.2.1.2 Forest fires

Clearing of forest canopy and the subsequent reduction of forest humidity, coupled with increasing forest floor temperatures, increases the likelihood of forest fires. The clearing of the forest floor allows for the rapid growth of invasive grasses and shrubs which can become very flammable in times of elevated temperatures and drought (Wooster *et al*., 2012).

1.2.1.3 Animal biodiversity

A field exercise in Benue state, Nigeria compared animal biodiversity levels between an undisturbed forested area and an adjacent site on which selective logging had taken place (Fig. 1.18). With exception of the Gambian giant rat, the study showed a significant reduction for all species in the selectively logged, compared with the forested areas (Amali *et al*., 2013).

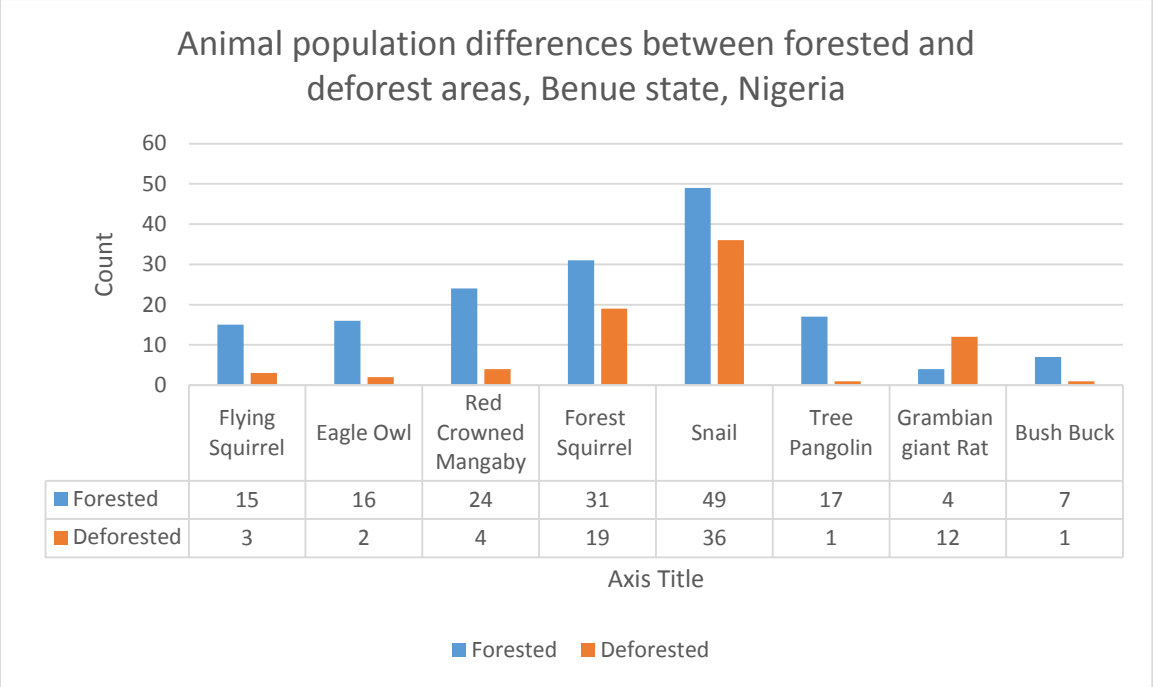

Fig. 1.18 Ecological effects of timber deforestation upon forest animal populations. Adapted from Amali *et al*. (2013).

1.2.2 Endangered timber species

Madagascar and Cameroon are home to as many as ten thousand tree and shrub species, the majority being unique to Madagascar. Researchers found 244 tree and shrub species in a plot of 0.79 hectares within the island (Armstrong *et al*., 2011) a level of diversity second only to Yanamomo in Peru, where a study found 292 species spanning one hectare (Whitmore, 1982).

Table 1.2 Species count within worldwide rainforests. Adapted from Armstrong *et al*. (2011).

Rainforest location	Species number	Sample area (ha)
Yanamomo, Peru	292	1
RNI Betamppona, Madagascar	244	0.79
Pasoh, W. Malasia	210	1
Bukit Lagong, Malasia	180	1
Wanariset, Kalimantan, Indonesia	239	1.6
Northewest Amazonia, Columbia	178	1
Sungei Menyala, Malasia	170	1
Korup National Park, Cameroon	140	0.63
Jaro, Kalimantan, Indonesia	135	1
Papua New Guinea	115	0.8
Papua New Guinea	75	0.8

1.2.2.1 Dalbergia

Rosewoods are types of legumes that are members of the genus *Dalbergia* and are listed on the CITES register, classified as vulnerable, at risk of extinction. The strong and heavy nature of its wood means that it has many specialist high end applications such as the production of chess pieces, guitar fingerboard components, billiard cues and luxury flooring. *Dalbergia bathiei* and *Dalbergia monticola* are types of Rosewood unique to Madagascar and are major components of the oriental forest in the country.

1.2.2.2 Diospyros

The Genus *Diospyros* encompasses over 700 species of trees, shrubs and small bushes, with the vast majority of the species growing in tropical climates. *Diospyros angabensis, Diospyros velutipes, Diospyros lohokoensis* and *Diospyros masoalensis* are all types of Ebony timber unique to

Madagascar. Many of the Madagascan species are on the CITES register, classified as vulnerable, and at risk of extinction. Ebony is a dark and dense wood which has many small use applications, particular in the manufacture of musical instruments, pool cues and hand gun grips. Rosewood and Ebony are both ecologically and economically important to Madagascar and are under threat due to large scale deforestation on the island (Harper *et al*., 2007).

1.2.2.3 Entandrophragma

Entandrophragma cylindricum and *Entandrophragma angolense* are types of Sapele timber commonly found in West Africa. Both species are listed on the CITES register as vulnerable, at risk of extinction, with restrictions such as felling limits and protected areas being put in place in an attempt to curb their trade. Species of *Entandrophragma* are often used in the production of furniture. Having a similar appearance to mahogany, they are used instead as a cheaper replacement.

Table 1.3 Summary of threat classifications for timber species of analysed. Adapted from: http://www.foe.co.uk/page/different-types-wood-timber.

Common name	Scientific name	Origin	Uses	Level of use in the UK	Global threat status
Ebony	*Diospyros*	Africa, Asia	Cutlery handles, musical instruments, craftwork.	Minor	VU: At risk of extinction
Rosewood	*Dalbergia*	Africa, South America, India	Furniture, musical instruments	Minor	VU: At risk of extinction
Sapele	*Entandophragma cylindricum*	West Africa	Furniture, joinery, decorative applications	Major	VU: At risk of extinction
Tiama / Edinam / Sapele	*Entandrophragma angolense*	Africa	Furniture, joinery, construction, flooring	Minor	VU: At risk of extinction

1.2.3 Law enforcement and regulations to combat illegal logging

1.2.3.1 EU and FLEGT

The forest law enforcement governance and trade (FLEGT) regulations were set up by the EU (European Union) in 2003 in response to the ongoing damage to the world's natural forests. The regulations aim to assist EU countries in implementing a joint code of practice in conjunction with the EU forest institute. As of the 3rd March 2013, it is a criminal offence to sell illegally sourced timber in the European market. After this date only importers holding a FLEGT licence are legally empowered to import exotic timbers into the EU. The National Measurement Office has the responsibility for enforcement and licensing FLEGT in the UK. Within the FLEGT framework, the EU has set up a number of voluntary partnership agreements (VPA) with a host of timber producing countries outside of the EU. A number of African countries including Cameroon, Central African Republic, Ghana and Congo are currently implementing the agreements, with Côte d'Ivoire (Ivory Coast), Democratic Republic of the Congo, and Gabon in the negotiation stage.

1.2.3.2 Lacey Act

The Lacey Act is a law enacted in the United States of America (USA) and enforced since 2008. It makes it illegal to import plants and plant products which have been harvested in violation of another country's laws. The law made the headlines in 2012 when an America guitar manufacturer was fined $300,000 for importing illegally sourced guitar fingerboard blanks made from Rosewoods and Ebonies from Madagascar and India. The Lacey regulations were enacted by US courts because the guitar manufacture continued to import the endangered timbers from India and Madagascar after 2006 when trade bans had been put in place.

1.2.3.3 CITES regulations

The Convention on International Trade in Endangered Species (CITES) was established in 1973 and is an international (often voluntary) agreement between governments to ensure that trade in endangered species does not threaten their survival. CITES is implemented in the EU by member

states through a framework of European wildlife trade regulations, covering the control of importation of endangered species of animals and plants. The convention also includes a classification threat list called the CITES register. International trade in animals and plants has increased twentyfold since 1975 with over twenty thousand species of plants and trees appearing on the CITES register.

1.2.3.4 The International Tropical Timber Organisation (ITTO)

The International Tropical Timber Organisation (ITTO) is an intergovernmental organisation whose main aim is to promote the implementation of sustainable and conservation management in the world's tropical rainforests. It was set up in 1986 following a United Nations report on the rapid diminishment of the world's tropical rainforests. The organisation works with tropical timber producing nations to develop sustainable logging and sourcing of timber.

1.2.3.5 Forest Stewardship Council

The Forest Stewardship Council (FSC) was founded in 1993 and aims to promote the use of sustainable sourced timber. The FSC operates a global forestry certification system and helps countries and business implement sustainable forestry. FSC certification involves application of a chain of custody system, ensuring that timber is accounted for as it passes along trade supply lines. The organisation offers three stages of certification for wood derived products: FSC 100% – where the wood product is produced from an FSC certified forest; FSC mixed sources – where a portion of FSC certified material is mixed wood products from other controlled sources, and FSC recycled, where the product is produced entirely from recycled timber or wood fibre.

1.2.3.6 INTERPOL's role in enforcement

INTERPOL carries out law enforcement in relation to illegally traded timber through an international consortium named project LEAF (Law Enforcement Assistance for Forests). LEAF is led by INTERPOL in partnership with the United Nations program and United States, Department of State. INTERPOL's first large scale international action against illegal logging took place in the autumn of 2012 across South America. More than 200 people were arrested with over 50 m^3 of tropical timber,

(worth approximately 8 million US dollars) being seized. Improved intelligence sharing among agencies has enabled INTERPOL to support countries in bigger and more effective police operations, leading to larger seizures of illegal timber and wildlife products. Another operation by INTERPOL resulted in the seizure of US$40 million of tropical timber and wood products from Costa Rica and Venezuela. The development of wood authentication and provenance tools would be a significant boost to the law enforcement activities of INTERPOL and government agencies worldwide.

1.3 Elemental analysis methods used to determine the provenance of timber

1.3.1 Stable isotopes

1.3.1.1 Introduction to stable isotopes and stable isotope ratio mass spectrometry

Isotopes differ from each other due to the number of neutrons present in the nucleus, making differences in the mass of an element. For example, when ^{13}C is compared to ^{12}C, the difference in the atomic mass of the two isotopes contributes a small, but significant difference in the way an element (in this case carbon) behaves during biological, chemical and physical processes. Compounds in which there are more than one isotope species are called isotopologues. A typical example of an isotopologue exists in mixtures of 'light' ($^{12}C^{16}O_2$) and heavier carbon dioxide ($^{13}C^{16}O_2$). There are two categories of isotopes; stable and unstable. The majority of isotopes are classified as stable, with a minority classified unstable. This research will focus on the stable isotopes of carbon, hydrogen and oxygen. A list of elements and respective stable isotopes is shown in Table 1.4.

Table 1.4 Relative abundance of the isotopes most commonly determined using IRMS. Adapted from Meier-Augenstein (2010).

Element	Isotope	Relative abundance (%)
Hydrogen (H)	^{1}H	99.984
	^{2}H	0.0156
Carbon (C)	^{12}C	98.892
	^{13}C	1.108
Nitrogen (N)	^{14}N	99.635
	^{15}N	0.365
Oxygen (O)	^{16}O	99.759
	^{17}O	0.037
	^{18}O	0.204
Sulfur (S)	^{32}S	95.02
	^{34}S	4.22

1.3.1.1.1 Stable isotope notation

Stable isotope compositions are expressed as a ratio of heavy to light concentrations of the isotopes under consideration, and are measured relative to certified standards issued by official bodies such as the International Atomic Energy Agency (IAEA), and the United States Geological Survey (USGS). The δ value for a sample is calculated using the following equation (1.1):

$$\delta^{13}C_{Sample} = \left\{ \frac{\left(\frac{^{13}C}{^{12}C}\right)_{Sample}}{\left(\frac{^{13}C}{^{12}C}\right)_{Reference}} - 1 \right\} * 1000 \qquad (1.1)$$

Stable isotope ratios are defined relative to an agreed international scale and expressed as the ratio of the heavy to light isotope. They are reported as a delta value (δ), and measured in units of per mil (‰ or parts per thousand) in order to express the subtle differences occurring to isotope ratios at natural abundance levels. Equation 1.1 shows an example of calculating δ for ^{13}C. In the case of carbon isotopes, the VPDB (Vienna Pee Dee Belemnite) scale is applied. For stable isotopes of hydrogen and oxygen, the VSMOW (Vienna Standard Mean Ocean Water) scale is used. In order to standardise isotopic measurements and reduce inter laboratory variation, the application of VPDB and IAEA scales was agreed by the IAEA (Coplen *et al*., 2006).

1.3.1.1.2 Stable isotope standards

Following the preparation, distribution, and calibration by a number of worldwide specialised isotope laboratories, the IAEA was able to issue a number of certified reference materials for use in isotopic analyses. Table 1.5 shows a list of isotopic reference materials issued by the IAEA.

Table 1.5 List of certified reference materials issued by the IAEA, Vienna, Austria. Adapted from Meier-Augenstein (2010).

International reference material	Code	$\delta^{13}C_{VPDB}$ (‰)[a]	$\delta^{15}N_{AIR}$ (‰)	$\delta^{2}H_{VSMOW}$ (‰)	$\delta^{18}O_{VSMOW}$ (‰)
TS-limestone	NBS-19	1.95			-2.2
Lithium carbonate	LSVEC	-46.6			-26.6
Oil	NBS-22	-30.031		-118.5	
Sucrose	IAEA-CH-6	-10.449			
Polyethylene foil	IAEA-CH-7	-32.151		-100.3	
Wood	IAEA-C4	-24			
Wood	IAEA-C5	-25.5			
Wood	IAEA-C9	-23.9			
Sucrose	IAEA-C6	-10.8			
Oxalic acid	IAEA-C7	-14.5			
Oxalic acid	IAEA-C8	-18.3			
Caffeine	IAEA-600	-27.771	(+1.0)a		
Cellulose	IAEA-CH-3	-24.724			
Water	VSMOW			0	0
Water	GISP			-189.5	-24.8
Water	SLAP			-428	-55.5
Benzoic acid	IAEA-601				23.3
Benzoic acid	IAEA-602				71.4

(a)This $\delta^{15}N$ value is based on data from one laboratory only.

1.3.1.2 Isotope effects

The term isotope effect refers to the variation in atomic mass of a chemical element due to physical and chemical differences. Isotope fractionation is dependent upon the equilibria of thermodynamic and kinetic processes to which a given element is subjected. Although isotopes behave in a similar manner, they differ in the quantities of energy required to make them undergo identical reactions, such as physical changes where destruction and formation of chemical bonds occur (Kelly, 2003)

1.3.1.2.1 Equilibrium fractionation

Equilibrium fractionation occurs during the conversion of one physical phase to another, and in a number of very different physiochemical processes. In closed systems, or where the reaction is

allowed to reach completion, no net fractionation occurs between the substrate and its product, meaning that only changes in the isotope distribution occur between different phases, substances, or individual molecules (Hoefs, 2009). During equilibrium processes, the forward and reverse reactions proceed at the same rate. The precipitation of calcium carbonate from water can be described as an equilibrium process, during which the calcium carbonate containing heavier ^{18}O atoms drops out of solution in preference to carbonate containing ^{16}O atoms.

The degree of isotope fractionation is expressed as an equilibrium constant (*K*) but can also be expressed as the fractionation factor (α). The equilibrium fractionation of ^{16}O and ^{18}O between calcium carbonate and water is given in the following in equation (1.2):

$$H_2{}^{18}O + \frac{1}{3}CaC^{16}O_3 \rightleftharpoons H_2{}^{16}O + \frac{1}{3}CaC^{18}O_3 \qquad (1.2)$$

The fractionation factor corresponding to the above exchange reaction can be defined in the following equation (1.3):

$$\alpha = \frac{\left(\frac{^{18}O}{^{16}O}\right)_{CaCO_3}}{\left(\frac{^{18}O}{^{16}O}\right)_{H_2O}} \qquad (1.3)$$

1.3.1.2.2 Kinetic fractionation

Kinetic isotope fractionation occurs in mass dependant reactions such as in biological systems. Kinetic isotope effects are mostly the result of enzymes discriminating against isotopes, resulting in a difference between the isotopic composition of the substrate and resulting product. The effect tends to be associated with incomplete and irreversible processes such as evaporation, dissociation reactions, biologically mediated reactions and diffusion. Quantum effects mean that less energy is required to break the bonds in a light isotope than those involving heavier isotopes (Hoefs, 2009). Bond cleavage in $^{12}C^{16}O_2$ has slightly lower activation energy than in $^{13}C^{16}O_2$. For example, in plant metabolism, ^{12}C and ^{13}C in CO_2 is first fixed by RUBISCO (ribulose-1, 5-bisphosphate carboxylase/oxygenase). The process leads to ^{12}C becoming enriched in the plant, whereas the ^{13}C heavier isotope is discriminated

against and becomes depleted. This has an overall effect of modifying the $\delta^{13}C$ value from that of the atmospheric CO_2 introduced through the plant leaf stomata, approx. -8 ‰ , typically to within the range -22 to -30 ‰ in the cellulose of C3 plant tissues (Farquar, 1984). Another example of a kinetic effect occurs with evaporation of water. In an open system containing liquid phase water with equivalent concentrations of deuterium and hydrogen, evaporative processes will lead to an enrichment of $^{1}H_{2}{}^{16}O$ and a depletion of $^{2}H_{2}{}^{18}O$ in the vapour phase, while a proportional enrichment of $^{2}H_{2}{}^{18}O$ / depletion of $^{1}H_{2}{}^{16}O$ occurs in the liquid phase. Hydrogen typically undergoes the greatest degree of fractionation due to the mass difference of its element and corresponding isotope. Irreversible chemical reactions have a tendency for products of reaction to become enriched with lighter isotopes. This is largely governed by the laws of quantum theory where molecules undergo a restriction to a certain energy level. The zero point energy is above the curve minima and is equivalent to ½ *hv*, where *h* is Planck's constant and *v* is the frequency with which the atoms in the molecule vibrate with respect to each other (Hoefs, 2009). Therefore, zero point energies vary for the molecules with the same chemical formula but differing isotope species. The corresponding heavy isotope of a given element (for example; ^{13}C compared to ^{12}C) has a lower vibrational frequency of its chemical bonds, while the opposite can be said for the lighter parent element.

Fig. 1.19 shows the potential energy curve for the interaction of two atoms, E_L and E_H referring to the energy intervals between the continuous and zero-point energy levels for the light isotopic and heavy isotopic species respectively.

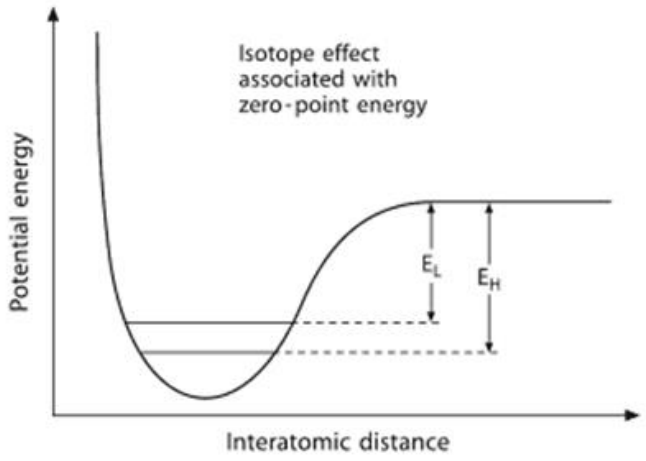

Fig. 1.19 Potential energy curve for the interaction of two atoms in a liquid or solid state. Adapted from Hoefs (2009).

1.3.1.3 Applications of carbon, oxygen and hydrogen stable isotope ratio analysis

The analysis of carbon, oxygen and hydrogen isotopes has been applied in a wide range of disciplines, such as animal migration studies, ecology, healthcare, forensic investigations, paleoclimatic reconstruction, and product authenticity. Although the analysis of single isotope species can answer a great deal of questions relating to authenticity, isotopic analysis of multiple species can reveal further information enabling the application of multivariate statistics. Hydrogen and oxygen isotopes vary with geographical location (Dansgaard, 1964; Boner, 2004), hence they are a popular choice of analysts seeking to answer questions of authenticity and traceability. Of particular relevance to this study is the use of isotopic analysis as a tool to answering questions of provenance. Horacek *at al.* (2009) showed that carbon and oxygen isotope ratio analysis of bulk timber was sufficient to differentiate samples of Siberian and Austrian larch wood. The study demonstrated the possibility of analysing whole (bulk) wood without the need for further purification of samples. However, to demonstrate the simplicity of the method, the study depends heavily upon a latitude separation of 6000 km between the sampling sites. The analysis of only carbon and oxygen isotopes, and relying only on the bulk timber for measurement, means that samples originating from locations separated by lesser distances of latitude may result in a reduced level of discrimination between sampling sites. Nor

does the analysis allow for the same technique to be applied to other tree species where the timber ratio of components cellulose/lignin may differ from larch. Kagawa & Leaveritt (2010) examined the possibility of applying the relatively new technique of isotope 'dendroprovenancing' to aid accurate origin determination of pinyon pine samples from the western United States. The study utilised the occurrence of high frequency variations of carbon isotope ratios from tree ring width series in order to establish a unique isotopic fingerprint that reflects the climatic history of its origin. The research demonstrated a high degree of accuracy for determining the origin of timber, but to be of use for purposes of enforcement, studies require large reference libraries, and extensive measurements of the individual tree ring width series of individual timber cores. Kepler *et al*. (2007) developed a method using compound specific GC-IRMS to analyse hydrogen isotope ratios in lignin methoxyl groups of wood. The method sought to overcome the problem associated with conventional measurements where exchangeable hydrogen has to be eliminated through nitration, or accounted for through equilibration techniques. Instead, the study focused on analysing the non-exchangeable carbon bound hydrogen of the lignin component in wood. The results of the analysis demonstrated a high degree of correlation when compared with the meteoric water line from the Online Isotopes in Precipitation Calculator (OIPC), (Bowen *et al*., 2003).

1.3.1.3.1 Carbon isotopes

Plants utilise atmospheric carbon dioxide during the process of photosynthesis, and depending upon the species, fractionation of ^{13}C in CO_2 is carried out to a greater or lesser extent. The majority of the earth's higher order plants, totalling more than 85% of planetary biomass, utilise the Calvin cycle (C3 pathway) for carbon fixation. The remainder use either the C4 or crassulacean acid metabolism (CAM) pathways. The terms C3 and C4 are defined by the number of carbon molecules present in the carboxylation reaction. In timber, CO_2 leads to the formation of 3-phosphoglycerate (3-PGA), hence plants using the 3-PGA pathway are commonly known as C3 plants (Meier-Augenstein, 2010). As previously shown in Table 1.4, carbon has two naturally occurring stable isotopes: ^{12}C with an abundance of 98.89%, and ^{13}C with an abundance of 1.108%. The ratio of the heavy and light isotope can be determined by isotope ratio mass spectrometry (IRMS) which can reveal information about

fractionation processes. Reported applications of the use of carbon stable isotopes are wide and varied, and a significant number of authors have applied carbon stable isotopes in food authenticity investigations:

Rhodes *et al.* (2010) used $^{13}C/^{12}C$ stable isotopes to identify the feeding regime of chicken labelled as corn fed. Corn is a C4 plant, thus chickens fed only a C4 diet are detectable by analysis of $^{13}C/^{12}C$ isotope ratios laid down in muscle protein. Adulteration of wine by the process of chaptalisation is known to involve the addition of cane sugar (C4) as a way of increasing alcoholic yield during fermentation. Roßmann *et al*. (1996) analysed $^{13}C/^{12}C$ ratios of distilled alcohol from wine providing a methodology for the detection of wine adulteration with cane sugar, the carbon isotope ratios of the cane sugar imparting distinct $^{13}C/^{12}C$ ratios in ethanol when compared to the carbon isotope ratios of ethanol derived solely from the grape (C3) sugars. Types of vinegar such as balsamic and wine vinegar are classified as protected geographical origin products (PGO), and therefore command a premium price when compared to cheaper non PGO vinegars, hence the potential for fraudulent mislabelling is significant. Thomas & Jamin (2009) studied vinegar authenticity by analysis of $^{13}C/^{12}C$ ratios of acetic acid. The study was able to characterise the botanical source of acetic acid as well as detect adulteration of vinegar with synthetic acetic acid. Jamin *et al*. (1997) also investigated wine and fruit juice authenticity using similar techniques to detect adulteration with cane and beet sugar. Furthermore, ecological studies such as those carried out by Mizutani *et al*. (1990); Hobson (1990) and Bearhop (2003), used $^{13}C/^{12}C$ stable isotopes to determine the feeding areas of sea birds. With regards to plants and trees, O'Leary (1981) and Farquar & Sharkey (1982), studied carbon isotope fractionation to understand metabolic processes in plants. Kiyosu and Kidoguchi (2000), carried out a study of city centre pollution analysing ^{13}C isotopes in the leaves of roadside trees, Kagawa *et al*. (2008); Kagawa & Leavitt, (2010) and Horacek *et al*. (2009), analysed $^{13}C/^{12}C$ stable isotopes as part of their research into timber origin, demonstrating that these isotopes were able to differentiate country of origin, sometimes alone, or when included in a multivariate analysis involving variables such as $^{18}O/^{16}O$ isotopes or ring width chronologies.

1.3.1.3.1.1 Carbon dioxide fixation in plants

Typical bulk natural abundance values for $\delta^{13}C$ in C3 plants range from -22 to -30 ‰, and for C4 plants, (such as cane sugar and tropical grasses) from -10 to -15 ‰. Fractionation in these metabolic pathways depends upon diffusion, dissolution and carboxylation processes (Kelly *et al*., 2002). Diffusion processes are largely governed by the rate of stomatal conductance (through leaf-air vapour pressure) between intercellular and atmospheric CO_2, controlling assimilation of carbon into the plant, influencing the plants water usage efficiency (Dawson *et al*., 2002). Plants relying upon the Calvin cycle are known to be inefficient with their water usage, and struggle to fix carbon under conditions of drought and water stress. Because of this, C3 plants tend to thrive in temperate areas of the earth where water is plentiful. On the other hand, C4 plants have adapted their biochemistry to survive in arid conditions and extremes of temperature, enabling their survival in areas of prolonged drought and sunlight intensity. Fig. 1.20 shows the typical ranges for $\delta^{13}C$ of C3 plants with respect to C4 plants and other carbon sources (Winkler, 1984).

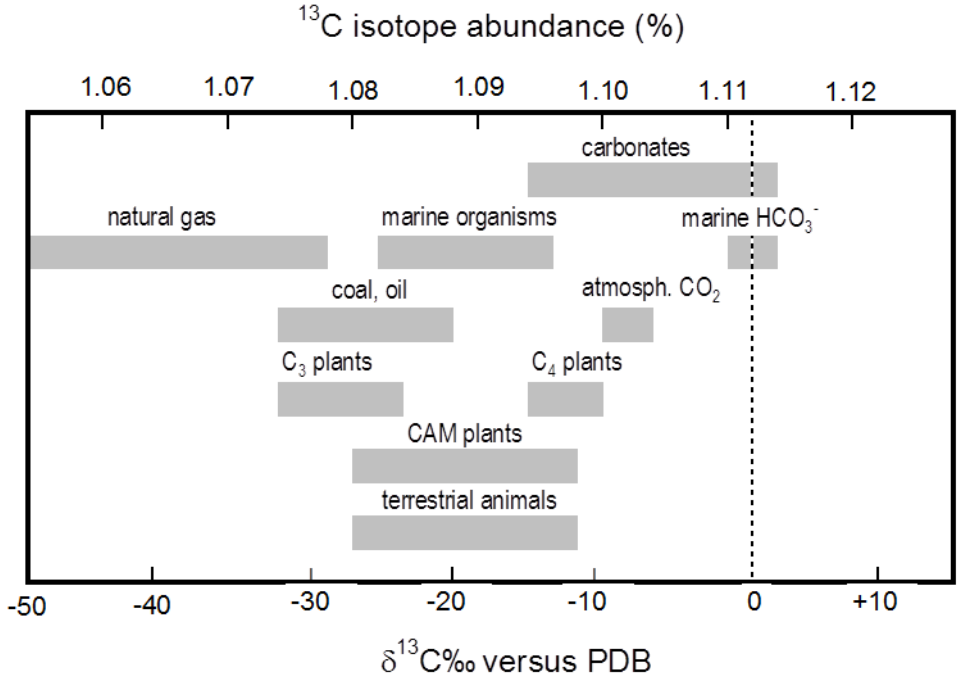

Fig. 1.20 Variation of $\delta^{13}C$ isotope in carbon sources. Adapted from Winkler, 1984.

The Calvin cycle (Fig. 1.21) is also known as dark reaction, named so because it is light independent. The cycle occurs in the chloroplast stroma, where ATP and NADPH fix atmospheric CO_2 into carbon skeletons which go on to be used in the biosynthesis of starch and sucrose (Woodrow & Berry, 1988; Geiger & Servaites, 1995; Quick & Neuhaus, 1997). The cycle comprises of 11 different enzymes, governing 13 different reactions, initiated by the enzyme ribulose-1,5-bisphosphate carboxylase oxygenase (RUBISCO) which catalyses the carboxylation of the CO_2 accepter molecule, ribulose-1,5-bisphosphate (RuBP). 3-phosphoglycerate (3-PGA) then undergoes a reaction forming triose phosphates, dihydroxyacetone phosphate (DHAP), and glyceraldehyde phosphate (G-3-P). The cycle also supplies a range of other metabolic processes in the chloroplast, including the shikimate pathway used for synthesis of amino acids and lignin (Raines *et al*., 2003).

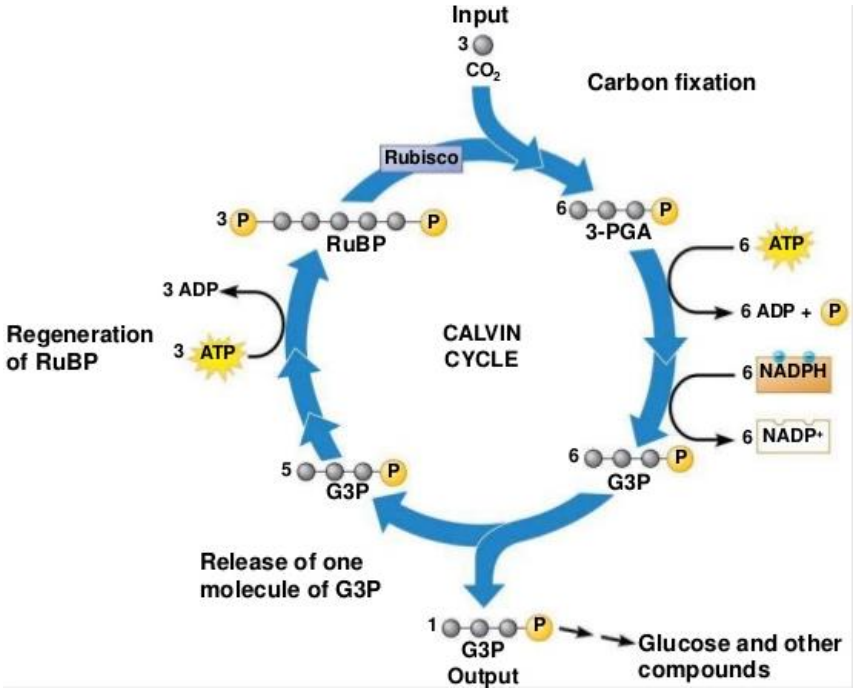

Fig. 1.21 Diagram showing a representation of the Calvin cycle, adapted to illustrate the formation of one glucose molecule. Taken from http://imgbuddy.com/calvin-cycle-diagram-mastering-biology.asp

In order to preserve moisture under conditions of water stress, C3 plants will close their leaf stomata (Fig. 1.22), limiting the proportion of CO_2 which can be absorbed. This has the consequence of decreasing the concentration of CO_2 in the plant leaves, reducing the proportion of CO_2 taking part in the carboxylation reaction of the enzyme RUBISCO. When a plant has insufficient CO_2, photosynthesis is inhibited and a cellular switch to photorespiration is made. The shape of the active site of the RUBISCO molecule means it is unable to discriminate O_2 from CO_2, and if the vascular concentration of CO_2 falls below a critical level, RUBISCO will preferentially absorb O_2, resulting in a net loss of carbon from the plant, stunting growth and eventually leading to death.

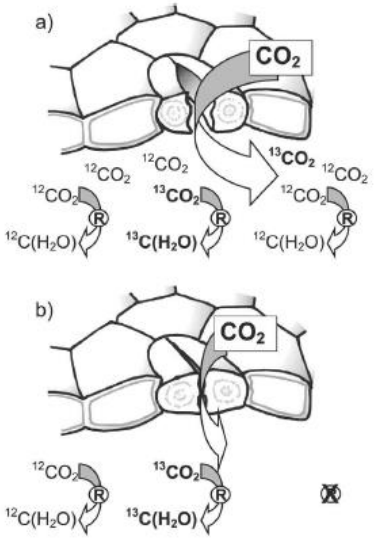

Fig. 1.22 Simplified schematic of the relationship between carbon isotope composition ($\delta^{13}C$) and stomatal conductance; (a) high stomatal conductance, low discrimination; and (b) low stomatal conductance, high discrimination. Taken from Ferrio *et al*. (2003).

Plants which utilise the C3 metabolic pathway therefore tend to be depleted in the ^{13}C when compared to C4 plants. Carbon isotope fractionation in plants has been shown to correlate with temperature. Sunlight intensity is often related to temperature, and assuming the water availability and atmospheric pressure remain constant, an isotopic gradient correlated temperature can be observed (Vogel, 1978; Francey *et al*., 1985; Berry *et al*., 1997).

1.3.1.3.2 Hydrogen and oxygen isotopes

Hydrogen and oxygen isotopes of alpha-cellulose largely reflect meteoric source water inputs, which in turn are influenced by isotope fractionation associated with transpiration and biological processes (Yapp & Epstein, 1982; Switsur & Waterhouse, 1998). Carbon isotopes of cellulose are shown to correlate with temperature, light intensity, water stress, and the isotopic composition of CO_2 assimilated during photosynthesis (Paweczyk & Pazdur, 2008).

1.3.1.3.2.1 Hydrogen

Hydrogen has two naturally occurring stable isotopes: ^{1}H and ^{2}H, each with a relative abundance of 99.984% and 0.0156% respectively. Hydrogen isotopes have a large mass difference. Therefore, fractionation leads to very distinct isotope ratios for this element. The distribution of ^{2}H stable isotopes in nature is shown in Fig. 1.23 (Winkler, 1984).

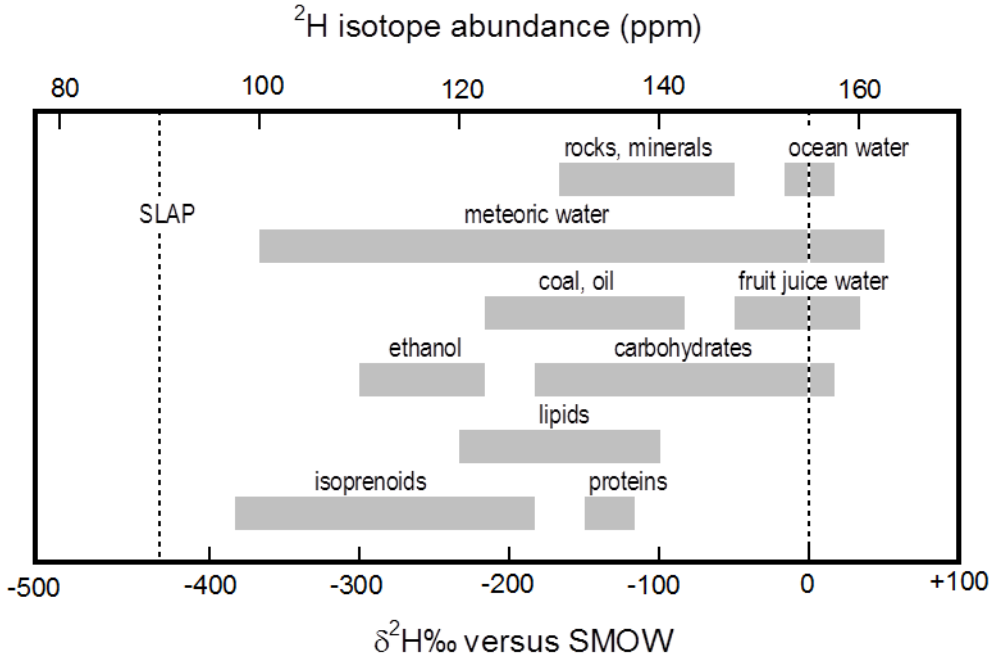

Fig. 1.23 Variation of $\delta^{2}H$ isotope in hydrogen sources. Adapted from Winkler, 1984.

1.3.1.3.2.2 Oxygen

Oxygen has three naturally occurring stable isotopes: ^{16}O, ^{17}O and ^{18}O, with relative abundances of 99.76%, 0.04% and 0.20% respectively. For the purposes of authentication and measurement by IRMS, and due to its low abundance, the isotope ^{17}O is rarely quantified. Instead, many analysts favour determination of the more abundant $^{16}O/^{18}O$ species. The determination of the ratios of the heavy and light isotopes of hydrogen and oxygen offers the potential to reveal information about fractionation processes. The distribution of ^{18}O stable isotopes in nature is shown in Fig. 1.24 (Winkler, 1984).

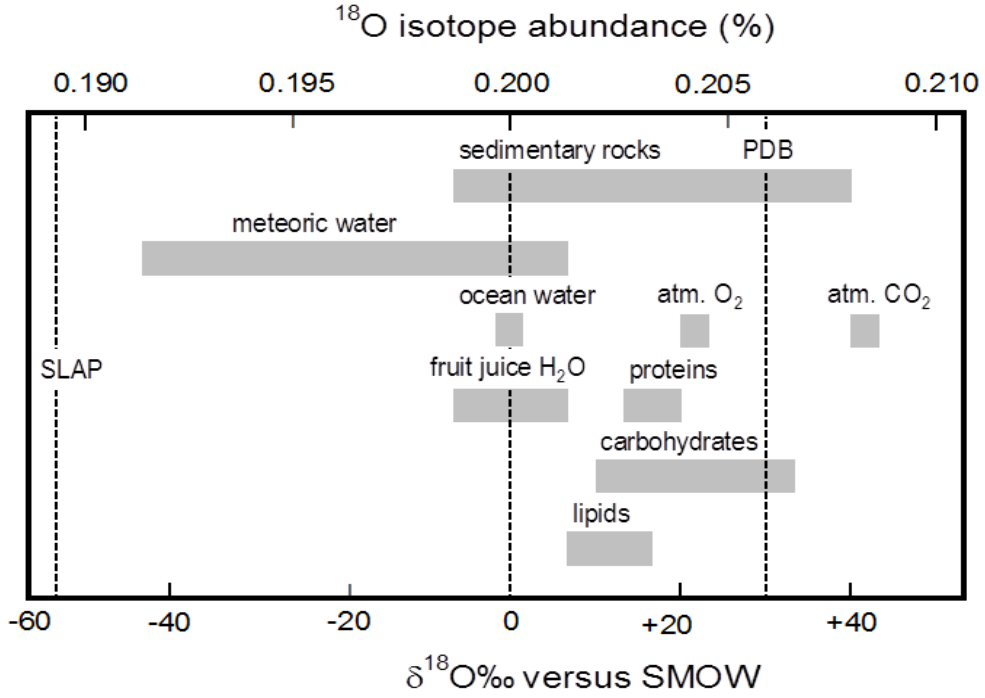

Fig. 1.24 $\delta\ ^{18}O$ isotope ranges of oxygen pools. Adapted from Winkler (1984).

1.3.1.3.2.3 Hydrogen and oxygen isotope fractionation

The isotopic variation of hydrogen and oxygen in global precipitation is heavily influenced by the Rayleigh type processes involving evaporation, condensation and precipitation. Oceans account for 96.5% of the hydrosphere, the starting point for the hydrological cycle, as water moves between the lithosphere, atmosphere, biosphere and back to the hydrosphere (Meier-Augenstein, 2010).

The influence of temperature upon the hydrological cycle results in water sampled from the tropics and North Sea posessing distinct ^{2}H and ^{18}O isotope signatures. Furthermore, latitude, altitude and distance to open seas all have an influence on the degree of ^{2}H and ^{18}O isotope fractionation. Fresh water ranges from +20 to –230‰ across the world, the positive ^{2}H and ^{18}O values typical of coastal/low latitude regions and more negative ^{2}H and ^{18}O values typical of inland/high altitude/high latitude regions (Meier-Augenstein, 2010). Fig 1.25 shows the global variation of ^{2}H in precipitation, the distribution largely mirrored by ^{18}O due to both ^{2}H and ^{18}O of precipitation undergoing the same fractionation processes.

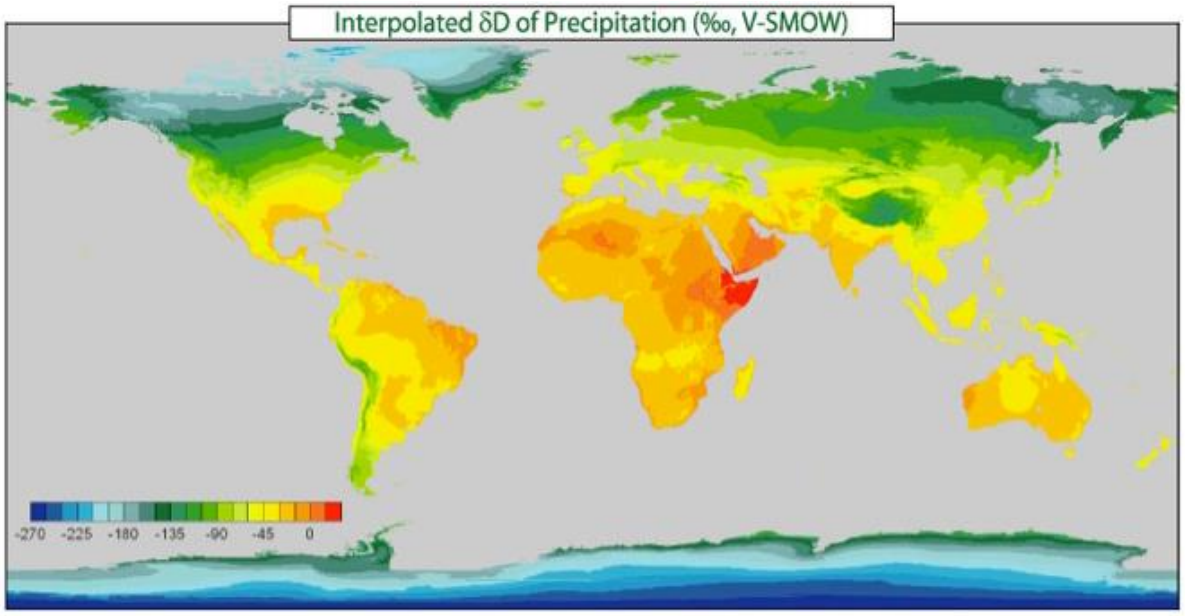

Fig. 1.25 Global variation of $\delta^{2}H$ in precipitation. Taken from: http://www.animalmigration.org/stable_isotopes/index.htm

In Fig. 1.26 the clouds are observed to follow an isotope gradient, becoming depleted in ^{2}H and ^{18}O as they move further inland from the sea. The initial phase of the loss of the heavier isotopes ^{2}H and ^{18}O from the clouds is known as “rainout effect”. The initial liquid phase of rain is enriched in ^{18}O and ^{2}H compared to the later precipitation. Similarly, the centre of a large land mass or continent has precipitation that is depleted in ^{18}O and ^{2}H, a phenomenon known as the "continental effect."

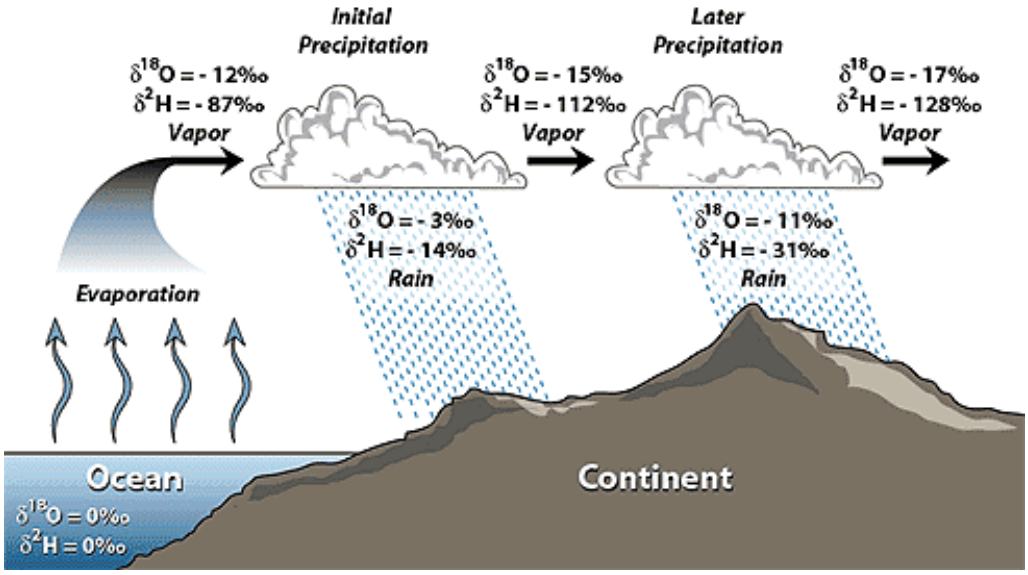

Fig. 1.26 Fractionation of δ^2H and $\delta^{18}O$ isotopes during evaporation and precipitation processes. Taken from Coplen *et al*., (2000). Available at https://iso-net.atlassian.net/wiki/display/IA/Water

1.3.1.3.3 The global meteoric water line

The relationship between $\delta\,^2H$ and $\delta\,^{18}O$ isotopes in global precipitation was first established by Craig (1961). Using data collected from IAEA weather stations across the world, he arrived at the following equation which describes the relationship, also known as the global meteoric water line (GMWL) shown in equation (1.4):

$$\delta^2H = 8\,\delta^{18}O + 10 \qquad (1.4)$$

The high degree of correlation is a consequence of ^2H and ^{18}O undergoing similar Rayleigh meteorological fractionation effects. Fig. 1.27 shows ^2H and ^{18}O measured in precipitation, with warm and cold regions of the earth at opposite ends of the global meteoric waterline.

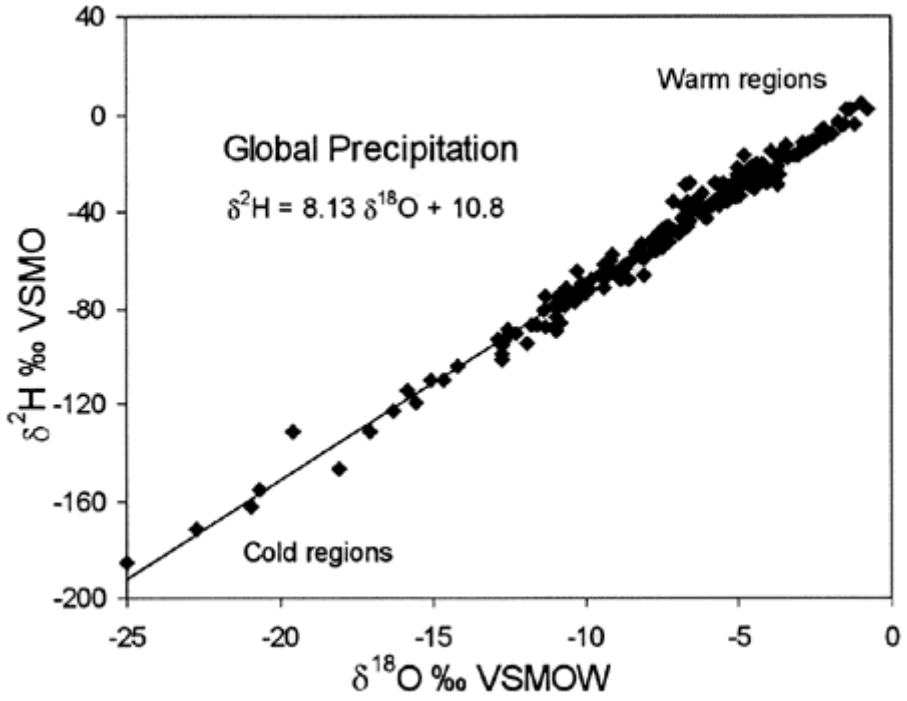

Fig. 1.27 Global meteoric water line. Taken from Clark and Fritz (1997). Available at http://web.sahra.arizona.edu/programs/isotopes/oxygen.html

Area specific meteoric water lines such as arid countries will exhibit the same slope as above, but increased evaporation means the slope will deviate more positively in relation to δ^2H because of increased evaporation in these areas. Furthermore, humid environments maintain the MWL slope of 8, but the line shifts towards toward increased $\delta^{18}O$ because the phase change tends toward liquid precipitation (Hoefs, 2009; Coplen *et al.*, 2000).

1.3.1.3.4 Hydrogen and oxygen fractionation in plants

Terrestrial plants have been shown not to fractionate ^2H and ^{18}O during root uptake and transport through the primary and secondary xylems, making the hydrogen and oxygen isotopic composition of the water absorbed by trees a predominant factor influencing the hydrogen and oxygen isotopic composition of tree cellulose (Fig. 1.28) (Dawson & Ehleringer, 1993). However, fractionation has been shown to occur within the leaf tissue of plants and trees, as ^2H and ^{18}O in leaf water exchanges with ^2H and ^{18}O of glucose during synthesis, the fractionation largely a consequence of leaf

evapotranspiration effects governed by temperature, humidity and water use efficiency (Kahmen *et al.*, 2011; Farquhar & Richards, 1984).

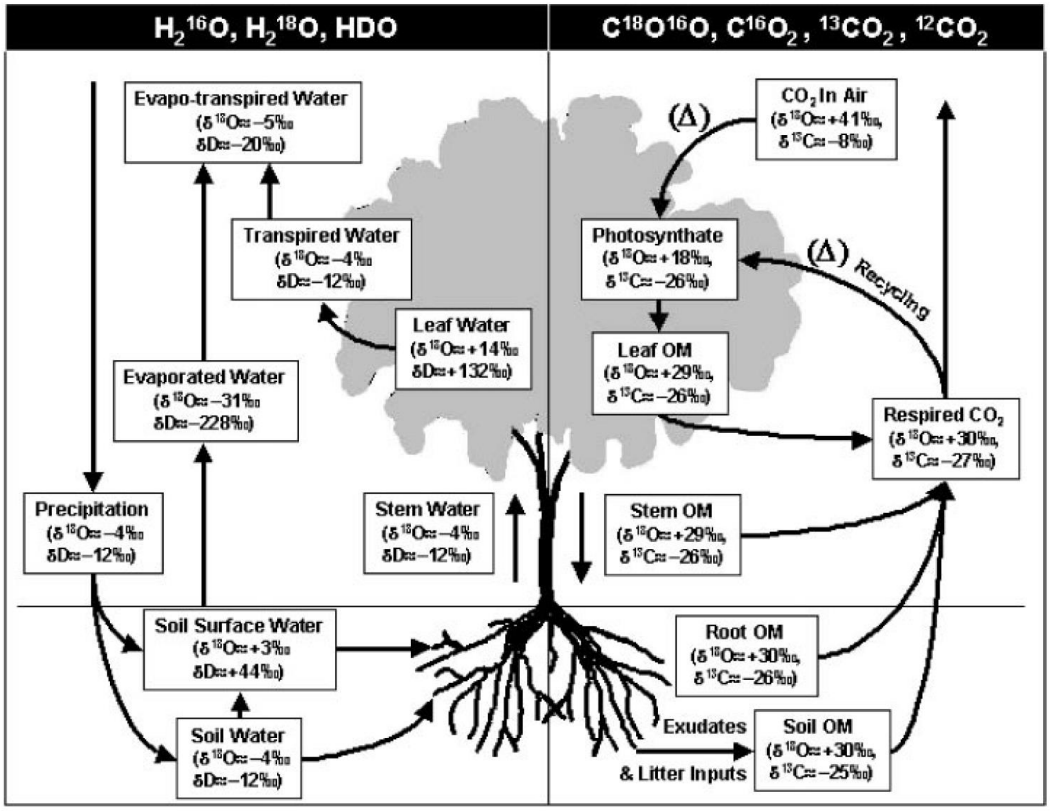

Fig. 1.28 Isotopic composition of C, O and H pools in the terrestrial carbon and water cycles. Taken from Dawson *et al*. (2002).

1.4 Analysis techniques

1.4.1 Principles of isotope ratio mass spectrometry (IRMS)

The subtle differences between the isotopic species of a given element require a very accurate means of quantification. IRMS instrumentation meets this challenge as it employs specialised static magnetic sector fields as well as Faraday cups for the simultaneous quantification of multiple isotope species. Most modern IRMS systems are based on a design by Nier (1940) who set the bench mark for measurement precision and reliability of operation. The Nier type IRMS (Fig. 1.29) has three basic components consisting of an ion source, mass analyser and ion detector or collector.

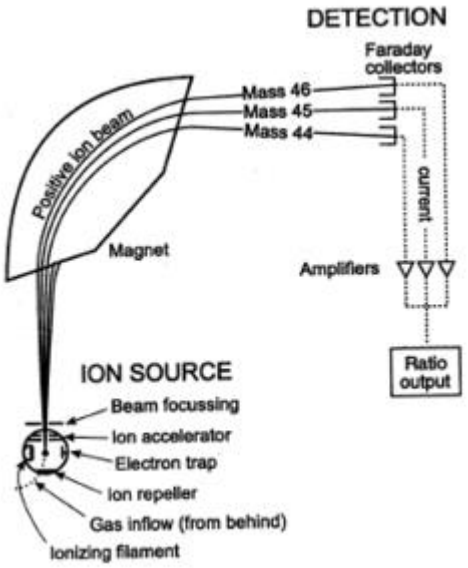

Fig. 1.29 Schematic of an isotope ratio mass spectrometer. Taken from http://ph12dt2-lestorjacksontimothy.wikispaces.com/Electromagnetism+Part+II

The IRMS relies upon sample gas species arriving in an inert stream of helium which are introduced to the IRMS source through a narrow capillary. In order to produce the gas species for determination, the sample in question must first undergo quantitative conversion into H_2, N_2, CO, CO_2 and SO_2. This is achieved through a variety of IRMS interfaces which have been designed to allow measurements of different sample phases (Kelly & Lees, 2003). Elemental analysis (EA-IRMS) is typically used to convert liquid or solid samples into the aforementioned gas species. Furthermore, GC or LC-IRMS can be applied for compound specific analysis of mixtures (Gremaud & Hilkert, 2008).

The sample gases reach the source once they pass through the narrow capillary. It is here where they undergo bombardment by a stream of electrons generated by thoria coated tungsten filament, the gas molecules undergoing ionisation. The interaction of the energetic electrons and the gas molecule generally results in an electron being removed from the valence orbital of the gas molecule, shown in equation (1.5):

$$M \xrightarrow{e^-} M^+ + 2e^- \qquad (1.5)$$

The resulting positively charged ion may result in bond dissociation (also termed fragmentation or cracking). A typical example of fragmentation occurs when CO_2 is ionised to CO, thus causing a

problem for N_2 analysis because of the similarity in masses (Kelly, 2003). Inside the mass spectrometer charged atoms are separated according to their mass to charge ratio ($^m/_z$). The mass to charge ratio is the common form of notation used to define dimensionless quantity derived by dividing the mass number (m) of an ion by its charge (z). During this process, positively charged ions are accelerated and collimated by a series of electrode lenses to which variable potentials may be applied. As the ions pass the magnet, the magnetic field deflects ions into circular trajectories, heavier isotopolgues undergoing less deflection than their lighter corresponding isotopes. The resolved beams then continue along the flight tube until they collide with the Faraday collectors. The resulting electron current that is produced upon impact allows for an accurate measure of the charge of a particular ion beam. The resulting voltages are amplified to enable conversation into a digital signal for interpretation by the IRMS software (Kelly, 2003).

1.4.2 Bulk stable isotope analysis

Bulk stable isotope analysis is carried out using an elemental analyser (EA) and is the most widely used approach for converting bulk samples into gases suitable for measurement by IRMS. Samples are first weighed or dispensed into silver or tin capsules which are sealed before introduction into the EA via an auto-sampler. Depending on the gas species being quantified, samples undergo either flash combustion, or high temperature pyrolysis, gas conversion techniques.

1.4.2.1 Flash combustion elemental analysis

The sealed capsule is introduced to the EA by the auto-sampler where it is initially purged with helium to remove atmospheric gas contribution. The autosampler is then actuated by the computer software and the capsule introduced to the combustion reactor containing chromium oxide maintained at 1020°C. The sample undergoes combustion in an enriched stream of oxygen, resulting in a momentary elevated temperature of up to 1800°C, a noticeable flash visible through the auto-sampler viewing window (Gremaud & Hilkert, 2008). The combustion gases CO_2 and NO_x are carried in a stream of helium and pass through a copper reducing furnace, maintained at 650°C, where oxides of nitrogen are reduced to N_2. A magnesium perchlorate water trap ensures residual moisture generated

from the combustion process is removed and does not interfere with the measurement acquisition. In order to accurately quantify the gas species in the IRMS, CO_2 and N_2 are resolved fully using a gas chromatography column maintained at 35°C before quantitative introduction to the IRMS via a stream of helium through the open split.

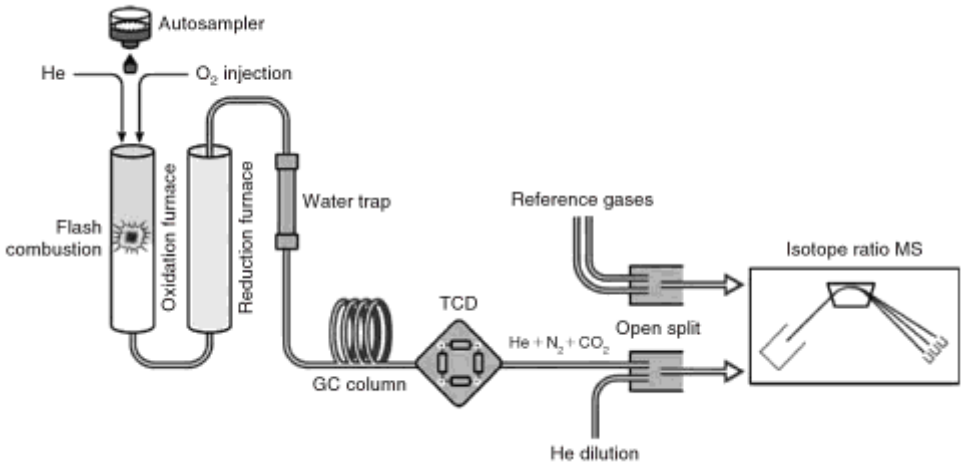

Fig. 1.30 Configuration of the elemental analyser IRMS system in flash combustion mode. Taken from Gremaud & Hilkert (2008).

The technique of flash combustion is typically used to measure isotope ratios of the gas species N_2, CO_2 and SO_2. It is not suitable for determining isotope ratios of the gas species H_2 and CO because of the contamination effects contributed from the use of excess oxygen and the formation of moisture from the combustion process.

1.4.2.2 High temperature pyrolysis elemental analysis

The sealed capsule is introduced to the EA by the auto-sampler where it is initially purged with helium to remove the contribution atmospheric gases. The auto sampler is actuated by the software and the capsule introduced to the pyrolysis tube containing glassy carbon chips and maintained at 1450°C. Once inside the pyrolysis tube, the sample undergoes thermal degradation in the absence of oxygen, resulting in the formation of pyrolysis gases H_2 and CO shown in Fig. 1.31 below. Depending upon the C:O elemental ratio of the sample, excess carbon may be deposited inside the glassy carbon tube.

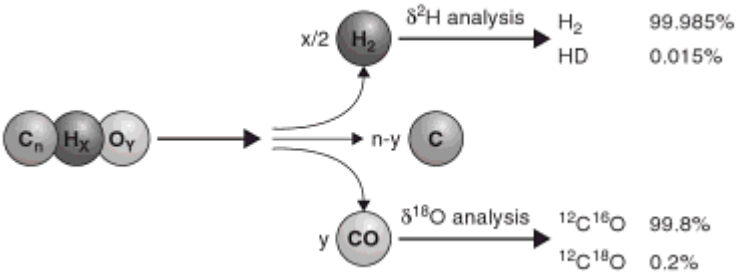

Fig. 1.31 High temperature conversion during pyrolysis. Adapted from Gremaud & Hilkert (2008).

The resulting pyrolysis gases are fully resolved using a molecular sieve column or CO trap (Elementar, Hanau, Germany) before quantitative transferred via the open split in a stream of helium to the IRMS for determination (Fig. 1.32).

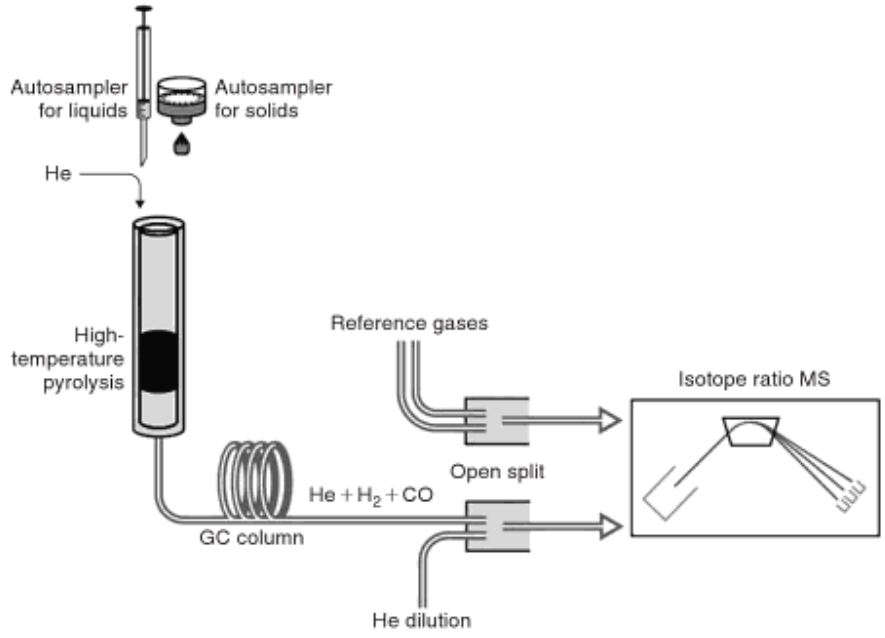

Fig. 1.32 Configuration of the elemental analyser IRMS system in high temperature pyrolysis mode. Taken from Gremaud & Hilkert (2008).

1.4.3 Measurement of trace elements

Preparation methods for a multi element analysis typically involve acid digestion taking place in open and closed systems (King & Barclay, 2003). Reflux systems in a beaker or using a laboratory hot plate are both types of open system (atmospheric pressure). Despite the long and inconvenient digestion times involved in open system acid digestions, the quality of the final sample has been not shown to be reliable following subsequent analysis (Soylak *et al*., 2004). Microwave acid digestion can be achieved in both open (atmospheric pressure) and closed systems (under pressure), and is mainly carried out by a fusion or a wet procedure based on an acid digestion with a heated mixture of mineral acids. In general, closed digestion systems are preferred, minimizing possible contamination of the digest, increasing reproducibility, and avoiding losses of volatile elements. Furthermore, they allow the acid digestion of many batches of samples to be carried out in a short space of time. Wet microwave digestion equipped with temperature and pressure control assisted by common mineral acids (such as nitric, sulphuric, perchloric and hydrochloric acids) is frequently used for sample digestion (Enamorado-Báez *et al*., 2013). A number of methodologies exist for the determination of trace element analysis, with inductively coupled plasma mass spectrometry (ICP-MS) used in the majority of applications in relation to food and nutritional studies or where determination of multi element composition is required (Stürup, 2004). The technique has come a long way since its development by Gray and Date (1983), and many of the elements of the periodic table can now be measured within detection limits below one part per billion (ppb). ICP-MS also has the advantage that it can be combined with an array of interfaces such as gas and liquid chromatography systems.

1.4.3.1 Microwave acid digestion

The use of an open vessel system allows for an even spread of radiation, but is disadvantaged by sample digestion times (Kou & Mitra, 2003). Increased sample capacity, throughput, and rapid digestion makes closed vessel microwave digestion the preferred choice for many analysts carrying out trace element analysis (Soylak *et al*., 2004). Closed vessel microwave systems typically employ a magnetron which generates radio waves (Fig. 1.33). The waveguide employs reflective materials

which direct microwaves generated by the magnetron, into the microwave cavity. Upon entering the cavity from the waveguide, the mode stirrer interrupts the flow of microwaves and creates an evenly distributed microwave field. Sample digestion vessels are also rotated ensuring they receive equal quantities of microwave energy (King& Barclay, 2003).

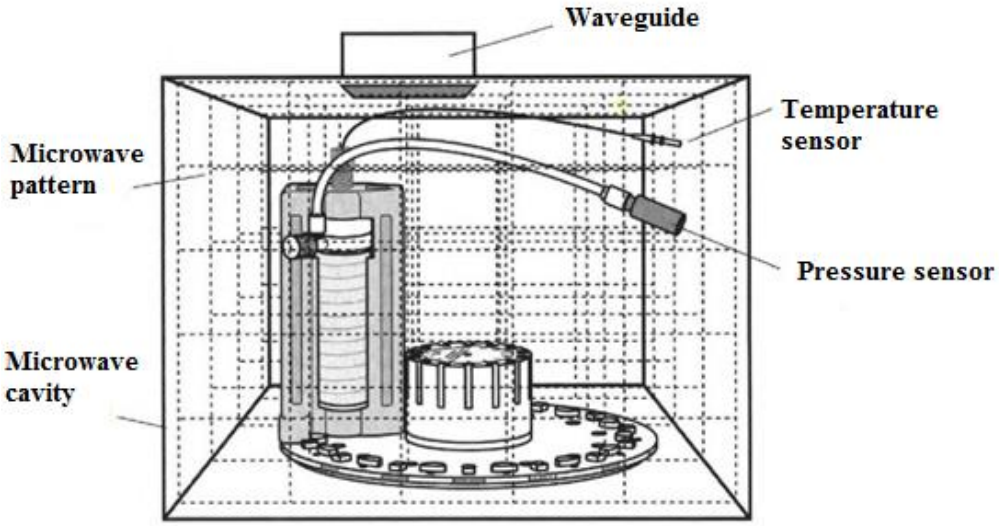

Fig. 1.33 Cavity type microwave digestion system. Taken from King & Barclay (2003).

Acid digestion illustrated in the closed system above involves several stages. Initially, microwave energy heats the acid through warming of the quartz vessel until the acid reaches it boiling point. The acid converts from liquid, into the gaseous phase and begins to condense on the cooler surfaces the quartz vessel. Sustained dynamic thermal non-equilibrium in the final stage of heating ensures the reaction temperature is maintained during digestion, the intensity of microwave energy governed by feedback sensors inside the microwave cavity. The use of microwave energy in a closed system enables sufficiently high temperatures to be achieved at lower pressures, enabling faster and efficient digestion processes compared to that of an open system (Kingston & Walter, 1997; King & Barclay, 2003).

1.4.3.2 Principles of inductively coupled plasma mass spectrometry (ICP-MS)

ICP-MS systems typically comprise an ion source, mass analyser and an ion detector as illustrated in Fig. 1.34.

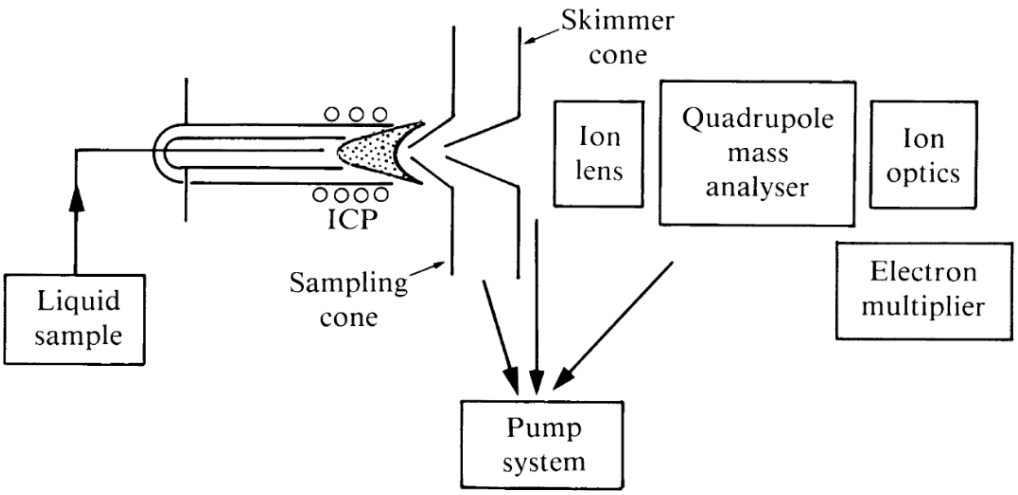

Fig. 1.34 Schematic of a typical ICP-MS system**.** Taken from O'Connor & Evans (1999).

Acid digested samples are introduced into the ICP-MS via a nebuliser which aspirates the liquid sample in combination with high velocity argon, resulting in a fine aerosol mist. The sample mist passes through a spray chamber, regulating the size of the droplets entering the plasma torch (Fig. 1.35). The argon ICP is mounted horizontally against sampling and skimmer cones and is generated by heating argon gas to over 6,000K (Fay & Kussmann, 2010). An intense radio frequency (rf) field ensures the temperature is maintained. A number of molecular processes (Fig. 1.36) occur upon the sample mist entering the argon torch; de-solvation separates solvent from the aerosol and residual particles of salt become vaporised. Dissociation and atomisation is followed by a small fraction super-heated plasma gas entering the ion lenses and skimmer cones before undergoing acceleration into the mass analyser and detection using electron multipliers (Dass, 2007).

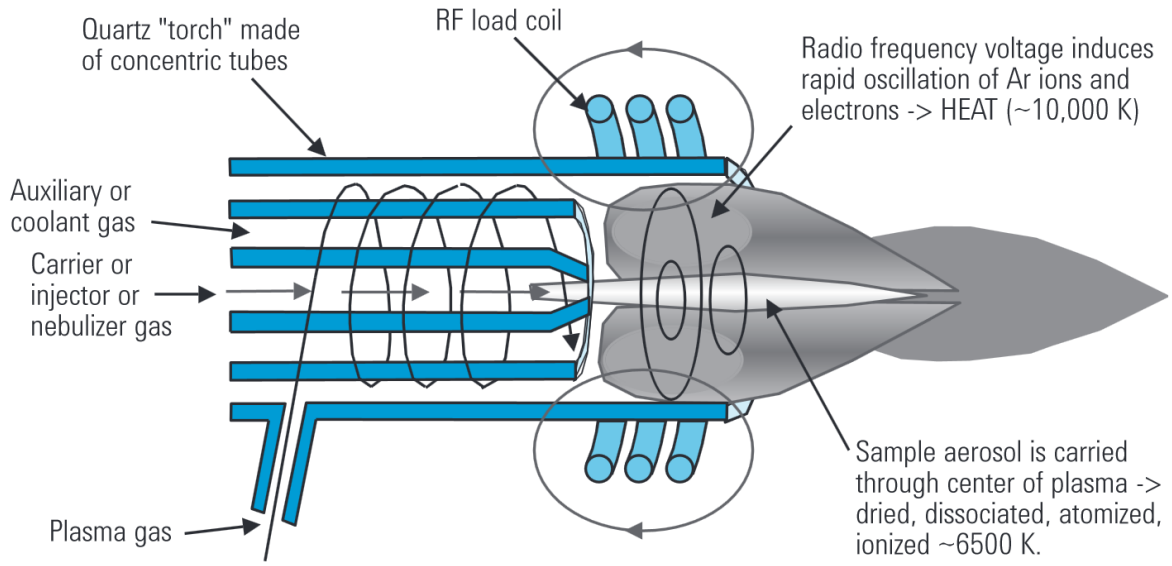

Fig. 1.35 ICP-MS plasma torch based on the Fassel design. Taken from: http://www.agilenticpms.com/primer/ICP-MS Primer.pdf

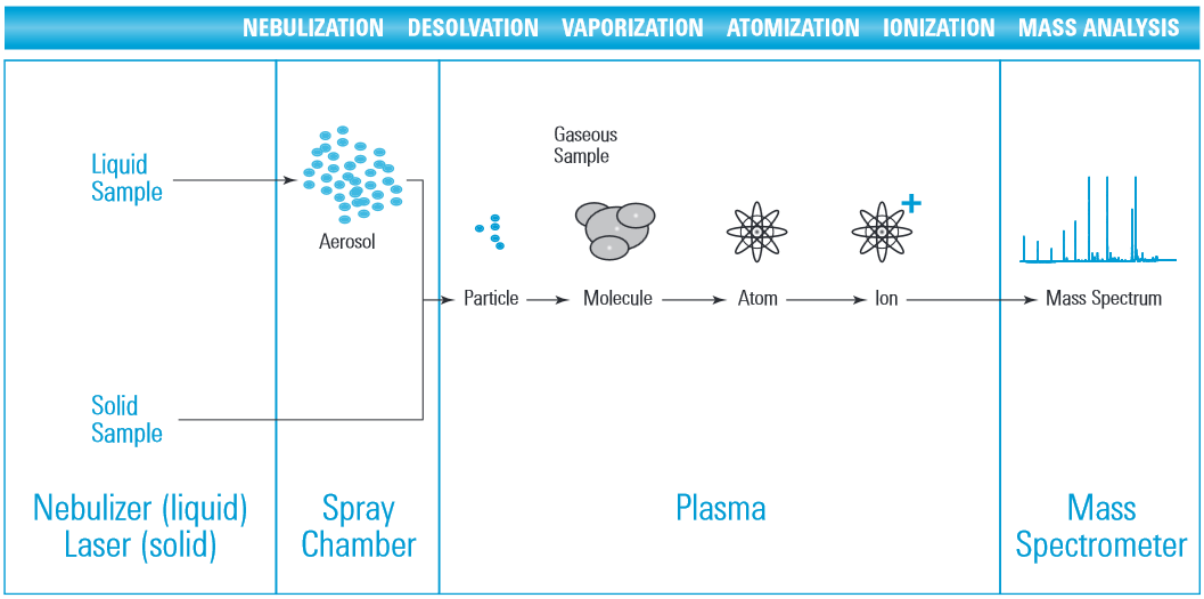

Fig. 1.36 Representation of ICP-MS processes following sample introduction. Taken from http://www.agilenticpms.com/primer/ICP-MS Primer.pdf

1.5 Research objectives

This research aims to establish if stable isotope and trace element profiles can be used to verify the declared origin of timber. The study seeks to apply the same analytical techniques of IRMS and ICP-MS to timber which have proven useful in geographical determination of a wide range of foodstuffs. Additionally, the study seeks to improve upon existing methodologies which use stable isotopes and trace elements in geographical origin determinations, by carrying out multivariate statistical analysis of the combined trace element and stable isotope data.

The objectives of the research presented in this thesis are:

i. To examine the relationship between the isotopic compositions of carbon, hydrogen and oxygen in timber cellulose, as well as differences contributing to the growth conditions and meteorological influences experienced by the trees.

ii. To investigate the link between the trace element profiles of the underlying lithology of the trees growing environment with that of the timber samples.

iii. To investigate whether multivariate statistical treatment of stable isotope ratio and trace element data enables discrimination of species of *Entandrophragma* from across Cameroon, Ghana, Congo, and the Democratic Republic of Congo, as well as *Diospyros* and *Dalbergia* from Madagascar.

Chapter 2 – Multi-element analysis of timber samples by ICP-MS

ICP-MS analysis

2.1 Introduction

This chapter will deal with the measurements and quality controls from the trace element analysis of tropical timber samples from West Africa and Madagascar. It will introduce multivariate statistical analysis and how this can be applied to the trace elements measured in the tropical timber samples in an attempt differentiate country of origin. The variation of a selection of trace elements measured in timber from across the sampling locations will also be covered in this chapter.

The large variation in continental geology and subsequent soil types influencing the incorporation of trace elements into plants has led to a number of studies investigating if trace element profiles can be used to differentiate country of origin for a range of commodities. Trace element profiling is now established as an effective means of determining provenance of a number of cultivated foodstuffs (Jakubowski *et al*., 1999; Kelly *et al.*, 2002; Moreda & Piñeiro, 2003; Boner *et al*., 2004; Coetzee *et al*., 2005; Anderson & Smith, 2005; Iglesia *et al*., 2007; Gómez-Ariza *et al*., 2006; Heaton *et al.*, 2007; Aritama *et al*., 2007; Pilgrim *et al*., 2010; Li *et al.*, 2013). The use of ICP-MS allows for a large number of elemental variables to be analysed, enabling robust comparison against established reference libraries to identify origin.

While the majority of publications involving trace element analysis relate to the provenance of foodstuffs, only small number of authors have attempted to analyse trace elements in timber (Kagawa *et al*., 2008; Watmough and Hutchinson, 2010; Doucet *et al*., 2012). Kagawa *et al*. (2008) combined $^{13}C/^{12}C$, $^{15}N/^{14}N$ and $^{18}O/^{16}O$ stable isotopes with trace elements to aid geographic origin determination of Rubroshorea wood from South East Asia. Soil type and water conditions were shown to influence trace element concentrations in the timber. However, no correlation was established between trace element concentrations of timber, and the longitude or latitude of the sample sites, indicating that trace elements alone were not useful for timber origin determinations. It is not clear how the elemental variables were selected in the 2008 study, or if many more were not deemed to

play any role in the discrimination of Rubroshorea wood, but the use of few elemental variables in the origin classification (Al, Ba, Ca, Fe, Mg, Mn, Sr, V, Zn) suggests that other useful trace elements were possibly overlooked. This study uses ICP-MS to analyse a further 57 trace elements (detailed later in this chapter), in order to increase the precision of the country prediction.

To answer the question of provenance, a robust reference library must be established against which a sample of unknown origin would be compared statistically. Furthermore, the statistical robustness associated with the compilation of a large reference library containing a sufficient number of elemental variables, is preferred over a small reference library, e.g. the British Beef Origin Project (Kelly, 2010), (based on samples from across the United Kingdom: England (n=500), Scotland (n=100) and Wales (n=118). This study aims to expand upon the work already carried out by Kagawa (2008) by establishing an authentic reference library of 75 samples of *Entandrophragma* from across Cameroon, Ghana, Congo, and the Democratic Republic of Congo, as well as core samples of *Diospyros* (n=12) and *Dalbergia* (n=13) from Madagascar.

2.1.1 Trace elements in timber

The trace element concentrations in timber are heavily influenced by the input of water soluble nutrients derived both from the underlying lithology and from anthropogenic activity (Baes & McLaughin, 1984). Hence, the trace element composition of forest biomass reflects the bio-available and mobilized macro and micro-nutrients present in the underlying soils, these being the main source of plant trace elements. Trace element availability depends on several factors including soil pH, humidity, porosity, clay type and content (Kim & Thornton, 1993). Table 2.1 details the typical bioavailability of a selection of trace elements including the influence of pH and soil oxidation conditions. The cation and anion exchange capacity (CEC, AEC) of the soil is also critically important and is highly correlated with the surface area of the soil particles (Pendias, 2004). Uptake of trace elements mostly takes place through the root system of the tree, the dissolved minerals entering through the epidermis, passing through the root cortex and finally reaching the stele and xylem.

Absorption takes place both through non-metabolic diffusion of ions, and through metabolic processes involving chemical gradients to mobilise nutrients (Pendias, 2004).

Table 2.1 Bioavailability of trace elements under different soil redox conditions. Taken from Pendias (2004).

Soil condition		**Bioavailabilty**	
Redox	**pH**	**High**	**Moderate**
Oxidising	<3	Cd, Zn, Co, Cu, Ni	Mn, Hg,V
Oxidising	>5	Cd, Zn	
			Mo, Se, Sr, Te, V
Oxidising	>5	Non	Cd, Zn
Fe-rich			
Reducing	>5	Sc, Mo	
			Cd, Zn, Cu, Mn, Pb, Sr
Reducing with H_2S	>5	None	Mn, Sr

Alkaline metals, especially rubidium (Rb) and caesium (Cs), are easily mobilised in the soil and readily transported into plants potentially making them useful indicators of geographical origin. Consequently, the range of soils present and range of bioavailability among metals mean that elemental compositions in timber may provide unique markers that characterise geographical origin (Branch *et al.*, 2003). Figure 2.1 details the surficial lithology for Africa, thus enabling assessment of the relationship of trace elements present in the lithology with those trace elements absorbed by the trees at the various sampling locations.

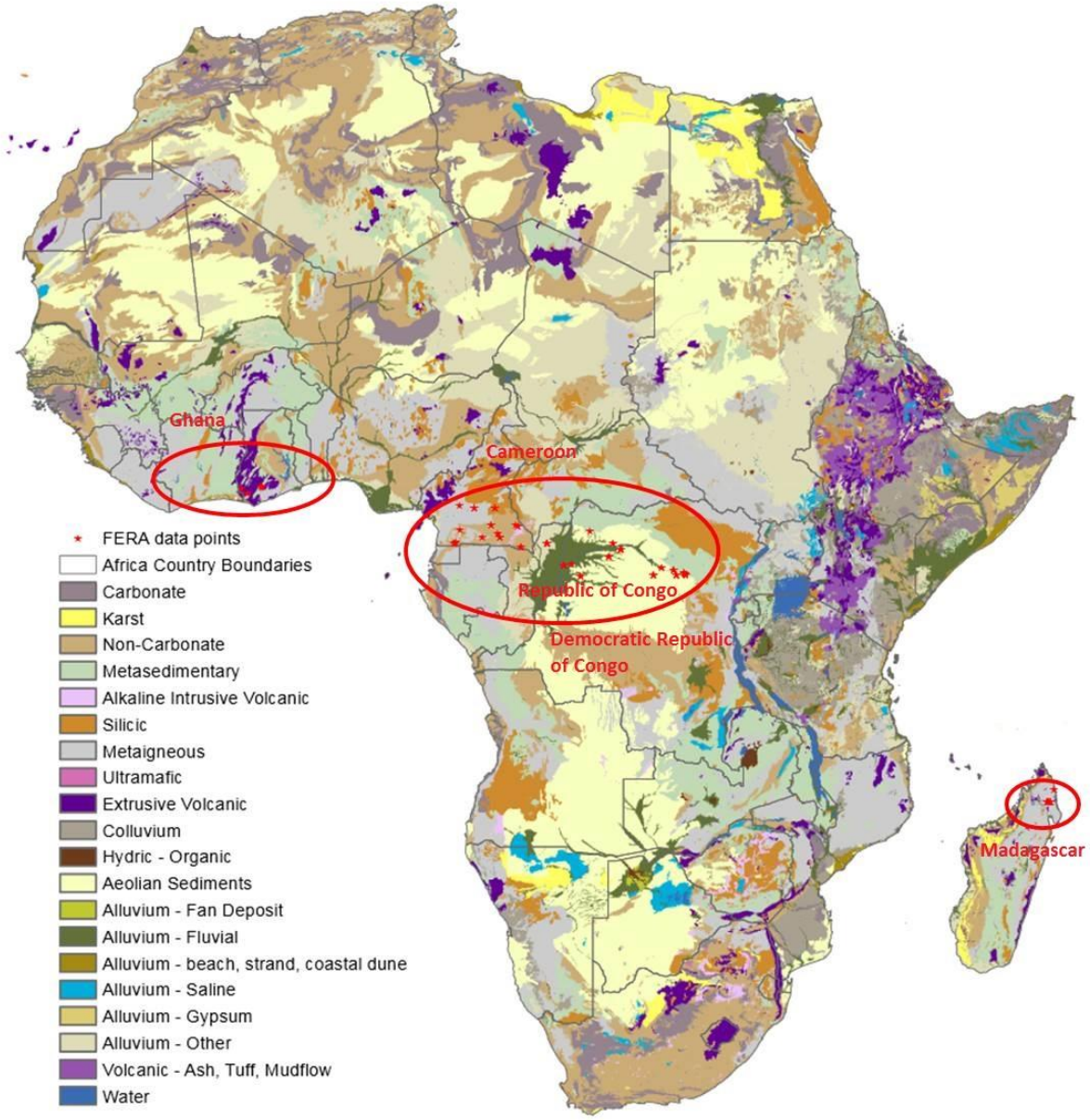

Fig. 2.1 African surficial lithology and timber sampling locations. Taken from the United States Geological Survey. http://rmgsc.cr.usgs.gov/ecosystems/africa.shtml

2.2 Multi element concentrations in timber

Timber samples (n=100) from West Africa and Madagascar were weighed (0.2 g ±10%) in quartz reaction vessels and subject to pressurised microwave acid digestion. During the process, sample matrix was broken down and trace elements liberated through a process of oxidation. The sample containing the dissolved trace elements was then introduced to the ICP-MS via a nebuliser, producing

an aerosol which underwent ionisation in a high temperature plasma beam, the resulting ion fragments passing into the mass analyser for measurement. For the purposes of quality control, approximately 25% of samples were randomly selected and analysed in duplicate. Each analytical batch contained a minimum of 3 procedural blanks, a spiked sample (for recovery estimate purposes) and the certified reference materials OBTL-5 oriental basma tobacco leaves and ZC73013 spinach. The number of trace elements quantified from the data acquisition was very much dependent upon elemental concentration, recovery and sensitivity of the ICP-MS (Agilent Technologies, Berkshire, UK), the sixty-six elements analysed as part of this study having been consistently measured on a routine basis (Kelly *et al.*, 2002: Li *et al*., 2014). Data was accepted if calculated recovery of the spike sampled for each analyte fell within the 60 - 140% tolerance. Additionally, at least 75% of the elements in the spiked sample had to fall within 80% - 120% recovery tolerance, otherwise acid digestion and ICP-MS analysis of the failed batch was repeated. The multivariate statistical processing discussed in Chapter 4 requires the analysis of variables to enable discrimination in the model. To enable the multivariate model the greatest chance of achieving country level classification of the timber samples, data for as many trace elements as possible were acquired by inductively coupled plasma mass spectrometry (ICP-MS). There was no prior hypothesis regarding the selection of elements acquired, rather the sixty-six element concentrations measured was the maximum range that could be acquired by ICP-MS for the multi-element analysis.

2.2.1 Limits of detection and quantification

Reagent blanks were taken through the same analytical procedure as the samples and four replicate blank determinations were divided by the weight of the sample used for the acid digestion in every analysis batch. The final limit of detection (LoD) used for each element was established by applying the median method LoD calculated across all the analysis batches measured on several different days.

Similarly, the limit of quantification (LoQ) was defined as ten times the standard deviation of the signal when corrected for sample weight and dilution. Elemental analysis parameters detailing the ICP-MS mode of operation, LoD and quality control results for each individual element can be found

in Appendix I. In order to overcome the problem of polyatomic interference from ions with similar masses, the ICP-MS octopole reaction system (ORS) was operated in standard and non-pressurised modes, details of which are shown in Table 2.2.

Table 2.2 Operation mode of the ICP-MS octopole reaction system (ORS) for the respective trace elements.

Octopole reaction system (ORS) operating mode	Element
H_2	Se
He	Ti, V, Cr, Fe, Ni, Cu, Zn, As.
Standard	Li, B, Na, Al, K, Ca, Mn, Co, Rb, Sr, Y, Zr, Mo, Pd, Ag, Cd, Sn, Sb, Cs, Ba, La, Ce, Pr, Nd, Sm, Eu, Gd, Tb, Dy, Ho, Er, Tm, Yb, Lu, Hf, Tl, Pb, Bi, Th, U.

2.2.2 Instrument stability

During the course of several weeks of data acquisitions by ICP-MS, repeat analysis of calibration standards containing multi element solutions no.1 (Ce, Dy, Er, Eu, Gd, Ho, La, Lu, Nd, Pr, Sc, Sm, Tb, Th, Tm, Y, Yb) and no. 2a, (Ag, Al, As, Ba, Be, Ca, Cd, Co, Cr, Cs, Cu, Fe, Ga, K, Li, Mg, Mn, Na, Ni, Pb, Rb, Se, Sr, Tl, U, V, Zn) were performed at regular intervals during each analytical batch sequence, enabling assessment of instrument stability. The standards were selected because their elemental composition encompassed a wide range of masses and concentrations, making them a suitable check of ionisation efficiency of the instrument. Additionally, each calibration check enabled monitoring of the performance of the octopole reaction system over time. The set acceptance criteria of the results for the re-analysed standard was set at ± 20 % of the initial value, and only elements which passed this QC criteria were included in the final multivariate statistical analysis. The samples were also re-analysed in a separate acquisition if more than 10% of the elements failed to meet this quality control criteria within a batch.

2.2.3 Quality controls

Accepted results had to be within the range of 40% of the accepted or certified value as detailed in Appendix 1 and where indicative values were shown on certificates, measured concentrations had to be within a factor of 2 of the quoted value. Data were accepted if results for >75% of reference materials passed the criteria above. Additionally, replicate agreement for 25% of total samples analysed had to achieve a relative standard deviation ≤ 20 % or less than 10 times standard deviation of the blanks, whichever was greater. Failure of the samples to meet the acceptance criterion required the batch in question to be re-analysed. Table 2.3 details those elements which passed the QC acceptance criteria, and were used in the multivariate statistical processing. Data for the failed elements (16) were not improved upon despite several repeat analyses, many of them known to be difficult to quantify when analysed as part of a multi element acquisition. In order for those failed elements to pass the QC acceptance criteria, it would be very likely they would require re- analysing in single element batches. However, it was deemed acceptable that the fifty elements passing the QC criteria would provide the multivariate model a great enough number of variables**.**

Table 2.3 Quality control results of the trace element analysis.

Element	QC pass or fail	Element	QC pass or fail	Element	QC pass or fail	Element	QC pass or fail
7 Li	Pass	66 Zn	Pass	121 Sb	Pass	175 Lu	Pass
9 Be	Fail	71 Ga	Fail	125 Te	Fail	178 Hf	Pass
11 B	Pass	72 Ge	Fail	133 Cs	Pass	181 Ta	Fail
23 Na	Pass	75 As	Pass	137 Ba	Pass	182 W	Fail
24 Mg	Pass	78 Se	Pass	139 La	Pass	185 Re	Fail
27 Al	Pass	85 Rb	Pass	140 Ce	Pass	189 Os	Fail
39 K	Pass	88 Sr	Pass	141 Pr	Pass	193 Ir	Fail
44 Ca	Pass	89 Y	Pass	146 Nd	Pass	195 Pt	Fail
45 Sc	Fail	90 Zr	Pass	147 Sm	Pass	197 Au	Fail
47 Ti	Pass	93 Nb	Fail	153 Eu	Pass	201 Hg	Fail
51 V	Pass	95 Mo	Pass	157 Gd	Pass	205 Tl	Pass
52 Cr	Pass	101 Ru	Fail	159 Tb	Pass	208 Pb	Pass
55 Mn	Pass	103 Rh	Fail	163 Dy	Pass	209 Bi	Pass
56 Fe	Pass	105 Pd	Pass	165 Ho	Pass	232 Th	Pass
59 Co	Pass	107 Ag	Pass	166 Er	Pass	238 U	Pass
60 Ni	Pass	111 Cd	Pass	169 Tm	Pass		
63 Cu	Pass	118 Sn	Pass	172 Yb	Pass		

2.3 Introduction to canonical discriminant analysis

The multivariate statistical method chosen was one that falls under the umbrella of supervised 'pattern recognition'. The learning or training set comprised of the database of 100 stable isotope and trace element parameters from the authentic timber samples. The specific statistical technique used was canonical discriminant analysis (CDA) (Klecka, 1980), which was applied with the aim of finding a rule that allocated timber samples of unknown origin to be assigned to the correct group: Congolese, Cameroon, Democratic Republic of Congo, Ghanaian or Madagascan origin.

The procedure is based on finding the directions in multivariate space which discriminate best between the origins of timber samples. When the most important direction is found, the method searches for the next direction with the same property, but with the restriction that the variability along the axis is uncorrelated with the one(s) already determined. The procedure continues until the desired number of components has been extracted. Usually, scores for the first discriminant axis are plotted versus scores for the second discriminant axis for visual inspection of the data. The selection of the most significant variables was performed by forward 'stepwise' analysis. The variables were included in the model one by one, choosing at each step the variable that made the most significant additional contribution to the discrimination (i.e. with the largest F value - the value of F provides a test for the statistical significance of the observed differences among the means of two or more groups). Measured variables were excluded from the model if they were shown to be redundant. On the basis of the selected variables, different independent discriminant functions were computed by canonical discriminant analysis. Their maximum number is equal to either the number of variables or the number of groups (in this case geographical origins) minus one, if the latter is smaller. The statistical significance of each discriminant function was evaluated on the basis of the Wilks' Lambda factor after the function was removed. The function is used to test which variables contribute significance in discrimination functions. Wilk's Lambda values fall between 0 and 1, and the closer the value Wilk's Lambda is to 0, the greater the influence of that variable plays in the discriminant function. Increasing values play a decreasing influence in the canonical discrimination function, and no group differences are observed when Lamba is equal to 1. To test the robustness of the multivariate

model, a 'leave-one-out' cross validation assessment of the data was performed. The cross validation was achieved by removing in turn, a known sample from each dataset and testing the classification accuracy after assignment of the individual data points in multivariate model (Heaton *et al*., 2008).

2.4 Results of the multivariate analysis of timber samples

The concentrations of the fifty trace elements determined by ICP-MS were processed statistically using canonical discriminant analysis (CDA) in order to determine if geographical distinction of timber samples could be achieved. A multivariate model was produced using country classification, with samples grouped into their respective country (1-5) of origin (Fig. 2.1). The spread of data points for each country is represented by the group centroid, with 85.7% of original group cases correctly classified and 80.6% of cross validated grouped cases correctly classified. Function 1 (*x*-axis) and function 2 (*y*-axis) accounted for 65% and 24% of the variance, respectively. A total of 11 trace elements, listed in order of providing the greatest to the least discrimination, were selected by the software for the multivariate analysis: zirconium (Zr), molybdenum (Mo), strontium (Sr), manganese (Mn), arsenic (As), antimony (Sb), selenium (Se), boron (B), magnesium (Mg), titanium (Ti), cobalt (Co). Functions derived from the trace element parameters are illustrated in the cross plot below (Fig 2.2) and the interval plots for the respective trace elements illustrated in Fig. 2.3.

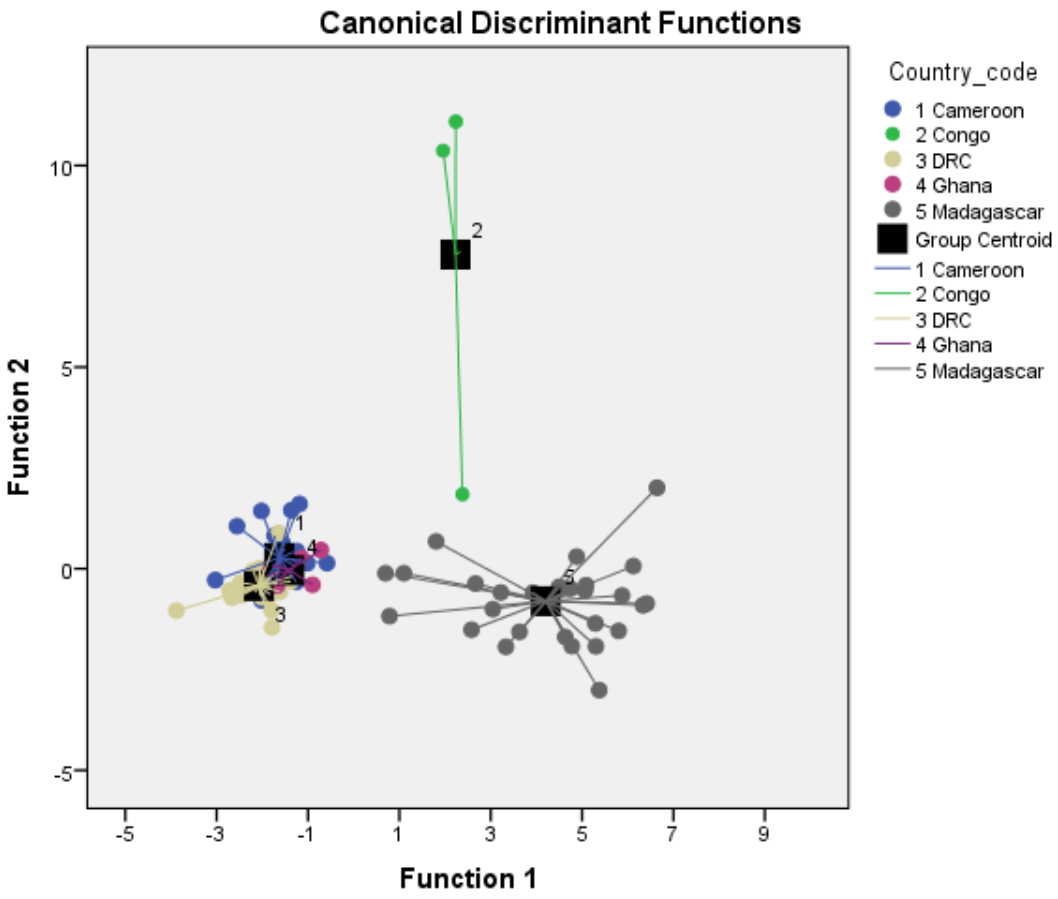

Fig. 2.2 Cross plot of all countries timber multi element data separated by two discriminant functions calculated from the step-wise canonical discriminant analysis.

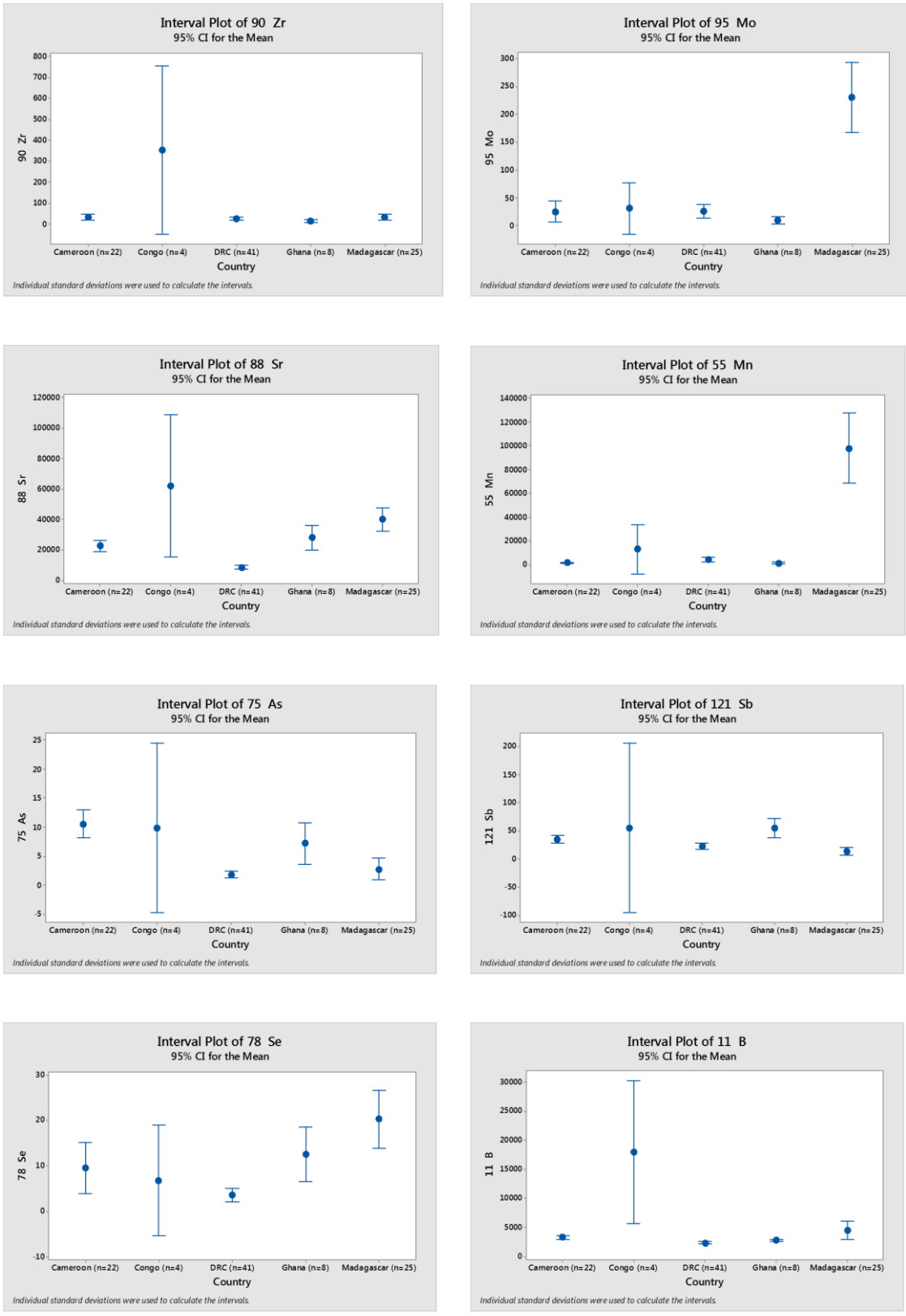

Fig. 2.3 Interval plots of trace elements selected by the canonical discriminant analysis. The mean values for each country are represented by solid circles, and the error bars represent the 95% confidence interval.

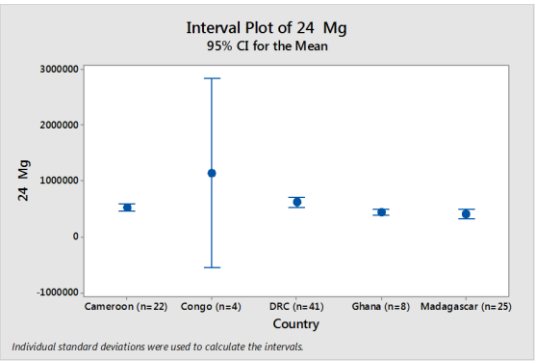

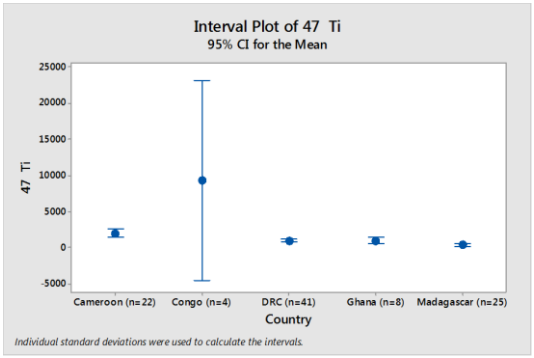

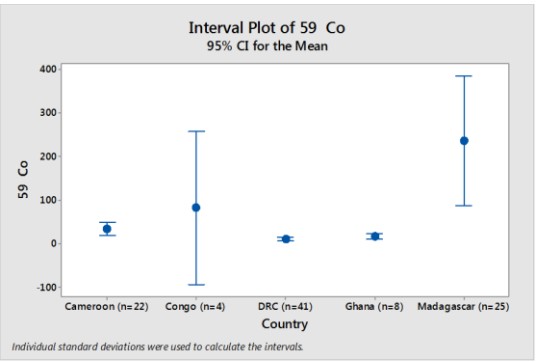

Fig. 2.3 continued Interval plots of trace elements selected by the canonical discriminant analysis. The mean values for each country are represented by solid circles, and the error bars represent the 95% confidence interval.

2.4.1 Discussion of the multivariate analysis

The CDA based on the multi element data reveal a clear distinction of the Madagascan samples from the West African sample groups (Fig. 2.2). The Congolese sample set is also clearly discriminated from all other countries, but this must be viewed with caution due to the very small number of Congolese samples included in the statistical analysis. Sample groups for Cameroon, DRC and Ghana were not clearly discriminated clearly from one another, possibly as a result of a dominance introduced through elevated concentrations of trace elements observed in the Congolese samples. Zirconium (Zr) is not known to have any role in biological development, although it can be found at low levels in a wide range of biological systems (Schroeder & Balassa, 1966). It can be released into the environment as a by-product of tin and titanium extraction (Callaghan, 2008). Molybdenum (Mo), boron (B), and manganese (Mn) are all essential plant micronutrients. Study of Fig. 2.3 reveals

molybdenum is present in the timber samples from Madagascar at significantly higher concentrations than the timber samples from West Africa. Molybdenum is the 54th most abundant element in the Earth's crust, and is an essential component of the enzymes reductase and nitrogenase, both of which are involved in nitrogen fixation and protein synthesis in plants (Albrigo *et al*., 1966; Emsley, 2001). The elevated concentration of molybdenum in the Madagascan samples could be largely attributed to the growing environment of the trees where the pH of the soil influences the mobility of ions absorbed through the tree roots (Fig. 1.13). However, if soil alkalinity was a significant contributing factor in the elevated concentration of molybdenum observed in the Madagascan samples, it would not be anticipated to observe similarly elevated concentrations of manganese and cobalt, the mobility of these trace elements favouring acidic conditions (Schulte & Kelling, 1999; King, 1988).

Many of the trace elements selected by the multivariate analysis (Fig. 2.2) are known to be toxic to plants and have no known biological role. Arsenic (As) is a highly toxic metalloid, found naturally in all soils (Culler and Reimer, 1989). It has no known cellular role in the growth of plants, but forms inorganic arsenate and arsenites which are readily absorbed by plant roots, resulting in plant cell membrane damage by induced electrolyte leakage (Singh, 2006). Manganese is the 12th most abundant element in the earth's crust (Emsley, 2001), and its ions play an active role in the Krebs cycle as an enzymatic activator, playing an important role in nitrogen metabolism and photosynthesis (Peterson & Anderson, 1990). The presence of these trace elements in all of the tropical timber at differing concentrations supports the understanding that many toxic trace elements can be passively absorbed by tree roots (Marschner, 1995). Additionally, this highlights the role forests act as biological buffer, reducing the volume of toxic trace elements which would otherwise leach into water courses posing a risk to forest biodiversity (Lombardozzi *et al*., 2003).

2.4.2 Further multivariate analysis of timber samples

In order to test if the separation of sample groups Cameroon, DRC and Ghana could be improved, it was decided to re-run the CDA (Fig. 2.4) excluding the Congolese samples. Exclusion of the Congolese sample set could support the hypothesis that the elevated concentrations of a large number of elements could be introducing dominance when processed by multivariate statistical analysis.

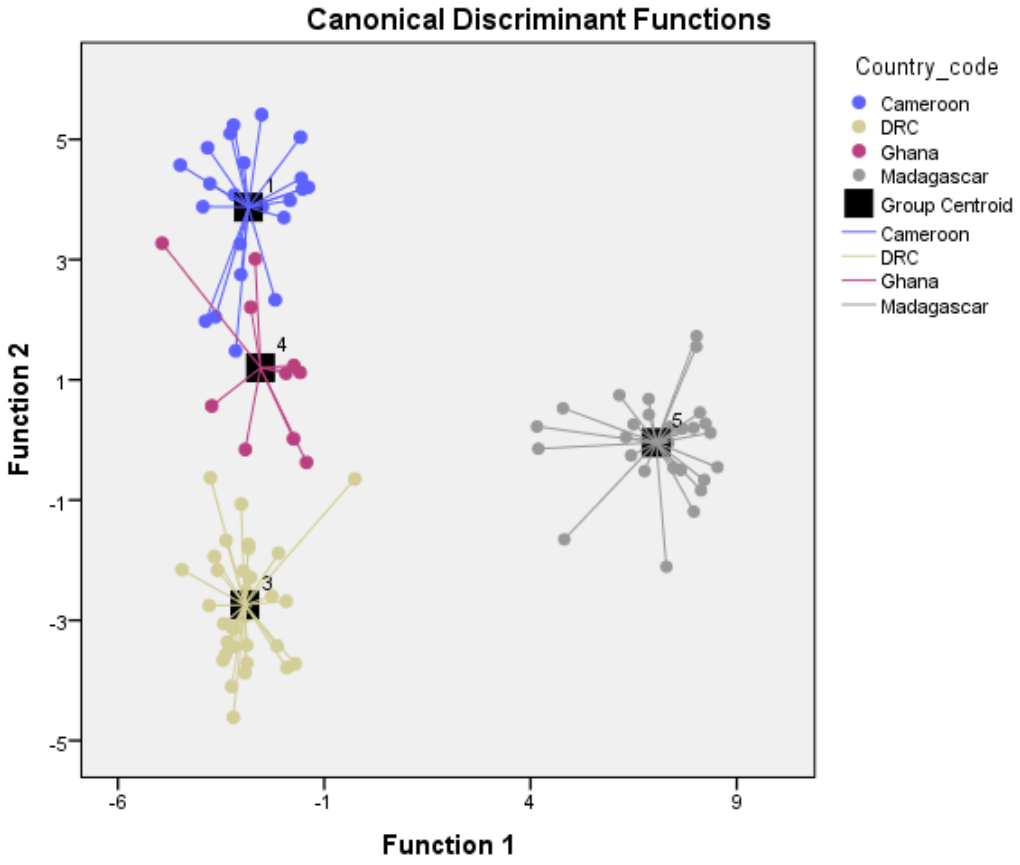

Fig. 2.4 Cross plot of all countries timber multi element data (minus Congolese) separated by two discriminant functions calculated from the step-wise canonical discriminant analysis.

Following the exclusion of the Congolese samples in the CDA, 98.9 % of original group cases were correctly classified and 83% of cross validated grouped cases correctly classified. Function 1 (*x* axis) and function 2 (*y* axis) provided 71.4% and 23.1% of the variance respectively, with 11 trace elements (Fig. 2.5), listed in order of providing the greatest discrimination, selected by the software for the multivariate analysis: Holmium (Ho), erbium (Er), thulium (Tm), ytterbium (Yb), lutetium (Lu),

hafnium (Hf), thallium (Tl), lead (Pb), bismuth (Bi), thorium (th), and uranium (U). The trace elements are plotted below (Fig. 2.5) as interval plots.

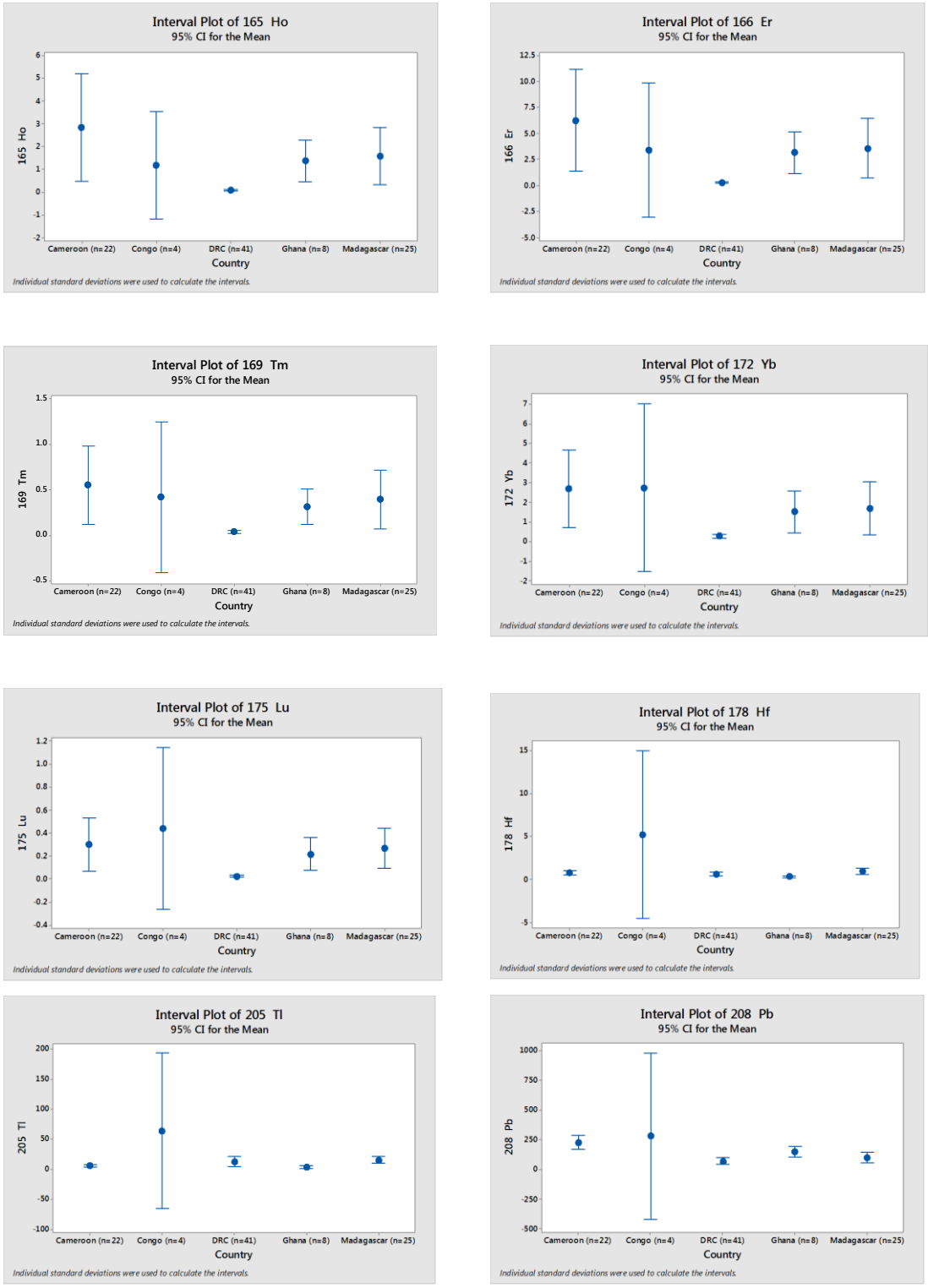

Fig. 2.5 Interval plots of trace elements selected by the canonical discriminant analysis. The mean values for each country are represented by solid circles, and the error bars represent the 95% confidence interval.

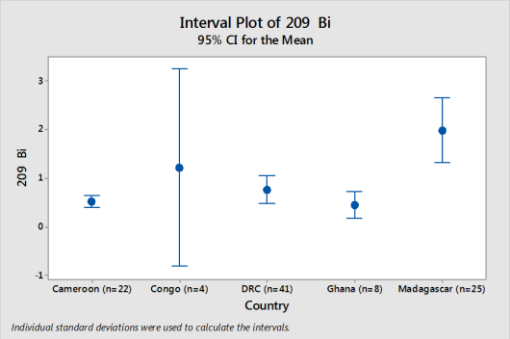

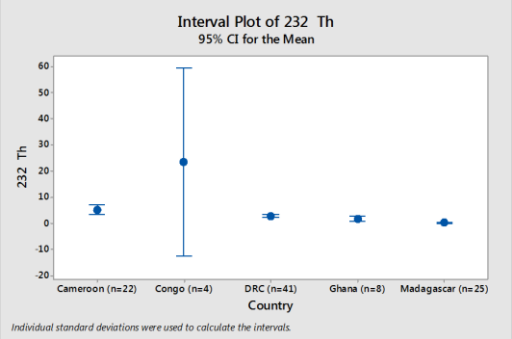

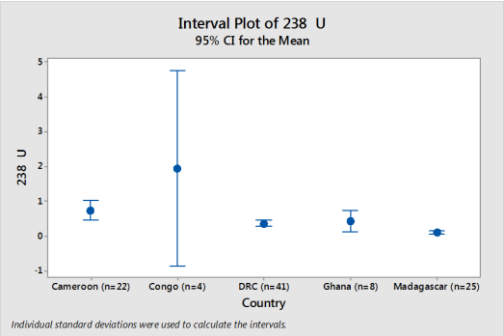

Fig. 2.5 continued Interval plots of trace elements selected by the canonical discriminant analysis. The mean values for each country are represented by solid circles, and the error bars represent the 95% confidence interval.

2.4.3 Discussion of the 2nd multivariate analysis

The CDA of the multi-element concentrations shows that trace element concentrations in timber vary significantly among the geographical locations examined. Study of the trace elements selected by the canonical discriminate analysis may give an insight into the relationship of the sampled trees with the local underlying geology, soil and forest biomass. The small number of timber samples from the Congo all contained significantly greater concentrations of zirconium, strontium, antimony, boron, magnesium and titanium than other West African samples in the study. Further investigation of the data revealed elevated concentrations of the elements; aluminium, vanadium, iron, palladium, nickel, copper and zinc. Sites from where the Congolese timber samples were collected are very near to the Sangha River. Hence, it is possible that these elements appear at elevated concentrations in the timber samples due to upstream pollution from anthropogenic activity such as mining in neighbouring

Cameroon and the Central African Republic, as the tributaries of the Sangha River originate in those countries (Joshi & Balasubramanian, 2010). The improvement in discrimination following removal of the Congolese samples from the second canonical discriminant analysis indicates that the elevated trace element concentrations mask the discrimination, impacting on the country classification. This was demonstrated as the analysis of correct classification of original group cases increased from 85.7% to 98.9 %, and classification of cross validated groups increased from 80.6% to 83% following exclusion of the Congolese samples. Holmium (Ho), erbium (Er), thulium (Tm), ytterbium (Yb), lutetium (Lt), hafnium (Hf), and thorium (th) are all rare earth metals with no known biological roles (Emsley, 2001). Thallium (Tl) has no known biological role in plants and is known to be highly toxic to certain plant species. McMurtrey & Robinson (1938) demonstrated that as little as 35 ppm in sandy soils was able to inhibit the growth of plants. Smith & Carson (1977) observed that many plant species are injured by the presence of thallium at concentrations of above 7 ppm in soils. Lead (Pb) is a phytotoxic transition metal, with no known biological role in plants (Peterson & Anderson, 1990). Absorption of lead by plant roots is largely governed by soil pH, soil particle size and cation exchange capacity. Lead is thought to intefere with the mechanisms ADP and ATP, inhibiting enzymatic activity and damaging DNA (Pourrut *et al*., 2011). Bismuth (Bi) is a pentavalent post-transition metal with no known biological role in plants. Its bio-availability is dependent upon leaching through soil acidification processes (Kovacs, 1984). Occurrences of the element are thought to be anthropogenic, such as from smelting and industrial activity. Volcanic emissions are also known to be a source of the element, resulting in a worldwide spread through atmospheric ash deposits. Uranium (U) can be found at low levels in the soil and rock all over the world (Hammond, 2000). It is not known to have a biological role in plants, although it has been demonstrated that plants are able to absorb this actinide. Atmospheric weapons testing in the middle of the 20th century led to uranium isotopes being spread throughout the globe at differing concentrations (Warneke *et al*., 2002). This global variation could explain why the element appears at differing concentrations across the sample sites, proving useful in the country discrimination. The presence of these elements adds further support the research by

Marschner (1995) and the findings discussed in section 2.4.1, that tree roots are able to passively absorb many non-essential trace elements.

2.5 Conclusions

Exclusion of Congolese samples from the statistical analysis increased the robustness of the model, with country and cross-validation classifications improving. Inclusion of stable isotope data in the canonical discriminant analysis may further improve the robustness of the model, and may reduce the dominance of the Congolese samples in the discrimination.

It is highly likely a significant number of the trace elements appearing at elevated concentrations in the Congolese timber cores occur as a result of anthopogenic activity. The sourcing of the timber samples for the authentic dataset from natural forest means that it is highly unlikely that trace element contribution arise from application of anthropogenic fertilizers (Kitata & Chandravansh, 2012). Further investigation of the trace elements in individual tree ring denrochronology for the samples analysed in the study could reinforce this claim (Peterson & Anderson, 1990; Watmough & Hutchinson, 2003).

Chapter 3 – Stable isotope ratio analysis of timber samples

3.1 Introduction

As discussed in Chapters 1 and 2, stable isotope analysis has been applied to a wide range of research studies with the aim of determining the provenance of consumer goods, and is now a commercially accepted method of certifying provenance of high value products. In order to achieve precise country of origin assignments required for provenance studies, many authors combined stable isotope analysis with other measured variables such as trace elements (Kelly, 2002; Boner *et al.*, 2004; Heaton *et al.*, 2007; Aritama *et al*., 2007; Pilgrim *et al*., 2010; Li *et al.*, 2013). Far fewer studies have applied the same combined methodologies in timber provenance research (Kagawa et al., 2008), many authors instead focusing on stable isotopes alone (Kepler *et al.* 2007; Horacek *et al* 2009; Kagawa *et al.* 2010; Gori *et al*. 2013). Additionally, stable isotopes have played an important role in the study of climatic reconstruction and environmental monitoring using isotope dendrochronology techniques (Eckstein *et al*. 1975; Pilcher *et al*. 1984; Epstein & Krishnamurthy 1990; Kiyosu *et al.* 2000).

This chapter will deal solely with the stable isotope component of this study, attempting to explain the geo-physical, and biological inputs influencing the $^{13}C/^{12}C$, $^{2}H/^{1}H$, and $^{18}O/^{16}O$ stable isotope profile of timber, and how these may be used to differentiate tropical timber samples from countries in West Africa and Madagascar. As well as investigating the results of the stable isotope analysis, this chapter will also cover standards and quality controls used in the analysis. The multivariate statistical treatment of the $^{13}C/^{12}C$, $^{2}H/^{1}H$, and $^{18}O/^{16}O$ stable isotope data will be investigated in Chapter 4 where it will also be assessed alone, and in combination with the results of the trace element analysis from Chapter 2. Methodologies relating to the IRMS analyses are described in Chapter 6. The specifics governing elemental isotope fractionation and how this influences the stable isotope ratios measured in this study will be discussed in this chapter, comparing the stable isotopes measured in cellulose with those isotopes calculated from local precipitation, as well as investigating the influence of geophysical and meteorological factors including wind, humidity and water availability.

3.2 Analysis of stable isotope of carbon ($^{13}C/^{13}C$ ratio)

Species of timber can vary in their morphological makeup, with some species having a greater proportion of lignin and hemicellulose relative to alpha cellulose (Sjostrom, 1993; Saurer *et al.*, 1997). In addition, the lignin, cellulose ratio of secondary xylem can vary between early wood and late wood (Wilson & Grinsted, 1977). There are a number of metabolic pathways involved in the formation of these components, introducing a source of measurement uncertainty if carrying out isotopic measurements on bulk wood (Gray & Thompson, 1977; Mazany *et al.*, 1980; Marshall & Monserud, 1996). To reduce the uncertainty associated with bulk wood measurements, it was decided to perform the isotopic analysis on the cellulose component of the timber samples. One hundred purified timber cellulose samples were weighed in duplicate and analysed using combustion IRMS to determine the $^{13}C/^{12}C$ ratio. Data acquired by the IRMS software was corrected offline, first using a drift correction and then a stretch correction to the PDB (Pee Dee Belemnite) scale. Detailed parameters for the stable isotope ratio analysis are listed in Chapter 6.

3.2.1 Quality controls for the carbon stable isotope ratio analysis

For the purposes of monitoring and instrument performance, quality controls IAEA (International Atomic Energy Agency) CH6 and JRC sucrose (Joint Research Commission) were routinely analysed in duplicate and the $^{13}C/^{12}C$ ratios measured along with each batch of purified timber cellulose samples. Standard deviation warning and action limits were set at 2 and 3 standard deviations of 0.2‰ respectively. Batch precision for the ^{13}C measurements of the JRC sucrose and IAEA CH3 cellulose are shown in Tables 3.1 and 3.2. Illustrated data is available in Figures 3.1 and 3.2, all of the data points falling within 0.1 and 0.15 standard deviations of the assigned values for JRC sucrose and IAEA CH3 cellulose respectively. To test the repeatability of the cellulose extraction procedure, wood in house reference material (WIHR) was also extracted and analysed with each analytical batch. Data for the wood in house reference material is available in Table 3.2 and Figure. 3.3, all of the data points falling within 0.25 standard deviations of the assigned value.

Table 3.1 Compilation of JRC sucrose average $\delta^{13}C$ ‰ values from the analytical batches

Date of analysis	Average $\delta^{13}C$ ‰ $_{vs.PDB}$	SD or ABS (‰)	n
01-Oct-13	-11.34	0.03	2
03-Nov-13	-11.34	0.03	2
08-Nov-13	-11.24	0.03	3
12-Nov-13	-11.30	0.10	4
13-Nov-13	-11.32	0.14	5
15-Nov-13	-11.32	0.14	5
26-Nov-13	-11.39	0.06	4
27-Nov-13	-11.38	0.07	4
28-Nov-13	-11.42	0.07	4
02-Dec-13	-11.35	0.13	2

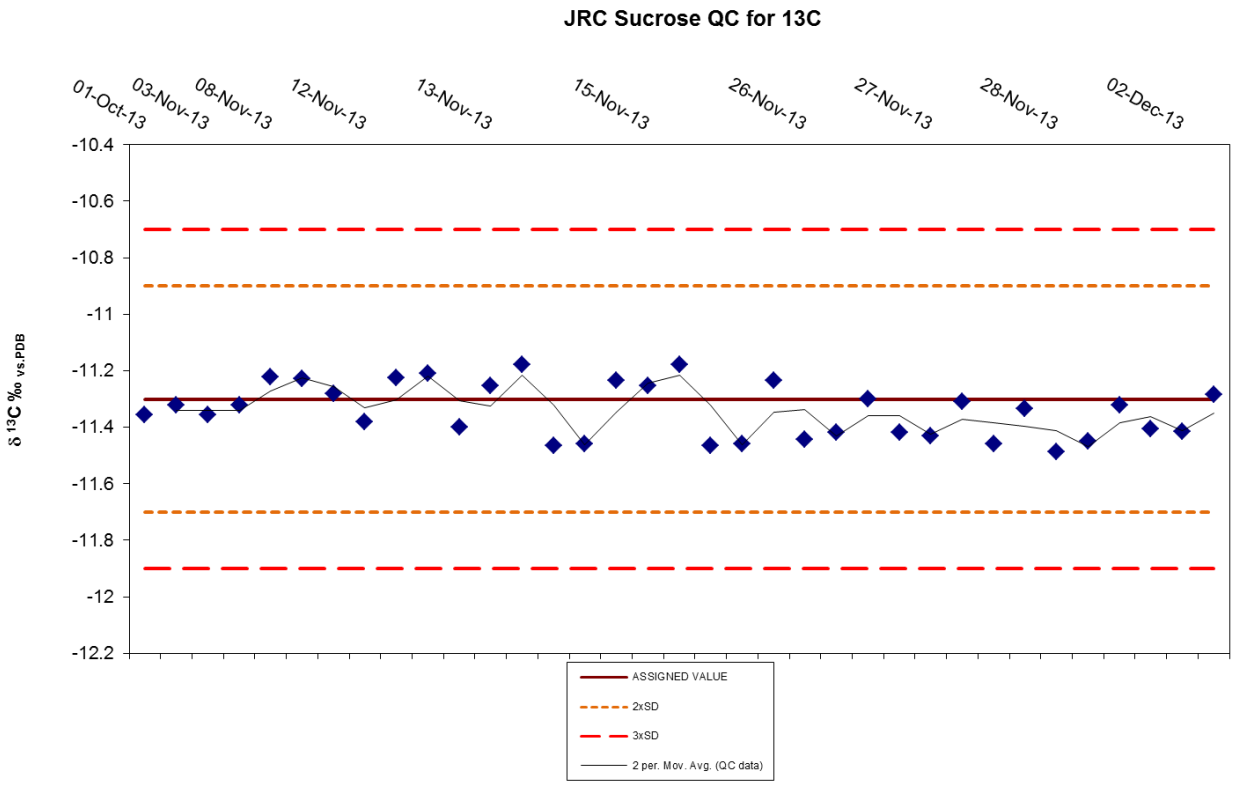

Fig. 3.1 Mean $\delta^{13}C$ values measured in JRC sucrose QC material across analytical batches. (Assigned value for sucrose from inter-laboratory comparison was -11.30‰).

Table 3.2 Compilation of IAEA CH3 cellulose average $\delta^{13}C$ ‰ values from the analytical batches.

Date of Analysis	Average $\delta^{13}C$ ‰ $_{vs.PDB}$	SD or ABS (‰)	n
01-Oct-13	-24.83	0.01	2
03-Nov-13	-25.21	0.02	3
08-Nov-13	-24.79	0.13	2
12-Nov-13	-24.78	0.10	3
13-Nov-13	-24.81	0.12	3
15-Nov-13	-24.87	0.16	3
26-Nov-13	-24.78	0.14	3
27-Nov-13	-24.82	0.08	3
28-nov-13	-24.69	0.03	3
02-Dec-13	-24.78	0.05	3

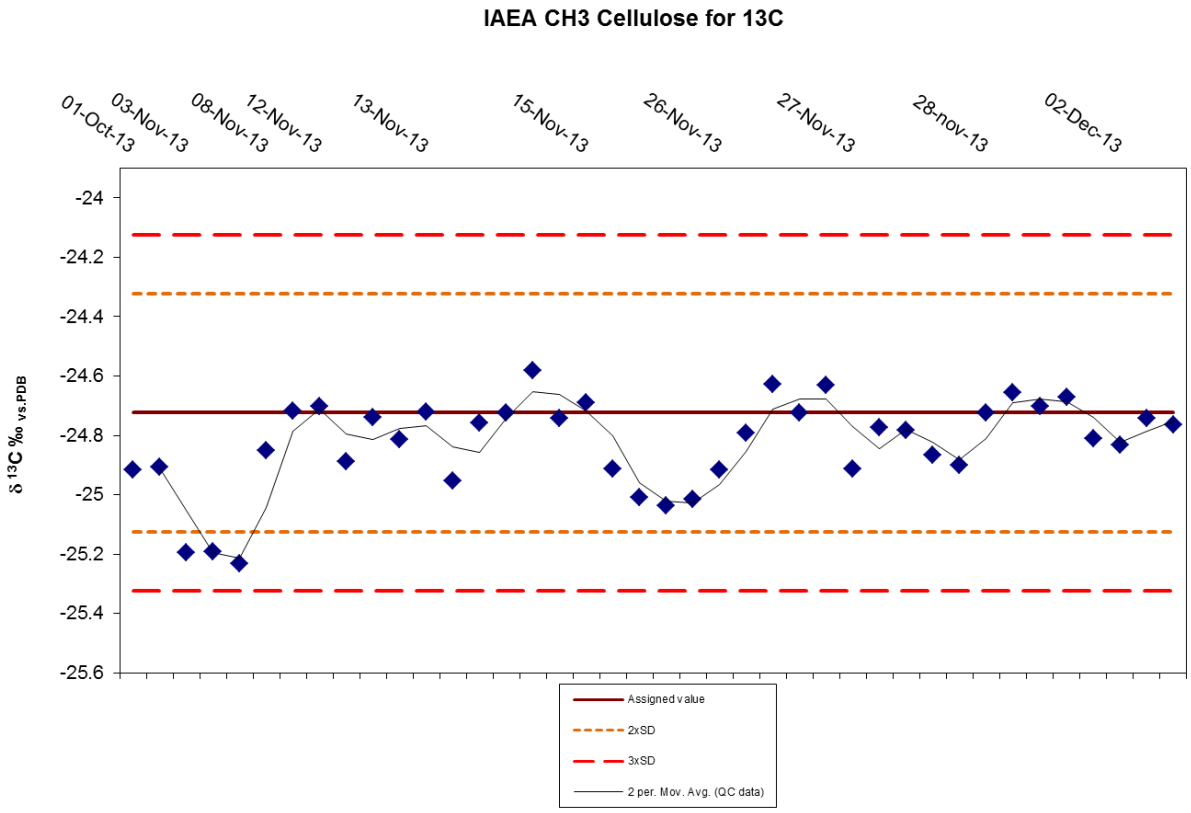

Fig. 3.2 Mean $\delta^{13}C$ values measured in IAEA CH3 cellulose across analytical batches. (Assigned value for sucrose from inter-laboratory comparison was -24.72‰, IAEA, Vienna).

Table 3.3 Compilation of wood in house reference material (WIHRM) average $\delta^{13}C$ ‰ values from the analytical batches.

Date of analysis	Average $\delta^{13}C$ ‰ $_{vs.PDB}$	n
01-Oct-13	-26.43	2
02-Oct-13	-26.33	2
03-Nov-13	-26.37	2
08-Nov-13	-26.06	2
10-Nov-13	-25.71	2
11-Nov-13	-26.09	2
12-Nov-13	-26.22	2
13-Nov-13	-26.28	2
15-Nov-13	-26.33	2
26-Nov-13	-25.99	2
27-Nov-13	-25.86	2
28-Nov-13	-26.5	2
02-Dec-13	-26.44	2

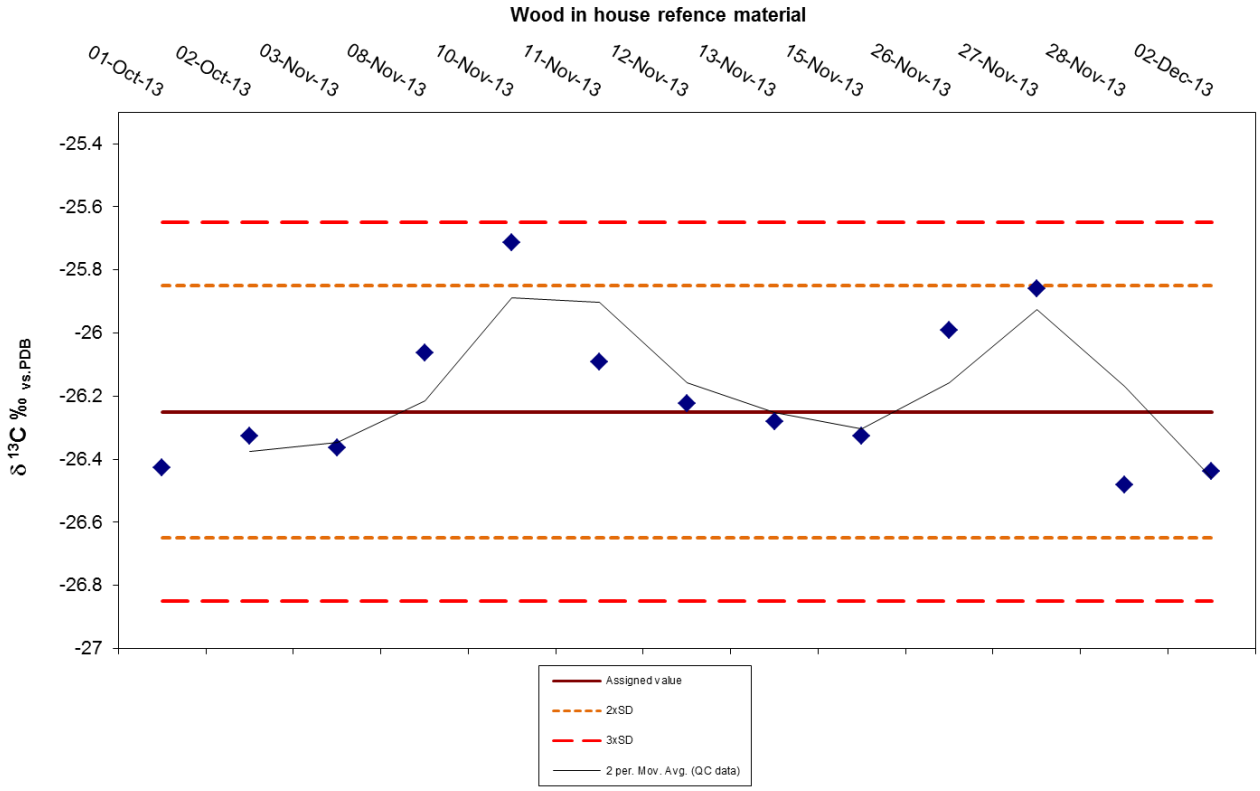

Fig. 3.3 Performance of mean $\delta^{13}C$ measured in WIHRM cellulose with analytical batches (assigned value for WIHRM cellulose was -26.25 ‰).

3.2.2 Carbon isotope compositions of authentic timber samples

All data for the carbon analysis was expressed relative to the PDB scale, the $\delta^{13}C$ values shown in Table 3.3 for all of the samples falling in the range as expected for C3 plants. As shown (Fig. 3.4), no individual country can easily be identified using $\delta^{13}C$ isotopes alone, although Madagascan and Cameroonian sample groups were approximately 2 per mille more positive than the samples groups from DRC and Ghana. It was also discovered the sample group taken from the eastern most part of the DRC had significantly more negative (depleted) $\delta^{13}C$ values when compared with other samples taken from across West Africa, including the sample group in the north of the DRC (Fig. 2.1).

Table 3.4 Mean $\delta^{13}C$, standard deviation, max and minimum $\delta^{13}C$ values for timber cellulose classified by country of origin.

Country of origin	Mean $\delta^{13}C$ value (‰)	SD of Mean $\delta^{13}C$ value	Max $\delta^{13}C$ value (‰)	Min $\delta^{13}C$ value (‰)	No. of samples (n)
Cameroon	-26.67	0.86	-28.31	-24.82	22
Congo	-26.11	0.59	-26.76	-25.36	4
DRC	-29.38	2.13	-35.44	-26.59	41
Ghana	-28.77	1.37	-30.35	-27.96	8
Madagascar	-27.90	1.13	-28.78	-24.3	25

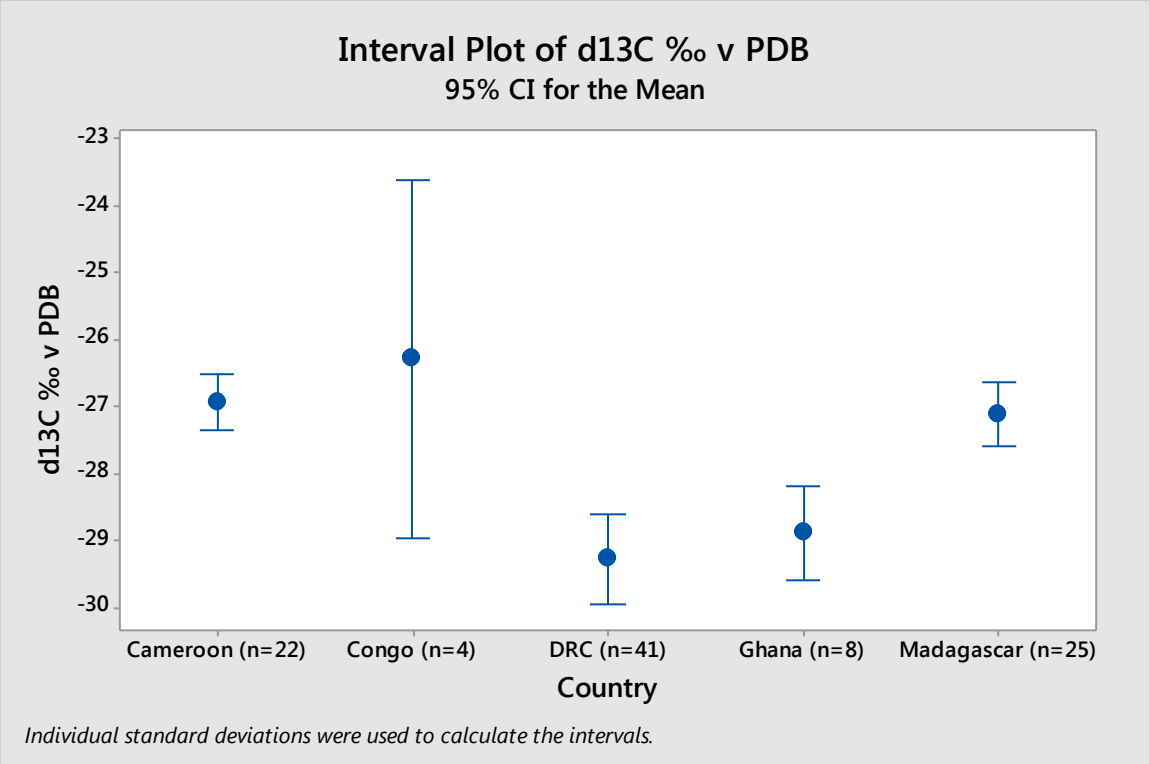

Fig. 3.4 Interval plot of timber cellulose $\delta^{13}C$ values classified by country of origin. Mean values for each country are represented by solid circles, the error bars representing the 95% confidence interval.

3.2.2.1 Discussion of the carbon isotope results

A number of isotope effects influenced by temperature, water availability, sunlight intensity and the localised atmospheric CO_2 concentration give rise to isotopic fractionation, resulting in a variation of the carbon isotopes in timber cellulose (Vogel *et al.*, 1970; Saurer *et al.*, 2007; Treydte *et al.*, 2007). These processes are usually classified as kinetic or thermodynamic, where reactions occur in non-equilibrium and equilibrium situations (Kelly *et al.*, 2002). The kinetic isotope effects of binary diffusion of atmospheric $^{13}CO_2$ and $^{12}CO_2$ in air, and the enzymatic fixation of $^{13}CO_2$ and $^{12}CO_2$ carried out by ribulose-bisphosphate carboxylase-oxygenase (RUBISCO) are both processes which discriminate against ^{13}C (Farquar *et al.*, 1989). Furthermore, decarboxylation reactions induced through photorespiration also discriminate against ^{13}C, the culmination of these isotope effects resulting in a measured offset of ~20‰ when comparing the carbon isotopes of atmospheric CO_2 with the carbon in cellulose (Igamberdiev *et al.*, 2004; Farquar *et al.*, 1989).

Information on canopy density was not recorded at the site of sample collection, nor were the local environmental conditions. Table 3.5 shows meteorological information for the respective countries of origin. Comparison of mean $\delta^{13}C$ values of the cellulose with long term mean weather data could give an insight into the contributing factors for the differences in $\delta^{13}C$ observed in the respective countries of origin. The similarity of temperatures across the respective countries did not produce a significant correlation with $\delta^{13}C$ of the cellulose. Instead, humidity data was compared with $\delta^{13}C$ of cellulose (Fig. 3.5).

Table 3.5 West African meteorological data. taken from: http://www.climatemps.com/

Region and country	Mean annual temperature (°C)	Mean annual precipitation (mm)	Mean annual relative humidity (%)	Mean annual wind speed (km/h)	Mean % un-interrupted sun exposure	Mean $\delta^{13}C$ Value (‰)
Douala, Cameroon	26.1	3812	85.1	10.83	62	-26.67
Brazzaville, Republic of Congo	25.3	1868	68.7	10.8	56	-28.77
Kinshasa, DR Congo	25.6	2265	54.5	14.16	60	-29.38
Kumasi, Ghana	25.6	1484	76.85	6.66	57	-26.11
Antsiranana, Madagascar	25.3	1196	59.5	11	29	-27.9

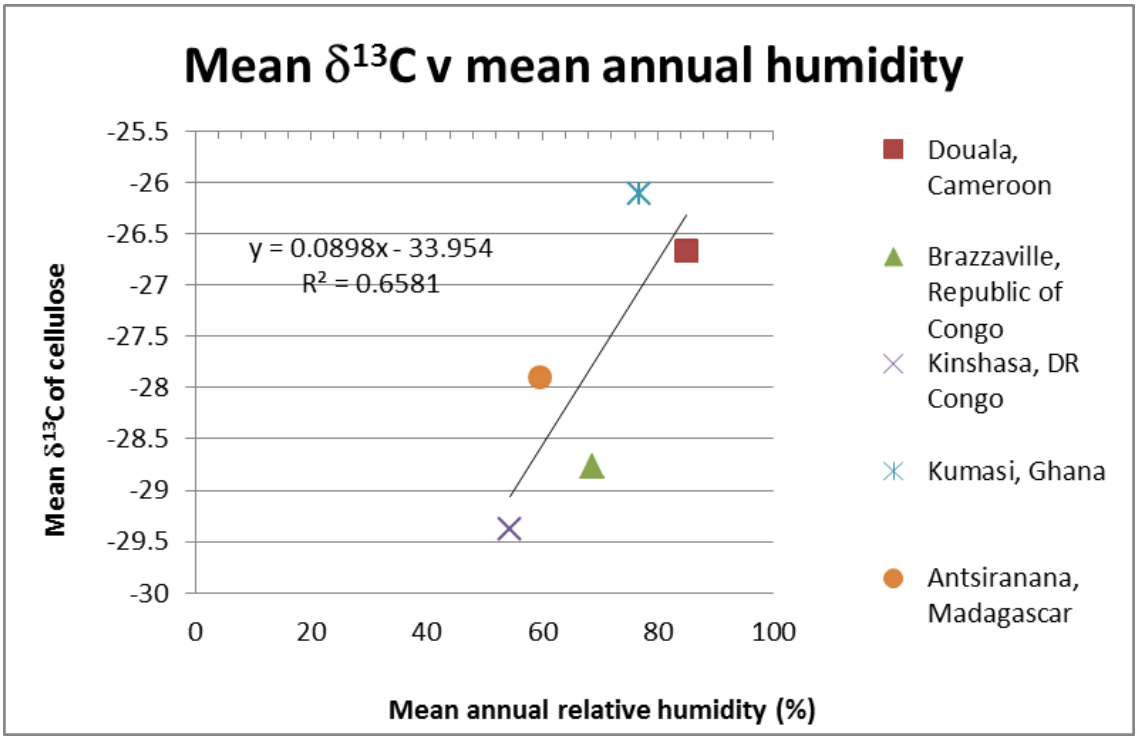

Fig. 3.5 Comparison between mean $\delta^{13}C$ values in tree cellulose and the mean annual humidity in West Africa and Madagascar.

The general trend observed was that discrimination against $\delta^{13}C$ increased with a corresponding reduction in relative humidity (R^2 =0.66). Assuming accuracy of the meteorological data, the correlation is surprising. Saurer *et al.* (1997) observed a depletion of $\delta^{13}C$ content in extracted cellulose when measured as a function of soil moisture index. One might expect humidity to be heavily correlated with soil moisture, especially as water stress is a significant factor governing photosynthesis, transpiration and leaf conductance (Farquar & Sharkey, 1982). To investigate this further, study of the Koppen-Geiger map (Fig. 3.6) revealed a band of elevated annual temperature and precipitation intersecting the north eastern part of the DRC. Furthermore, Fig. 3.7 reveals the DRC samples all originated from an area of high aquifer activity, whereas all of the other samples in the study were taken from areas with moderate or low aquifer activity. Water availability could go some way to explaining the differences in ^{13}C content of the cellulose from the various countries of origin.

Information on canopy cover and tree height was not recorded and therefore is impossible to verify, making an explanation for the trend in Fig. 3.5 difficult. Vogel *et al.* (1980) and Medina & Minchin (1980) described a significant difference in the ^{13}C content of growing leaves taken from near forest floor (-19‰) and canopy (-7‰). Notable differences are hypothesised to be attributed to the fixing of different sources of CO_2, such as lower leaf layers fixing CO_2 originating from respiration of forest floor soil microflora, and canopy leaf layers fixing atmospheric CO_2. Medina *et al.* (1986) also reported a CO_2 concentration difference of 20 ppm between the forest floor and canopy. This has huge significance for the study, as differing environmental factors such as canopy cover, tree height, temperature, wind speed, and vapour pressure could interfere with the distribution and mixing of the different sources of CO_2 in the forest, resulting in altered ^{13}C content of the cellulose.

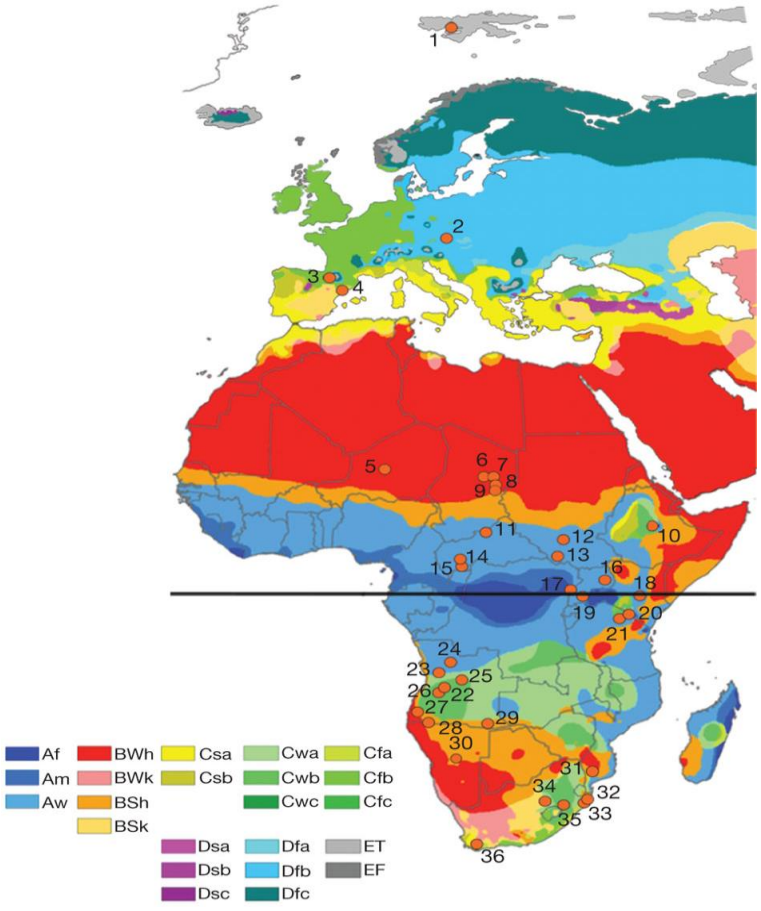

Fig. 3.6 Koppen-Geiger classification map (Af. represents tropical rainforest climate). Taken from Nature, 487, 358–361 (19 July 2012).

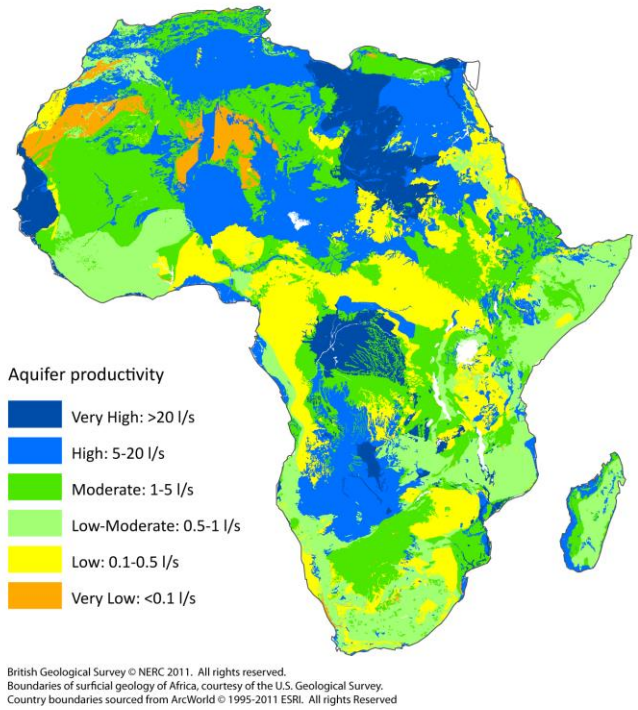

Fig. 3.7 Aquifer potential of continental Africa. Taken from: http://www.bgs.ac.uk/research/groundwater/international/africanGroundwater/maps.html

Assuming dense canopy at all of the sampling sites, the combination of reduced wind penetration, elevated levels of heat, and heavy rainfall would increase the relative humidity in those areas. However, in the case of the eastern DRC samples, it is possible they were taken from a deforested area, increasing the possibility of elevated levels of photosynthetic penetration and wind, subsequently increasing surface water evaporation. Fig. 3.8 shows a weak negative correlation (R^2=0.7) of $\delta^{13}C$ and wind speed, suggesting wind loading may be a factor in determining the $\delta^{13}C$ of the timber cellulose. Trees subjected to wind stress have been shown to concentrate their growth in the roots and lower portion of the trunk, reducing the long term height of the tree but providing mechanical stability and imparting wind resistance (Jacobs, 1954).

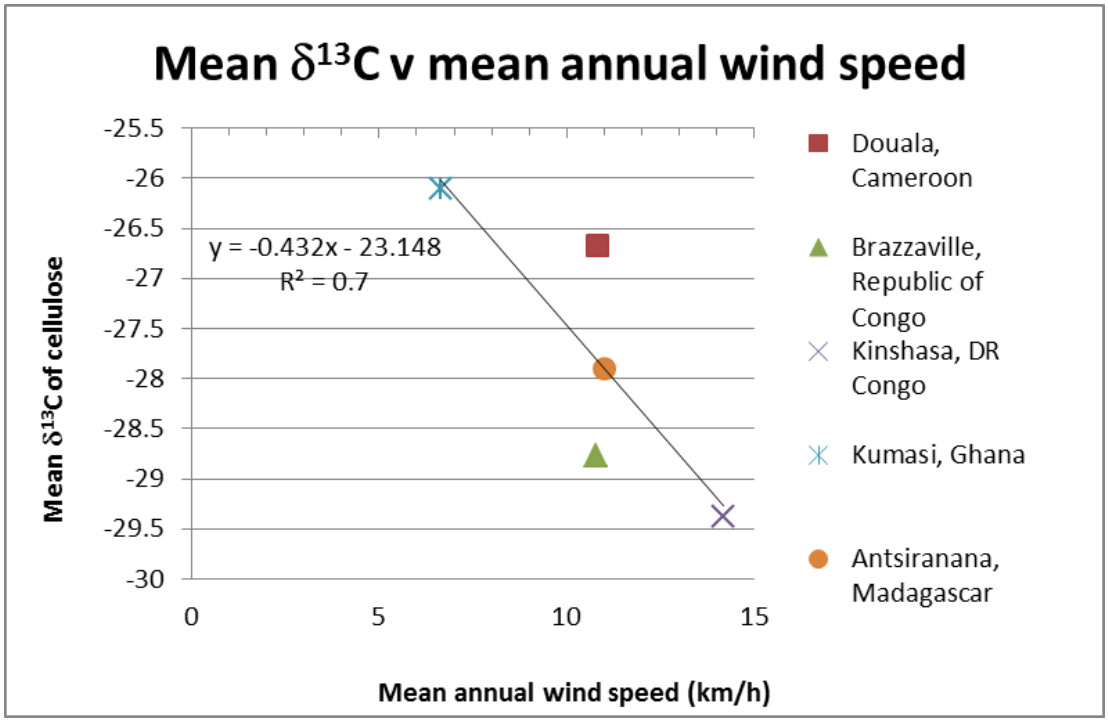

Fig. 3.8 Comparison between mean $\delta^{13}C$ values in cellulose and the mean annual wind speed in West Africa and Madagascar.

A lack of growth in the upper reaches of the tree, coupled with increased competition for sunlight with neighbouring trees could result in reduced photosynthetic activity, influencing the carbon isotope discrimination through reduced photosynthesis (King, 1991). Furthermore, leaves undergoing photosynthesis below the level of the canopy may be fixing greater volumes of CO_2 derived from forest floor microbial activity, already depleted in ^{13}C (Francey *et al.*,1985). Trapping and recycling of forest floor water condensate would be reduced in the absence of sufficient canopy cover, this in turn could reduce the localised humidity. The use of country level meteorological data may have introduced inaccuracies in the assessment of the isotope data. Higher resolution meteorological and environmental data of the specific sampling sites would likely increase the accuracy of data assessment and link further environmental factors governing the fractionation of ^{13}C in the cellulose.

3.3 Analysis of stable isotope of oxygen ($^{18}O/^{16}O$ ratio)

100 purified timber cellulose samples were analysed in quadruplicate and measured using pyrolysis IRMS to determine the $^{18}O/^{16}O$ ratio. Data acquired by the IRMS software was corrected offline, first using a drift correction and then a stretch correction to the VSMOW (Vienna Standard Mean Ocean Water) scale.

3.3.1 Quality controls for the oxygen stable isotope ratio analysis

Quality control IAEA CH3 sucrose was routinely analysed in quadruplicate for the purposes of monitoring and instrument performance. The $^{18}O/^{16}O$ ratios were measured along with each batch of purified timber cellulose samples. Standard deviation warning and action limits were set at 2 and 3 times the standard deviation of 0.75 ‰ respectively. Batch precision for the ^{18}O measurements of the IAEA CH3 cellulose is recorded in Table 3.6 and illustrated in Figure 3.9, all of the data points falling within 0.45 standard deviations of the assigned value. Repeatability of the cellulose extraction procedure was assessed using a wood in house reference material (WIHR). This was extracted and analysed with each analytical batch. Data for the wood in house reference material is available in Table 3.7 and Fig. 3.10, all of the results falling within 0.8 standard deviations of the assigned value.

Table 3.6 Compilation of IAEA CH3 cellulose average $\delta^{18}O$ ‰ values from the analytical batches.

Date of analysis	Average $\delta^{18}O$ ‰ $_{vs.}$SMOW	SD or ABS (‰)	n
25-Jul-14	31.33	0.38	2
29-Jul-14	31.47	0.25	2
30-Jul-14	31.02	0.54	3
15-Aug-14	31.28	0.17	3
16-Aug-14	30.98	0.18	3
19-Aug-14	31.12	0.64	3
21-Aug-14	31.32	0.33	3
22-Aug-14	31.01	0.90	3
28-Aug-14	31.85	0.91	3
02-Sep-14	31.54	0.06	3
03-Sep-14	30.99	0.35	3
05-Sep-14	31.17	0.69	3
08-Sep-14	31.00	0.07	3
10-Sep-14	31.15	0.33	3
12-Sep-14	30.95	0.32	3
22-Sep-14	30.82	0.61	3
26-Sep-14	31.36	0.57	3
29-Sep-14	29.70	0.19	3
02-Oct-14	31.15	0.56	3
03-Oct-14	30.68	0.85	3
06-Oct-14	31.65	1.02	3
08-Oct-14	31.88	1.30	3
10-Oct-14	30.65	0.19	3

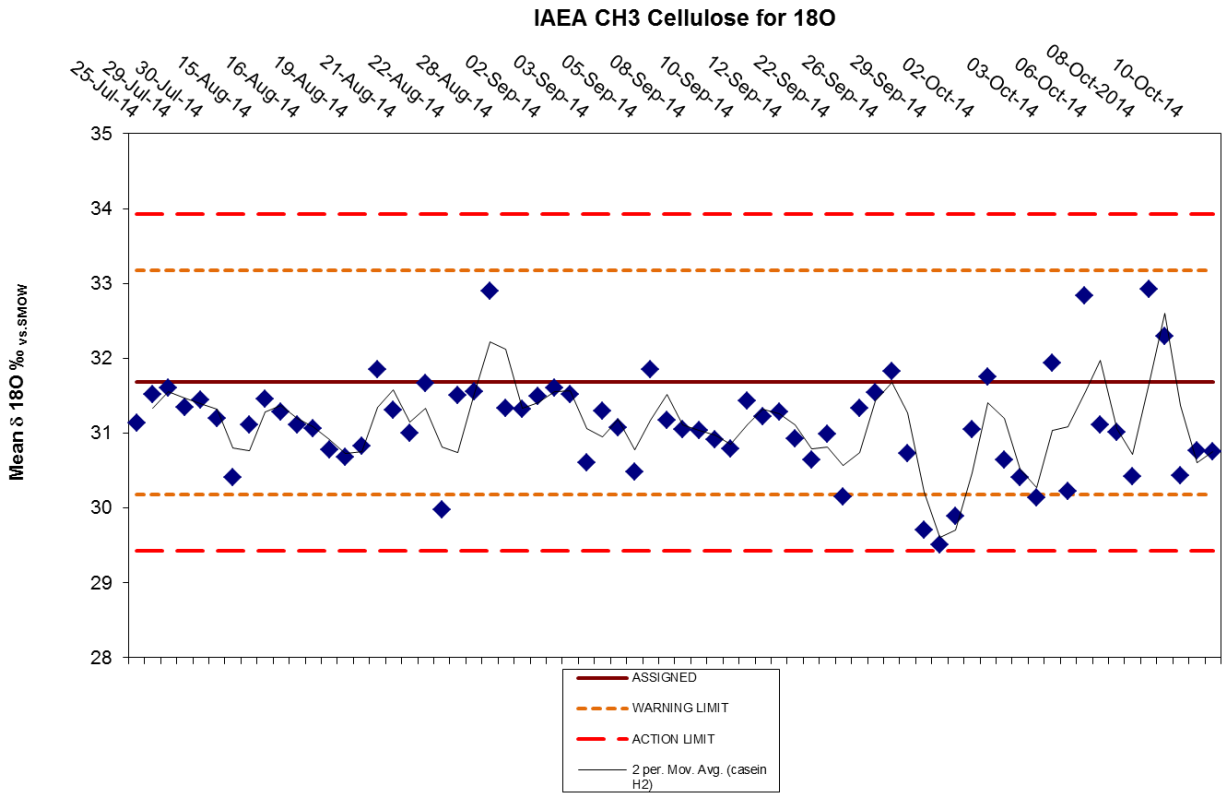

Fig. 3.9 Performance of mean $\delta^{18}O$ values measured in IAEA CH3 cellulose across analytical batches (assigned value for cellulose was -31.68 ‰, Loader *et al.*, 1999).

Table 3.7 Compilation of wood in house reference material (WIHRM) average $\delta^{18}O$ ‰ values from the analytical batches.

Date of Analysis	Average d ^{18O} ‰ $_{vs.}$ PDB	n
25-Jul-14	27.15	4
25-Jul-14	27.02	4
25-Jul-14	26.84	4
25-Jul-14	26.28	4
25-Jul-14	26.91	4
25-Jul-14	24.90	4
25-Jul-14	26.02	4
25-Jul-14	26.35	4
29-Jul-14	27.9	4
29-Jul-14	27.3	4
29-Jul-14	26.4	4
29-Jul-14	27.2	4
29-Jul-14	25.8	4

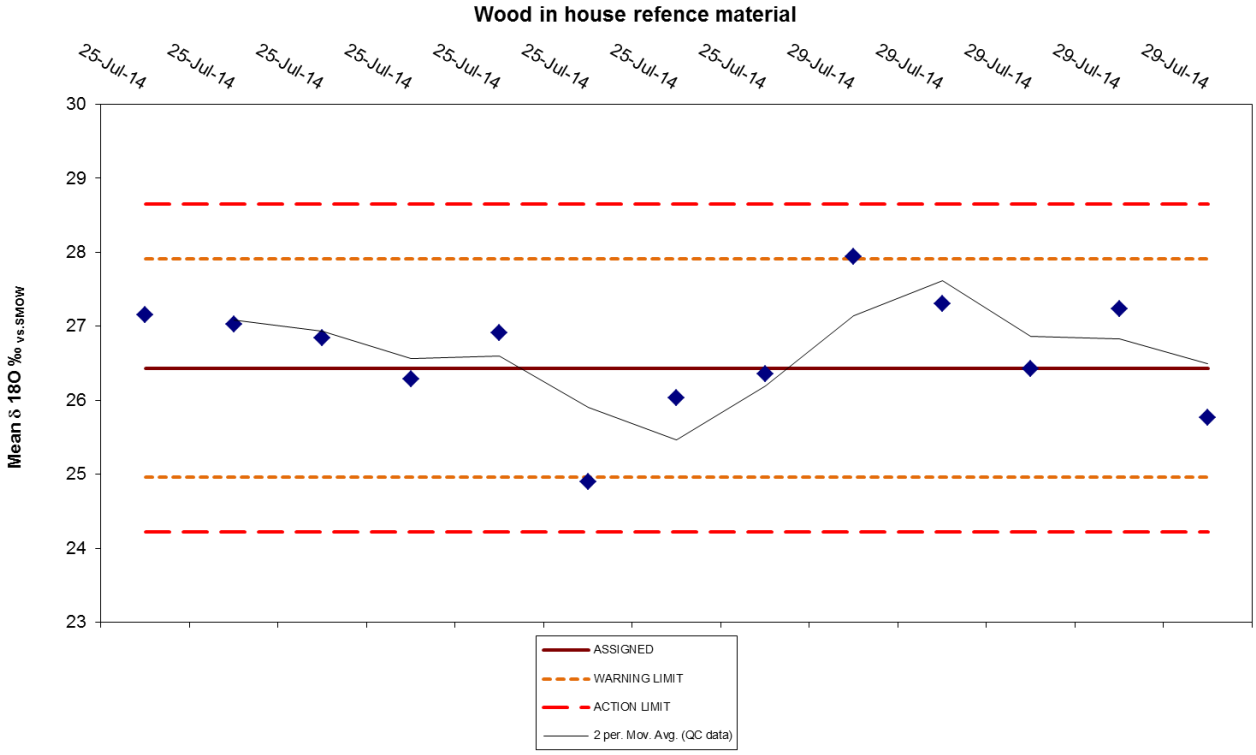

Fig. 3.10 Performance of mean $\delta^{18}O$ values measured in WIHRM cellulose with analytical batches. (Assigned value for WIHRM cellulose was 26.43 ‰)

3.3.2 Oxygen isotope composition of authentic timber samples

All data for the oxygen analysis was expressed relative to the VSMOW scale, the $\delta^{18}O$ values shown in Table 3.8. As shown in Fig. 3.11, sample groups originating from the DRC and Ghana were distinguishable from one another and the other countries in the study.

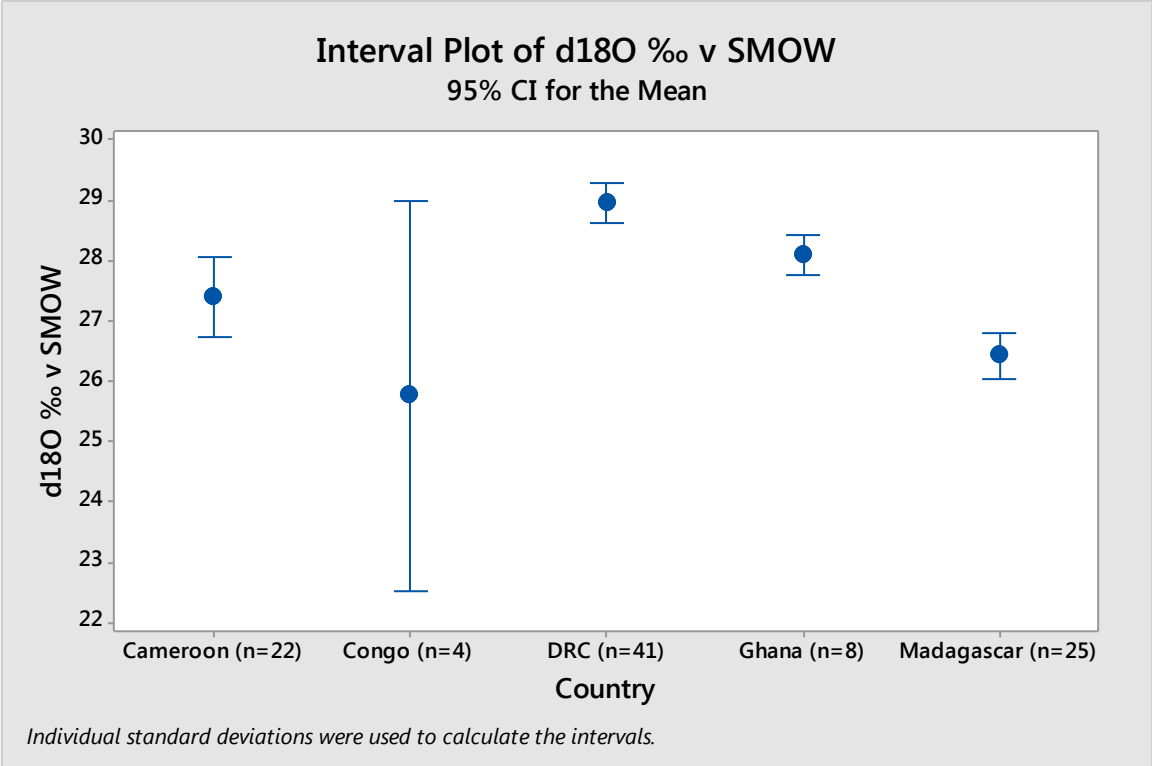

Fig. 3.11 Interval plot of timber cellulose $\delta^{18}O$ values classified by country of origin. Mean values for each country are represented by solid circles, the error bars representing the 95% confidence interval.

Table 3.8 Mean $\delta^{18}O$, standard deviation, max and minimum $\delta^{18}O$ values for timber cellulose classified by country of origin.

Country of origin	Mean $\delta^{18}O$ value (‰)	SD of Mean $\delta^{18}O$ value	Max $\delta^{18}O$ value (‰)	Min $\delta^{18}O$ value (‰)	No. of samples (n)
Cameroon	27.53	1.43	25.61	31.52	22
Congo	28.87	2.19	26.68	31.7	4
DRC	28.93	1.02	26.42	30.92	41
Ghana	29.06	0.78	27.74	28.57	8
Madagascar	27.94	1.71	24.98	28.2	25

The ^{2}H and ^{18}O isotope ratios of cellulose largely reflect the isotopic composition of the source soil water and its enrichment due to leaf and forest floor transpiration processes (Roden *et al.*, 2000; Yakir *et al.*, 2000; Barbour *et al.*, 2001). Furthermore, isotope ratios of ^{2}H and ^{18}O in soil water are influenced by localised precipitation and evapo-transpiration processes formed under equilibrium conditions, which in turn are driven by temperature (Kelly *et al.*, 2002). In tropical climates, ^{2}H and ^{18}O are more easily evaporated from the oceans, the resulting clouds isotopically enriched compared to clouds formed in sub-tropical climates. The isotopic composition of clouds slowly change with time, ^{2}H and ^{18}O, having greater affinity for the liquid phase, preferentially condensing over ^{1}H and ^{16}O as they are carried across land mass, the cloud becoming gradually enriched in ^{1}H and ^{16}O. The ^{2}H and ^{18}O isotopes of precipitation are distinct between the coast and interior (isotope gradient) of large land masses (Dansgaard *et al.*, 1964; Marshall *et al.*, 2007). Hence, latitude and altitude have a significant influence upon the fractionation of these isotopes (Dansgaard, 1964; Gat, 1980; Rozanski *et al.*, 1993; Kepler *et al.*, 2007; Horacek *et al.*, 2009).

Using the meteorological data from table 3.5, mean $\delta^{18}O$ values for the cellulose samples were plotted against mean annual temperature and rainfall for the respective countries (Fig. 3.12 & Fig. 3.13).

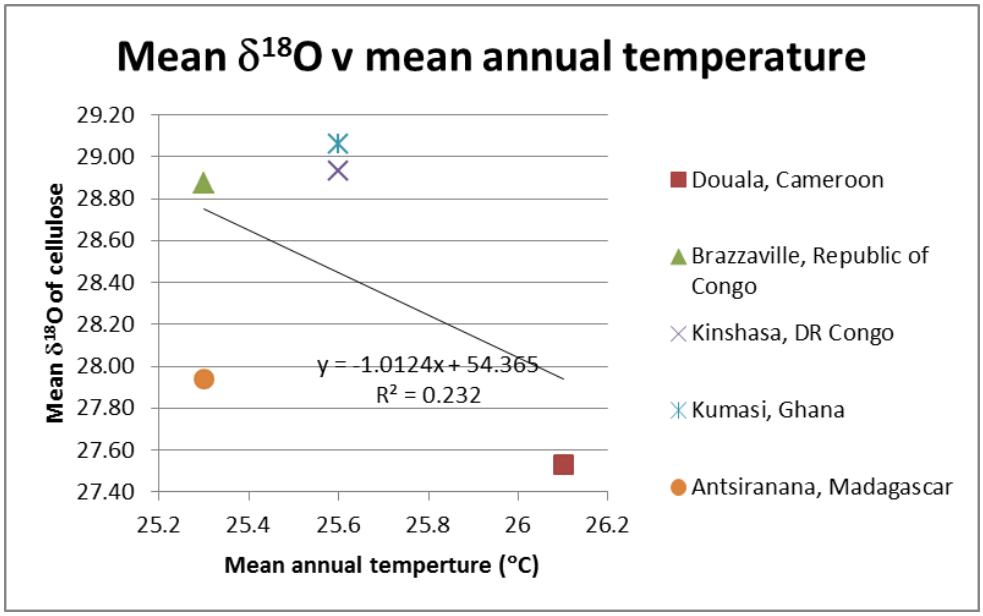

Fig. 3.12 Comparison between the mean $\delta^{18}O$ values of timber cellulose and mean country level annual temperature.

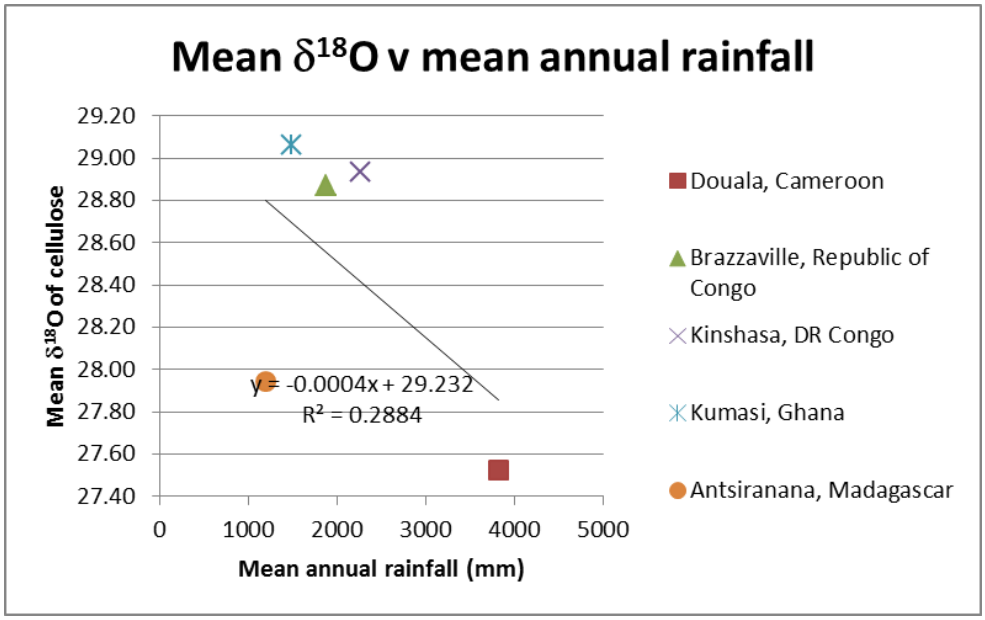

Fig. 3.13 Comparison between the mean $\delta^{18}O$ values of timber cellulose and mean annual rainfall in West Africa and Madagascar.

Fig. 3.12 and 3.13 show little correlation between the mean $\delta^{18}O$ of cellulose and mean annual temperature (R^2=0.232), as well as little correlation between the mean $\delta^{18}O$ of cellulose with mean annual rainfall (R^2=0.288). A correlation of annual rainfall with $\delta^{18}O$ of cellulose would be anticipated as this would be in agreement with the findings in literature (Craig, 1961; Dansgaard, 1964; Kelly, 2002). However, a negative, albeit small, correlation of $\delta^{18}O$ of cellulose with precipitation was unexpected. It should be considered that Douala is positioned on the Atlantic coast of Cameroon, and the temperature there may not be representative of the sampled area. Removal of the Cameroonian data point would produce a positive correlation for the line of best fit, this in agreement with literature where $\delta^{18}O$ is commonly reported as becoming correspondingly enriched with an increase in temperature (Craig, 1961; Dansgaard, 1964; Siegenthaler, 1980; Kelly, 2002).

3.3.2.1 Discussion of the oxygen isotope results

As discussed in Chapter 3.2.2, inaccuracies introduced through reliance on country level temperature and rainfall data may explain the lower than expected degree of correlation observed between the mean $\delta^{18}O$ of cellulose and mean annual precipitation. Kahmen *et al.* (2011) reported humidity, as well as temperature, has an influence on ^{18}O content of cellulose formed in tropical ecosystems. Leaf stomatal conductance and gas diffusivity are dependent upon atmospheric pressure, and the leaf-to-air-vapour pressure difference (VPD) was shown to govern the amount of exchange occurring between oxygen atoms of leaf water and cellulose, ~40% of oxygen atoms of glucose exchanging with water during cellulose synthesis, resulting in an overall enrichment of ^{18}O in leaf cellulose. This complicates interpretation of the results further, as relative humidity data was also applied at country level, and comparison with $\delta^{18}O$ of cellulose did not reveal a correlation. Clark & Fritz, (1997) reported that ^{18}O of aquifer water is the average of ^{18}O of mean annual precipitation. However, mean ^{18}O values of aquifers may vary due to evapotranspiration and enrichment of surface soil water (Marshall *et al.,* 2007). Comparing the relationship of ^{18}O in cellulose, with the variance in aquifer potential across respective countries may confirm the origin of the water, especially as the isotopes of source water undergo no fractionation during absorption by tree roots (Dawson & Ehleringer, 1993).

Assuming precipitation (rather than deep groundwater) is the main source of water for the trees and thus the hydrogen and oxygen of cellulose is derived from this water, the variability of aquifer potential across continental Africa (British Geological Survey, 2011) would be expected to have little influence on the $^{2}H/^{1}H$ and $^{18}O/^{16}O$ isotopes measured in the timber cellulose from the sampling locations in West Africa and Madagascar. However, Meinzer *et al.* (1999) reported that smaller tropical trees tended to rely on deeper water sources than nearby larger trees. Studies carried out by Thorburn & Ehleringer (1995) also found that tree roots did not always absorb water from within the same layer; instead the transportation of water through the root network was shown to be redistributed depending upon season and growing conditions. This further complicates the suggestion that ^{2}H and ^{18}O of cellulose reflect ^{2}H and ^{18}O of local precipitation. Altitude has also been shown to influence the isotopic composition (Craig, 1961; Dansgaard, 1964; Siegenthaler & Oeschger, 1980). Global positioning system (GPS) data recorded at the same time as sample collection from West Africa, enabled assessment of the influence of altitude upon the ^{18}O content of the cellulose (Fig. 3.14).

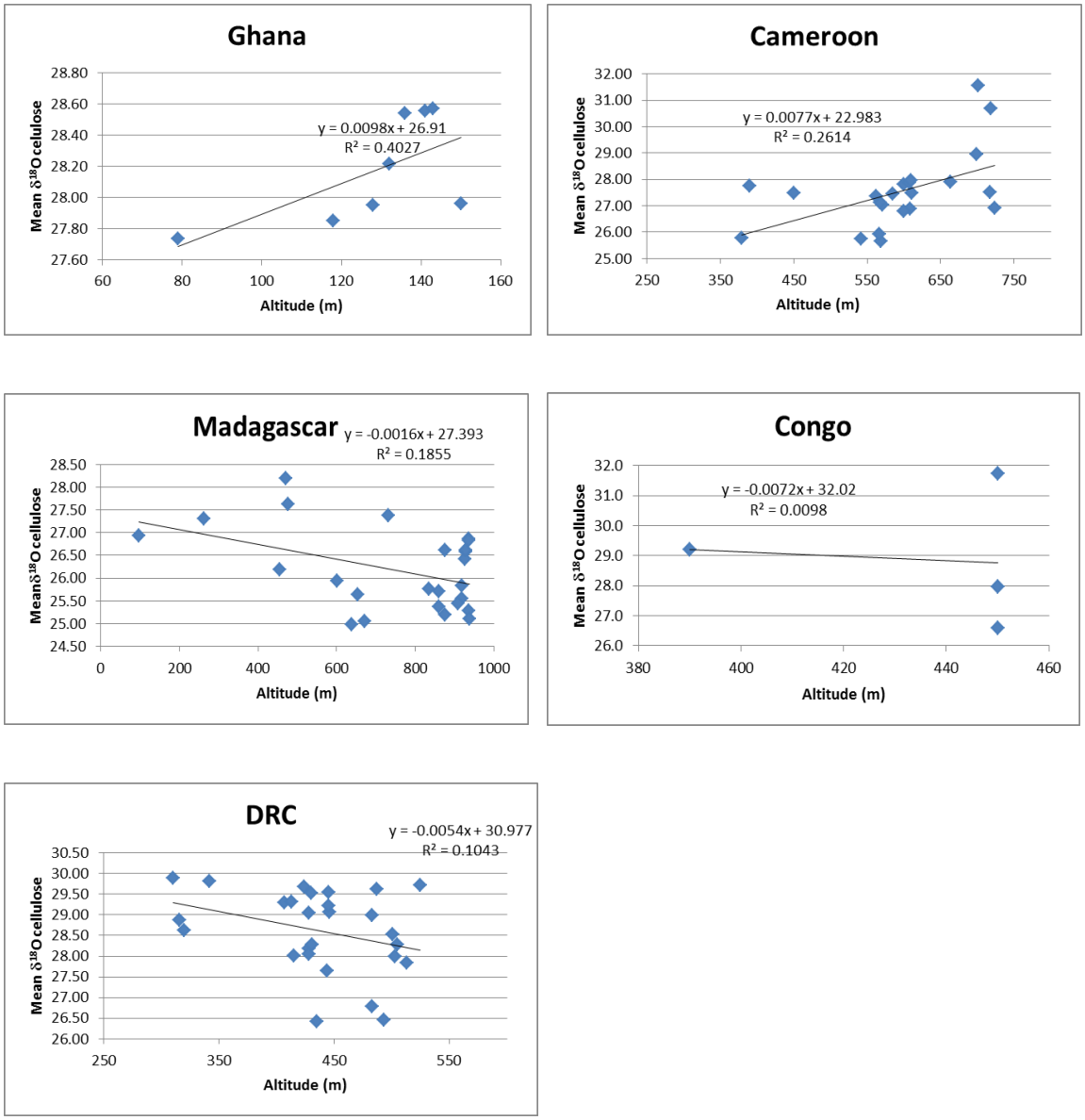

Fig. 3.14 Comparison between mean $\delta^{18}O$ of cellulose and altitude of the sampling locations for the respective countries.

Analysis of Figure 3.14 reveals a weak positive correlation for $\delta^{18}O$ of cellulose as a function of altitude for the Cameroon and Ghanaian sample sets. Very little correlation was observed for the Congolese data, however the small number of samples (n=4) makes it difficult to offer a robust evaluation. The positive correlation observed with the Cameroon and Ghanaian sample sets did not follow the widely accepted trend of increasing ^{18}O depletion as a function of increasing altitude. (Dansgaard, 1964; Marshall, 2007). However, studies assessing the correlation between increasing

altitude and ^{18}O depletion have often only been assessed from precipitation, and tend to overlook the effect of biological fractionation upon isotopic content of plants and trees. A possible explanation is the effect of atmospheric pressure upon the fractionation of ^{18}O (Kahmen, 2011). The relationship of decreasing pressure and increasing altitude has the effect of increasing gaseous binary diffusion of ^{18}O from plant leaves (Gohil *et al*., 2011). Elevated stomatal conductance has been shown to increase under these conditions, resulting in an enrichment of ^{18}O in plant tissue water, ^{16}O preferentially evaporating over ^{18}O (Kahmen *et al.*, 2011).

3.4 Analysis of stable isotope of hydrogen ($^{2}H/^{1}H$ ratio)

3.4.1 Quality controls for the hydrogen stable isotope ratio analysis

For the purposes of monitoring and instrument performance, quality control IAEA CH3 was routinely analysed in quadruplicate and the $^{1}H/^{2}H$ ratios measured along with each batch of purified timber cellulose samples. Standard deviation warning and action limits were set at 2 and 3 times the standard deviation of 3 ‰ respectively. Batch precision for the ^{2}H measurements of the IAEA CH3 cellulose are shown in Table 3.9 and illustrated data is available in Figure 3.15, all of the data points falling within 2.2 standard deviations of the assigned value. Repeatability of the cellulose extraction procedure was assessed using a wood in house reference material. This was extracted and analysed with each analytical batch. Data for the wood in house reference material is available in Table 3.10 and Fig. 3.16, all of the data points falling within 2.6 standard deviations of the assigned value.

Table 3.9 Performance of IAEA CH3 cellulose mean δ^2H values measured as part of analytical batches (assigned value was -41.73 ‰).

Date of analysis	Average δ2H ‰ vs.SMOW	SD or ABS (‰)	n
25-Jul-14	-37.1	2.70	2
29-Jul-14	-42.1	4.00	2
30-Jul-14	-43.4	1.69	3
15-Aug-14	-41.9	1.36	3
16-Aug-14	-45.2	2.83	3
19-Aug-14	-41.1	2.16	3
21-Aug-14	-41.3	2.99	3
22-Aug-14	-41.1	1.21	3
14-Sep-14	-41.1	1.29	3
01-Sep-14	-43.1	0.45	3
03-Sep-14	-43.2	1.77	3
05-Sep-14	-45.2	0.66	3
08-Sep-14	-41.0	1.91	3
10-Sep-14	-39.2	0.69	3
12-Sep-14	-41.9	2.82	3
22-Sep-14	-41.3	1.10	3
26-Sep-14	-38.4	2.44	3
29-Sep-14	-39.4	1.91	3
30-Sep-14	-45.6	1.75	3
03-Oct-14	-40.7	1.25	3
04-Oct-14	-44.1	2.25	3
06-Oct-14	-41.6	2.77	3
07-Oct-14	-41.3	1.10	3

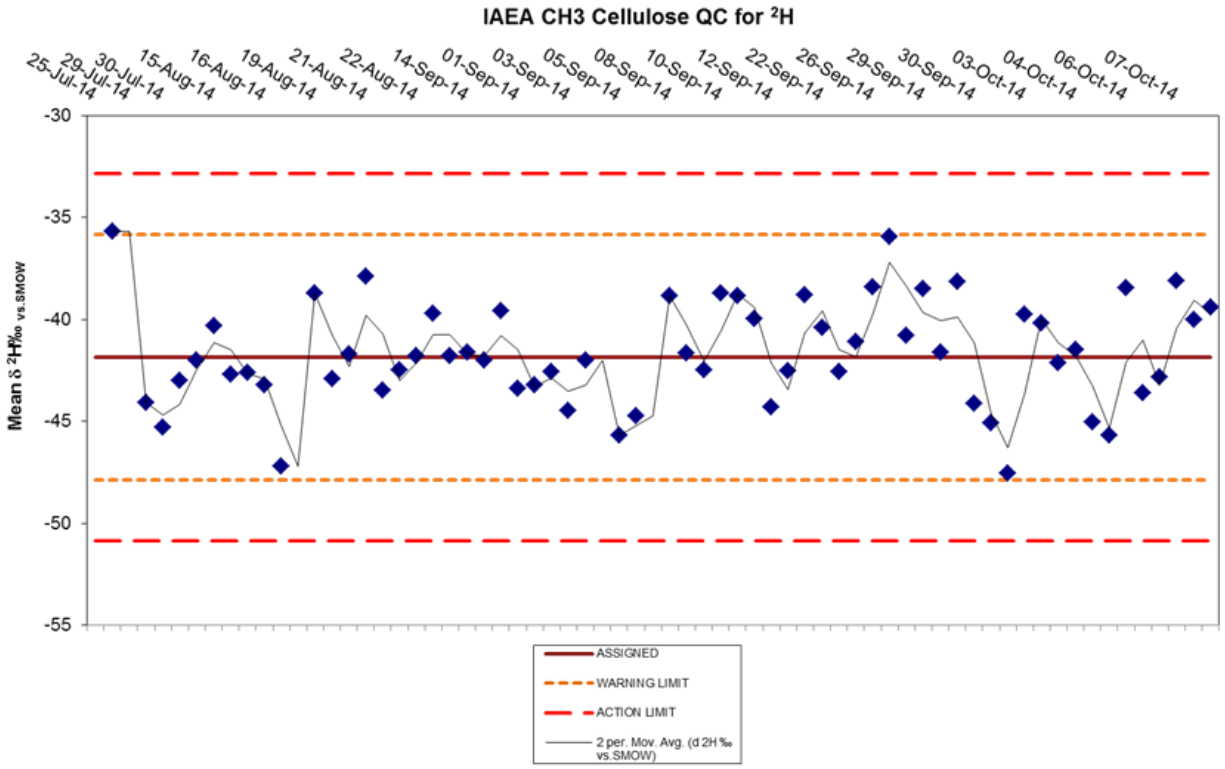

Fig. 3.15 Performance of IAEA CH3 cellulose measured as part of analytical batches.

Table 3.10 Compilation of WIHRM mean δ^2H ‰ values from the analytical batches (assigned value for WIHRM cellulose was -77.1 ‰).

Date of Analysis	Average δ^2H ‰ $_{vs.}$SMOW	n
25-Jul-14	-75.9	4
25-Jul-14	-77.5	4
25-Jul-14	-77.7	4
25-Jul-14	-80.3	4
25-Jul-14	-79.8	4
25-Jul-14	-79.3	4
25-Jul-14	-78.5	4
25-Jul-14	-81.1	4
29-Jul-14	-74.1	4
29-Jul-14	-74.6	4
29-Jul-14	-75.7	4
29-Jul-14	-73.4	4
29-Jul-14	-74.6	4

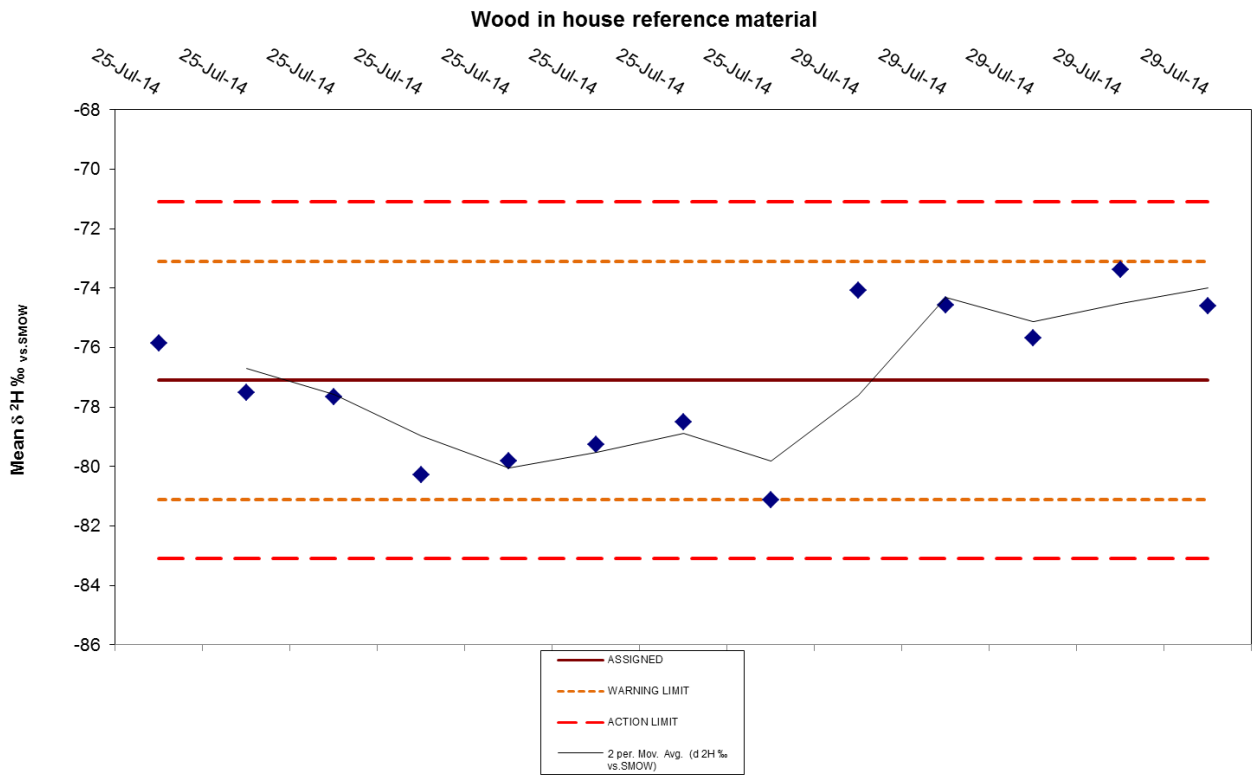

Fig. 3.16 Performance of WIHRM cellulose measured as part of analytical batches.

3.4.2 Hydrogen isotope composition of timber

All data for the hydrogen analysis was expressed relative to the VSMOW scale, the δ^2H values shown in Table 3.11. As shown in Fig. 3.17, only the Ghanaian sample group was distinguishable, and there was a noticeable inter-country variation for δ^2H of the timber cellulose.

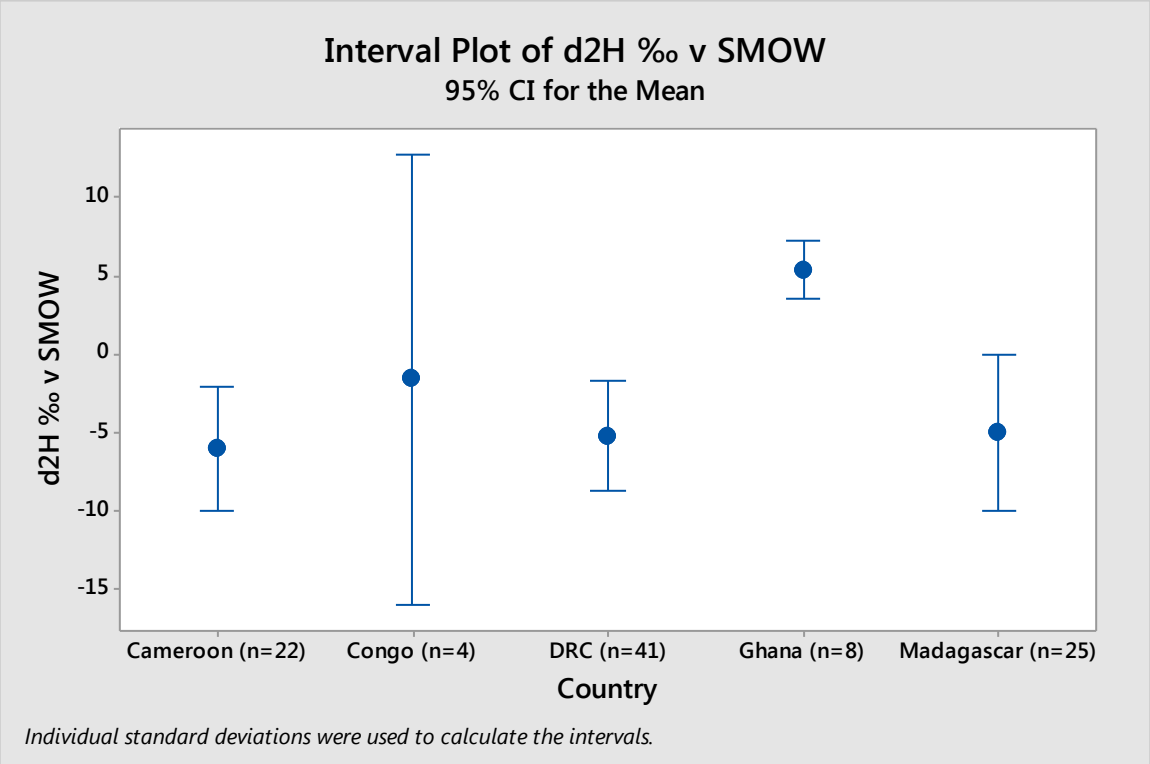

Fig. 3.17 Interval plot of timber cellulose δ^2H values classified by country of origin. Mean values for each country are represented by solid circles, the error bars representing the 95% confidence interval.

Table 3.11 Mean δ^2H, standard deviation, max and minimum δ^2H values for timber cellulose classified by country of origin.

Country of Origin	Mean δ^2H Value (‰)	SD of Mean δ^2H value	Max δ^2H value (‰)	Min δ^2H value (‰)	No. of samples (n)
Cameroon	-8.2	8.00	-19.4	4.7	22
Congo	2.6	3.10	-0.7	6.4	4
DRC	-5.4	9.49	-20.4	20.3	41
Ghana	-3.4	10.28	2.4	10.5	8
Madagascar	-4.3	12.44	-34.1	19.1	25

The standard deviations for the mean δ^2H of the respective countries samples are much greater than those ranges observed in the samples for ^{18}O. The noticeably wide standard deviations could be attributed to experimental factors such as measurement precision, a lack of suitable matrix matched standards within the δ^2H range of the samples, or fractionation caused by problems posed by exchangeable hydrogen during cellulose purification and analysis. Hydrogen also has the largest mass difference than any other elements resulting in the most variable δ values, this could also explain the observed variability for ^2H measured in cellulose.

As discussed previously, the ^2H and ^{18}O isotope ratios of cellulose have been shown to reflect the isotopic composition of local precipitation and tree root source water. (Craig, 1961; Dansgaard, 1964; Friedman *et al*., 1964). The relationship between hydrogen and oxygen isotopes of precipitation have also been shown to be closely related, plotted as the global meteoric water line (GMWL) and explained in the formula: $\delta^2H = 8\ \delta^{18}O + 10$ (Craig, 1961: Rozanski, 1993). The vapour pressure of ^2H_2O is nearly 40 torr lower than that of ^1H_2O, vapour pressure is inversely proportional to intermolecular forces and the ^2H—O bonds are stronger than the ^1H—O bonds. Thus, evaporation will

lead to observable fractionation, resulting in a depletion of ^{2}H in the vapour phase and an enrichment of ^{1}H in the liquid phase (Sulzman, 2008). If ^{2}H and ^{18}O of precipitation are shown to be highly correlated, and cellulose of timber is shown to reflect local source water and precipitation, one might expect the same correlation to be observed for ^{2}H and ^{18}O in the cellulose samples for the respective countries of origin. To investigate further, predicted mean ^{2}H and ^{18}O values of precipitation for the respective countries were calculated using the online resource at water isotopes: http://wateriso.utah.edu/waterisotopes/pages/data_access/form.html (Bowen and Revenaugh, 2003). Isotope data for ^{2}H and ^{18}O of the timber cellulose were plotted, as well as the predicted ^{2}H and ^{18}O values from the precipitation calculator, and a line of best fit applied to each set of results to enable comparison of data sets (Fig. 3.18).

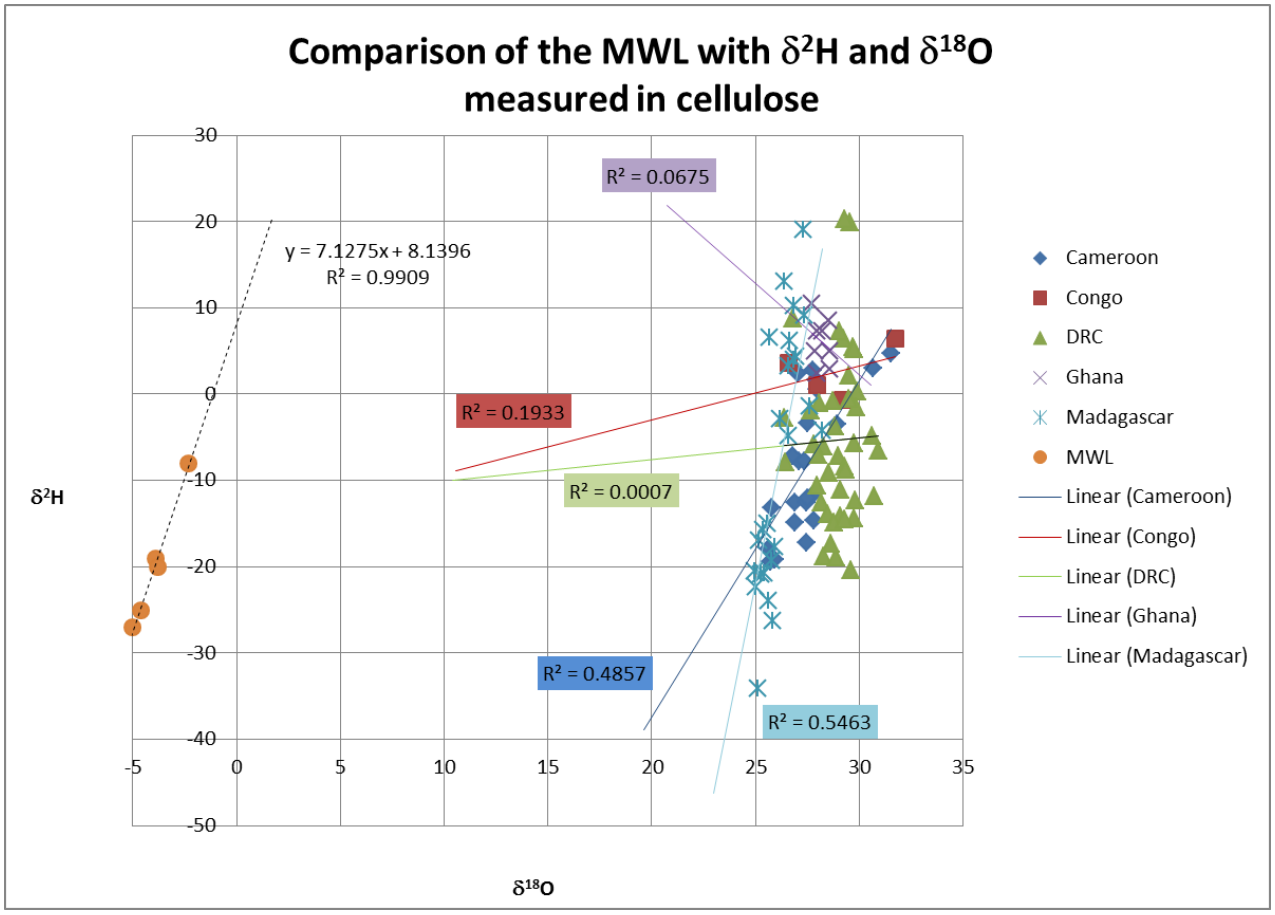

Fig. 3.18 Values for $\delta^{18}O$ and $\delta^{2}H$ calculated from precipitation (MWL) and measured in cellulose.

3.4.2.1 Discussion of the hydrogen isotope results

Linear relationships were obtained by plotting the respective countries mean values for predicted ^{2}H and ^{18}O of precipitation with ^{2}H and ^{18}O of cellulose. The degree of correlation of the cellulose samples with the MWL (Meteoric Water Line) was assessed by study of the calculated R^2 values. Correlation values for the country groups were as follows: Madagascar (R^2=0.55), Cameroon (R^2=0.49), Congo (R^2=0.19), Ghana (R^2=0.00) and DRC (R^2=0.00). The discrepancy in sample numbers between the country groups (Cameroon, n=22), (Congo, n=4), (DRC, n=41), (Ghana, n=8), (Madagascar, n=25), complicates assessment of the isotopic relationship of the MWL with the cellulose of tropical timber in the respective countries. The intercept and gradients for the lines of best fit for the country groupings are significantly different not only from one another, but also from the MWL. They show a deviation from unity indicating the source trees may have varied morphologically, and may have been subjected to a variety of localised environmental fractionation effects upon the isotopologues of water during cellulose biosynthesis. Fractionation of ^{2}H and ^{18}O of water does not take place during tree root uptake or during transfer through xylem (Dawson and Ehleringer, 1991), but it has been shown to undergo fractionation as leaf water exchanges with glucose at the site of biosynthesis within leaf tissue (Kahmen *et al.*, 2011). Atmospheric pressure governing gas diffusivity and leaf stomatal conductance, as well as the influence of photosynthetic activity upon cellular respiration all contribute to the fractionation of hydrogen isotopes during plant metabolism (Farquhar & Richards, 1984). Deviation of the sample line from the MWL is likely to be caused by deuterium excess, where the slower binary diffusion of $^{2}H^{16}O$, and the preferential evaporation of $^{1}H^{16}O$ into the gas phase, results in an enrichment of ^{2}H in the remaining leaf tissue water (Pfahl and Sodemann, 2014). As highlighted in the earlier sections of this chapter, measurements of local environmental conditions at respective sampling sites were not recorded, and hence, it is impossible to make a full assessment of influence of localised effects responsible for the enrichment of ^{2}H in the timber cellulose.

3.5 Conclusions

Analysis of stable isotopes of timber cellulose from Madagascar and West Africa could give useful insight into a number of environmental factors governing growth of the trees. Little variation of temperature between the respective countries meant that the influence of temperature upon isotopic fractionation could not be investigated further. However, carbon stable isotopes were shown to have the slight degree of correlation with wind speed and humidity, suggesting wind could be responsible for interrupting the flow of forest sources of CO_2, particularly the mixing of understory CO_2 with atmospheric CO_2 in the forest canopy. Increased wind speed was observed to correspond with a drop in relative humidity, thus influencing the water vapour pressure in the microclimate of the forest, in turn governing leaf stomata conductance and the degree of isotope fractionation taking place. The relationship between ^{2}H and ^{18}O of precipitation (MWL) and timber cellulose was shown to exhibit a low degree of correlation for the Cameroon and Madagascan samples, suggesting localised precipitation could be a main water source of the trees belonging to those sample sets. The offset between ^{2}H and ^{18}O of precipitation and cellulose confirmed these isotopes underwent a degree of fractionation during cellulose biosynthesis. Sample sets for the Congo (n=4) and Ghana (n=8), showed no correlation with the MWL, the low sample numbers in those data sets making interpretation of geophysical influences of the trees difficult. Furthermore, samples for the DRC group (n=41) also showed no correlation with MWL, the deviation from unity indicating that many of the trees in this sample group were exposed to elevated levels of humidity during cellulose biosynthesis (McGuire & McDonnell, 2007).

Climatic factors such as altitude and rainfall were also shown to potentially influence the degree of ^{18}O isotopic fractionation. Further study of climatic and environmental induced fractionation effects would have been made possible with the additional recording of physical and meteorological records at the various sampling sites. Moreover, the analysis of individual tree ring time series, in combination with meteorological and physical data, could add an extra level of confirmation into how climatic and physical variables contribute to isotope fractionation in timber cellulose. With the exception of Madagascar and Ghana, stable isotope analysis of timber cellulose alone may not

produce a clear enough distinction between the respective sample groups. A combination of isotopic and trace element data may offer more promise for increasing country classification and cross validation accuracy.

Chapter 4 – Identification of timber origin

4.1 Introduction

This chapter will deal with the statistical processing of the results, making assessment of the data acquired by the individual methodologies of stable isotope ratio and trace element analysis, and how this influences the country of origin classification when processed by multivariate statistical analysis. It will then assess whether the classification rate can be improved by combining the stable isotope and trace element data in the multivariate statistical analysis. Assessment of intra and inter site variation of stable isotopes and trace elements within a single timber species will also be covered, as well as a conclusion of those results.

4.2 Evaluation of the stable isotope ratio data

To assess the suitability of stable isotope ratio data in geographical origin classification, data for $\delta^{13}C$, $\delta^{2}H$ and $\delta^{18}O$ were subjected to a 'stepwise' canonical discriminant analysis (CDA). The multivariate model was produced using country classification, with samples grouped into their respective country of origin as shown in Fig. 4.1. The results of the CDA are represented by group centroids in Fig. 4.1, with 69% and 68% of group and cross validated cases correctly classified, respectively. Data for $\delta^{13}C$, $\delta^{2}H$ and $\delta^{18}O$ were all used in the multivariate discrimination. Function 1 (*x*-axis) provided 91% of the variance in the CDA, with $\delta^{13}C$ and $\delta^{18}O$ contributing the most to the discrimination, whereas function 2 (*y*-axis) provided only 8%, $\delta^{13}C$ and $\delta^{2}H$ contributing the most to the discrimination. Except for the Ghanaian sample group, $\delta^{2}H$ of the Cameroon, Congolese, DRC and Madagascan timber samples were shown to have a high degree of intra-country variation, and a significant overlap was observed at the inter-country level. This most likely explains why $\delta^{2}H$ contributed only a small influence in the multivariate discrimination, $\delta^{2}H$ contributing to the discrimination in only the 2^{nd} function of the CDA.

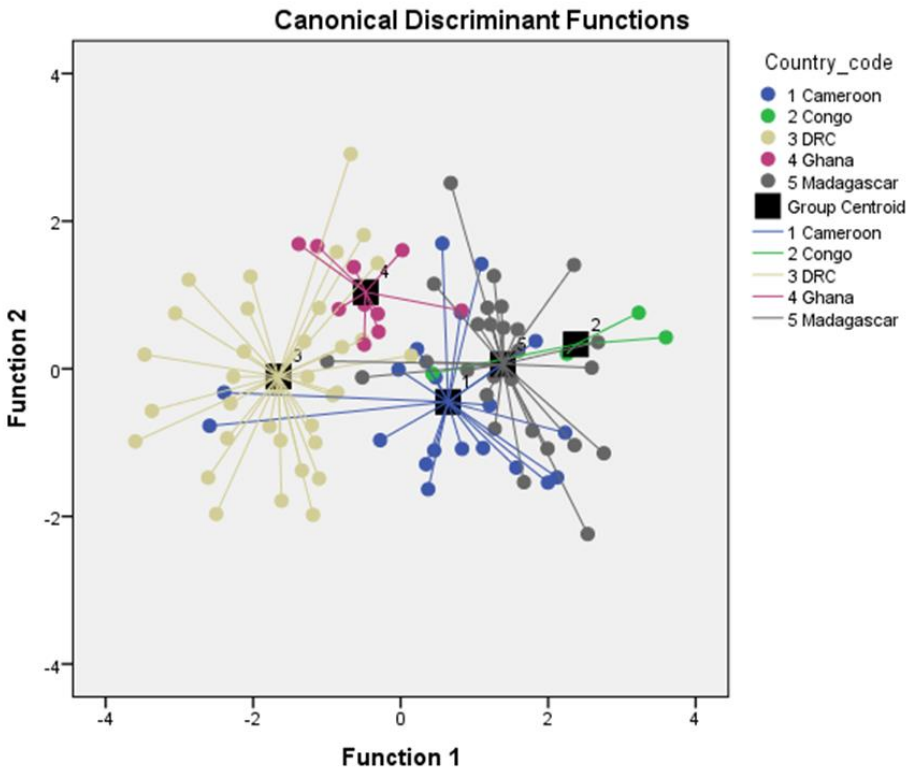

Fig. 4.1 Cross plot of timber cellulose stable isotope data for all countries, separated by two discriminant functions calculated from the step-wise canonical discriminant analysis.

Despite only three elements featuring in the isotope discrimination, there was a complete separation of the DRC sample group from Congo, and a nearly complete separation of DRC from Cameroon and Madagascar. Overlap is observed between Ghana and DRC, but the Ghanaian sample group is nearly completely resolved from the Cameroon, Congo and Madagascar sample groups.

4.3 Evaluation of the multi element data

The multi element dataset was interrogated by the same stepwise canonical discriminant analysis as the stable isotope ratio data for the timber samples. The multivariate model was produced using country classification, with samples grouped into their respective country of origin as shown previously in Fig. 2.2. The spread of data points for each country is represented by the group centroid, with 86% of original group cases correctly classified and 80% of cross validated grouped cases correctly classified. Function 1 (*x*-axis) and function 2 (*y*-axis) accounted for 65% and 24% of the

variance respectively. A total of 11 trace elements, zirconium (Zr), molybdenum (Mo), strontium (Sr), manganese (Mn), arsenic (As), antimony (Sb), selenium (Se), boron (B), magnesium (Mg), titanium (Ti), and cobalt (Co) were selected by the software for the multivariate discrimination.

As discussed in Chapter 2, the majority of the trace elements measured in the Congolese samples were significantly more concentrated than those measured in the Cameroon, Ghanaian DRC and Madagascan sample groups. The elevated concentrations, most likely a result of anthropogenic activity, appear to dominate the discrimination of the West Africa samples, resulting in those sample groups clustering together after multivariate processing. Exclusion of the Congolese sample set (Fig. 2.4) increased the grouped case classification rate of the multivariate model from 86% to 99%, the number of cases of cross validated groups also increasing from 81% to 83%. Function 1 (*x*-axis) and function 2 (*y*-axis) provided 71% and 23% of the variance, respectively, with 11 trace elements, (holmium (Ho), erbium (Er), thulium (Tm), ytterbium (Yb), lutetium (Lt), hafnium (Hf), thallium (Tl), lead (Pb), bismuth (Bi), thorium (th), and uranium (U) selected by the software for the multivariate discrimination. Complete separation of Madagascan and DRC sample groups was achieved, with the Ghanaian sample group nearly completely resolved from Cameroon.

4.4 Evaluation of the combined stable isotope ratio and multi element data

In order to construct a robust multivariate model and test if the classification rate of the sample groups could be improved, stable isotope ratios $\delta^{13}C$, $\delta^{2}H$ and $\delta^{18}O$ were included with the multi element data. The results of the CDA are represented by group centroids in Fig. 4.2, 100% and 87% of group and cross validated cases correctly classified, respectively. The twelve variables selected by the software for this multivariate discrimination were Mo, Zn, Ca, As, $\delta^{13}C$, $\delta^{18}O$, Sb, Mn, Pb, Cu, La, and Ba. Function 1 (*x*-axis) provided 51% of the variance in the CDA, and was primarily correlated with Mo, Ca, Sb, and $\delta^{18}O$, while function 2 (*y*-axis) provided 27% of the variance, and was mainly influenced by Mn, Cu, La, and $\delta^{13}C$.

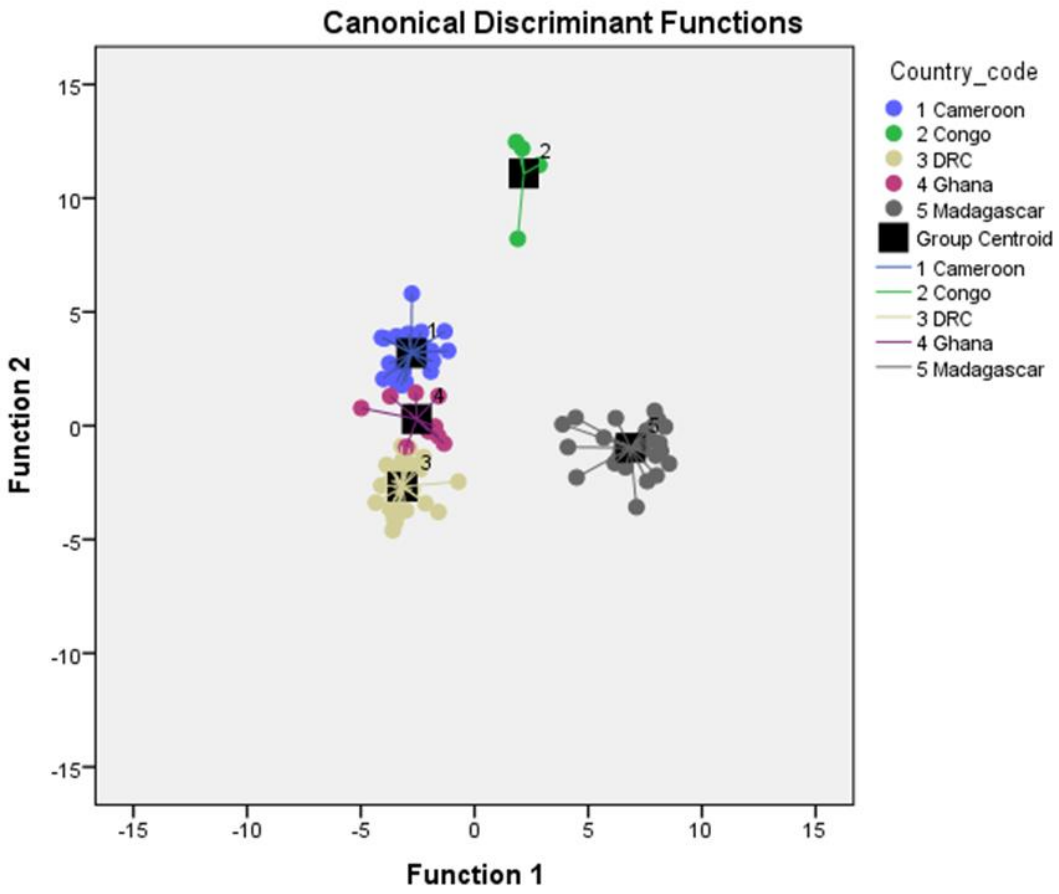

Fig. 4.2 Cross plot of timber multi element and stable isotope data for all countries, separated by two discriminant functions calculated from the step-wise canonical discriminant analysis.

4.5 Evaluation of inter and intra-site variation of stable isotopes and trace elements within the same species

To assess the inter-site and intra-site variation of stable isotope and trace element concentrations, and test the hypothesis that both geology and geography has an influence on the stable isotope and trace element profile of timber, two sampling locations separated by a distance of 355 kilometres were selected from within Cameroon and the stable isotope and trace element profiles of the timber samples from those locations compared. Goume-Goffi foret secondaire lies approximately 700 meters above sea level and is situated on silicic geology in the east of the country, 460 kilometres from the sea. Foret, UFA lies approximately 200 meters above sea level on metaigneous geology, 135 kilometres from the sea, in the west of the country. Samples taken at the respective sites were taken from the same species of tree and at no more than 10 metres apart.

Distance from sea and altitude have previously been shown to influence the stable isotopes of δ^2H and $\delta^{18}O$ (Keppler *et al*., 2007; Horacek *et al.*, 2009). Study of Figure 4.3 reveals δ^2H varied at both inter-site and intra-site levels. This is a likely explanation as to why hydrogen did not influence the discrimination of the CDA in Fig. 4.2. Variation of ^{18}O was only observed within site at Goume-Goffi foret secondaire and there was a notable offset of ~3 per mil for ^{18}O between the site and Foret, UFA. Altitude and distance from the sea could be possible contributors to ^{18}O isotopic difference between the sites, as well as precipitation and evapotranspiration.

Figs. 4.4 to 4.7 show significantly lower concentrations of lithium, aluminium, copper, titanium, yttrium, neodymium trace elements were present in timber at Foret, UFA. Furthermore, calcium and strontium concentrations were shown to be greatest at the Foret, UFA site. Despite significant differences in concentrations of many of these elements between the two locations, in some instances the intra site variation was greater, making study of the relationship between the underlying lithology and trace element concentration in timber difficult. However, calcium and strontium concentrations varied the most between sites and were highly correlated, suggesting these may be derived from the same lithology.

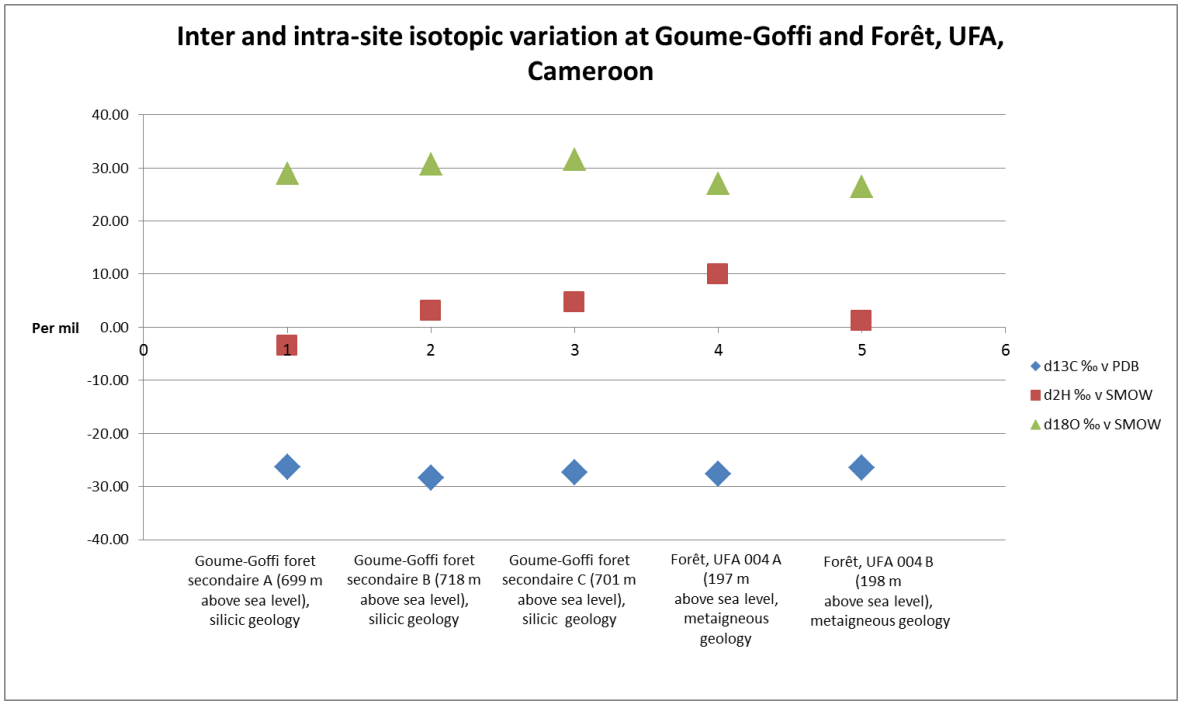

Fig. 4.3 Comparison of inter and intra-site isotopic variation of $\delta^{13}C$, $\delta^{2}H$ and $\delta^{18}O$ in timber samples of *Entandrophragma cylindricum* at sampling locations in eastern and western Cameroon.

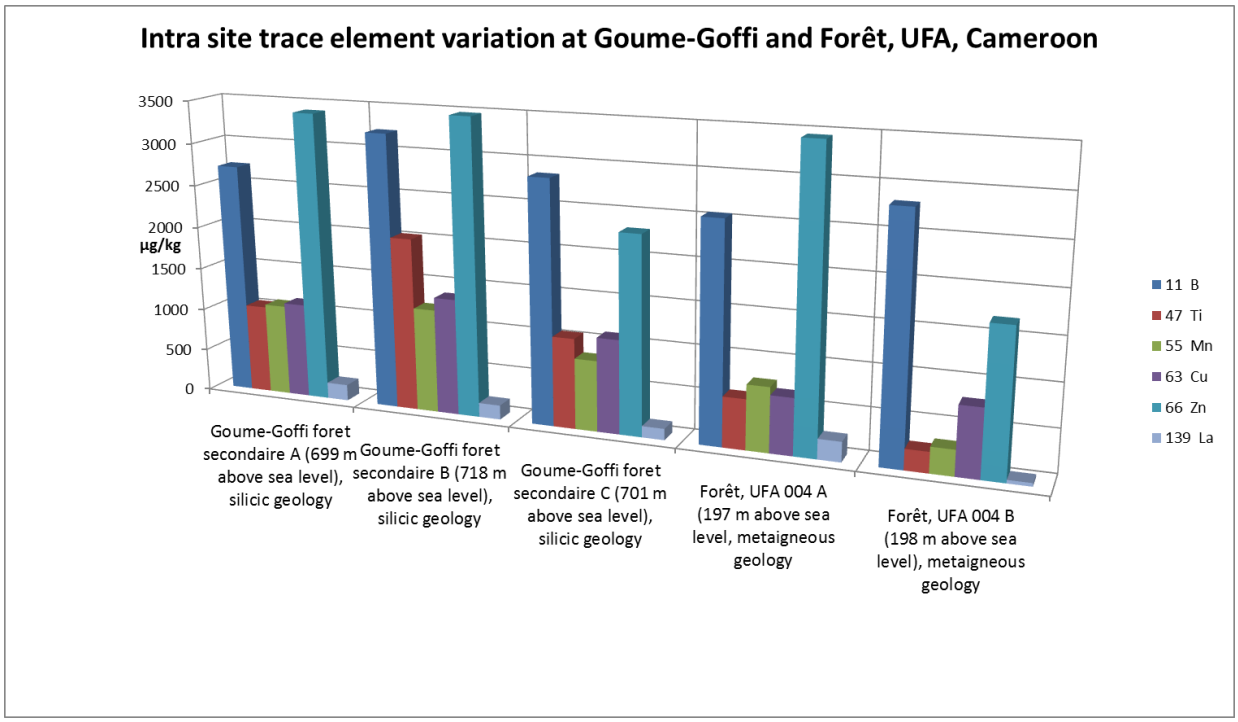

Fig. 4.4 Comparison of inter and intra-site variation of B, Ti, Mn, Cu, Zn and La trace element concentrations in timber samples of *Entandrophragma cylindricum* at sampling locations in eastern and western Cameroon.

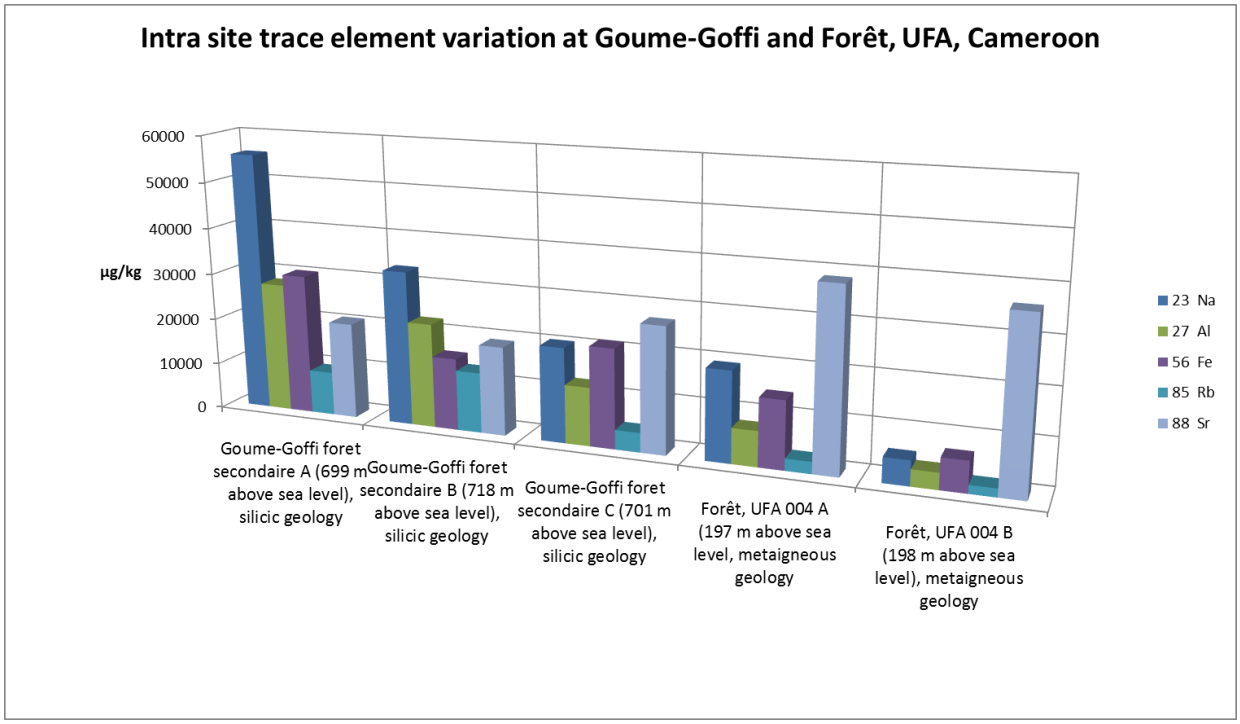

Fig. 4.5 Comparison of inter and intra-site variation of Na, Al, Fe, Rb, and Sr trace element concentrations in timber samples of *Entandrophragma cylindricum* at sampling locations in eastern and western Cameroon.

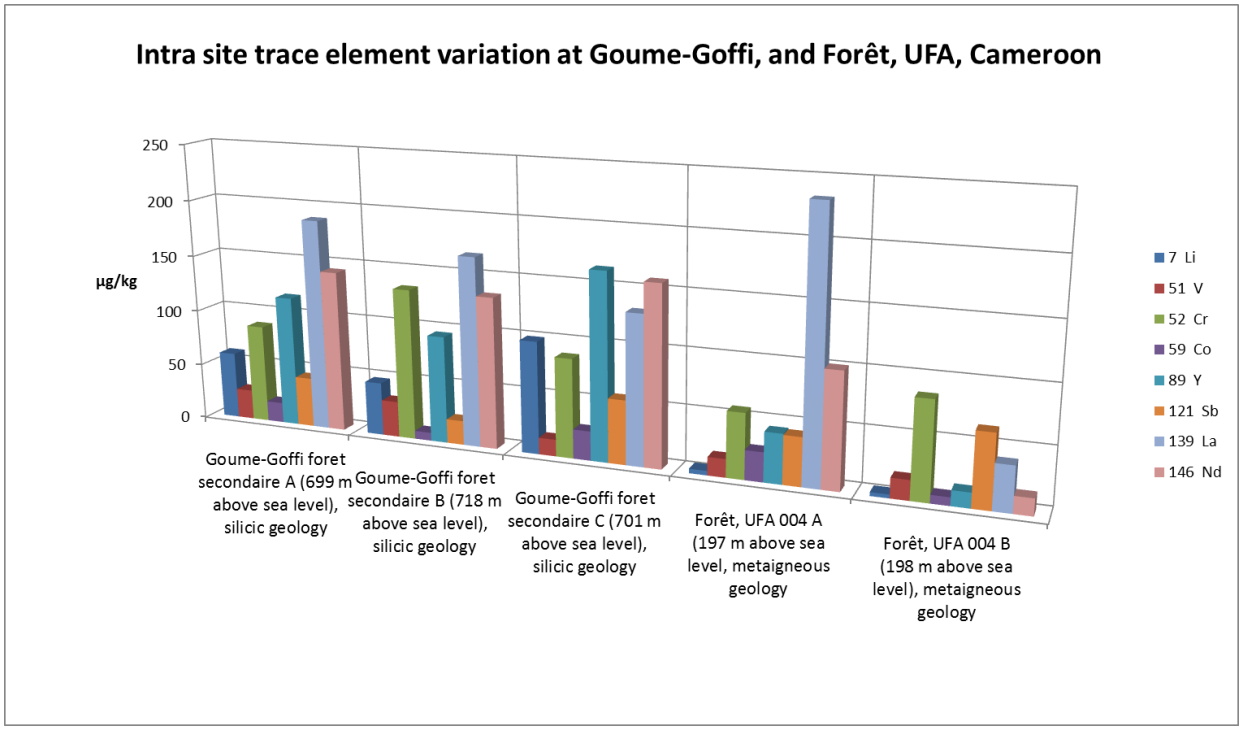

Fig. 4.6 Comparison of inter and intra-site variation of Li, V, Cr, Co, Y, Sb, La, and Nd trace element concentrations in timber samples of *Entandrophragma cylindricum* at sampling locations in eastern and western Cameroon.

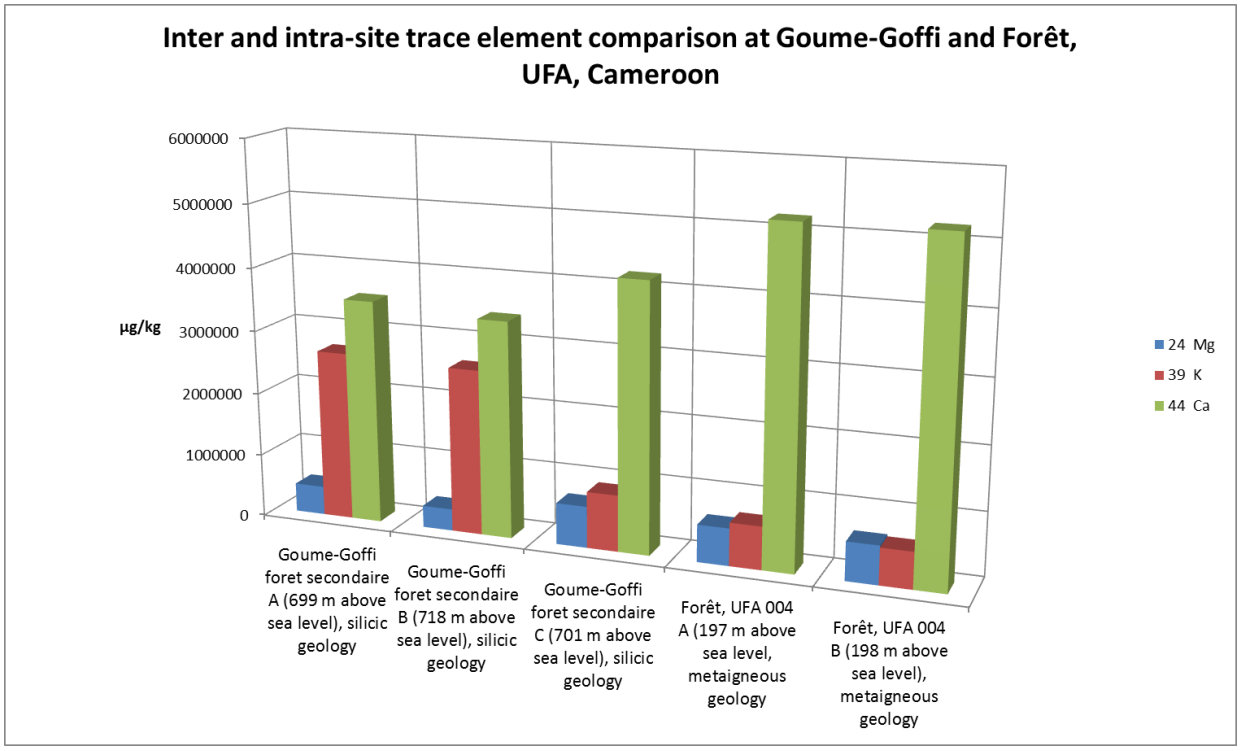

Fig. 4.7 Comparison of inter and intra-site variation of Mg, K, and Ca trace element concentrations in timber samples of *Entandrophragma cylindricum* at sampling locations in eastern and western Cameroon.

4.6 Conclusions

The combination of stable isotope ratio and multi element data was found to achieve the highest degree of discrimination between the sample sets, the combined approach proving more powerful than either individual analysis technique in providing accurate country of origin classification. The high degree of overlap and intra-country variability of δ^2H across the respective sample groups resulted in δ^2H providing only a small degree of discrimination in the cross plots where only isotopes were applied (Fig. 4.1). The high degree of variability meant that δ^2H was not selected by the CDA for origin classification when isotopes and trace elements were combined. Improvements to the preparation techniques and an increase in the measurement precision for δ^2H could improve the group and cross validation classification rates, increasing the robustness of the multivariate discrimination model. The great distance of tropical rainforests from industrial activity often means they are less prone to the influence of pollution from anthropogenic sources. In this study, it was hypothesised that the trace element profile of the Congolese samples was influenced by anthropogenic activity through their locality and subsequent exposure to the Sangha River, of which, passes through neighbouring Cameroon and Central Africa Republic where industrial mining takes place. In a wider study, anthropogenic inputs may prove limiting to the country level discrimination, especially if the selected trace element parameters are prone to contamination in nature. To account for only natural variation in trace element concentrations, the Congolese sample set was removed from the CDA. With respect to Figs. 2.2 and 4.2, exclusion of the Congolese samples from the multivariate discrimination improved group and cross validation classification rates for the remaining West African and Madagascan sample groups. Only the Ghanaian and Cameroon sample groups could not be completely resolved. Ti was shown to play a role in the multivariate discrimination both before and after exclusion of the Congolese samples, although the other ten elements selected by the software for the first CDA (Fig. 2.2) did not enable sufficient discrimination in the second multivariate analysis (Fig. 4.2). This is not surprising as Mo, B, Mg and Mn are all nutrients which play a role in tree biochemistry, hence measurable concentrations of these elements would be expected within all of the timber samples (Barker & Pilbeam, 2007). The majority of the eleven trace elements selected by the

software for the second multivariate discrimination have no known biological role, with Pb known as a phytotoxic transition metal (Peterson & Anderson, 1990). As and Pb contributed to the discrimination of both the first and second multivariate models, indicating that concentrations of these elements varied inter-site. Concentrations of heavy metals such as As and Pb, as well as a number of other trace elements measured in timber have been shown to be susceptible to fluctuation above background levels normally measured in nature (Tangahu *et al*., 2011). Therefore, it is important to make careful consideration of the trace elements involved in multivariate discrimination, especially if the model is to maintain its robustness during the course of several years where changes in the concentrations of trace elements may occur. Of the individual analysis techniques, multi element analysis was proven to offer the greatest classification rate in determining the country of origin of West African and Madagascan timber samples. However, the long term stability of the trace element profile for the respective sample groups is unknown, hence, inter-year variation of those elements selected for the multivariate analysis may result in a reduction in the long to medium term accuracy of the prediction model. In order to account for this, analysis of new samples from the same sites as those included in this study would be required to assess the long term stability of the prediction model. Furthermore, long term study of the respective sampling sites could reveal the trace elements which are less influenced by anthopogenic activity and short term physical effects, making them more suitable for inclusion in the prediction model. The mulitvariate model produced solely from the stable isotope ratios may compensate for potential mis-classification problems brought about by reliance on trace elements alone, which could be influenced by pollution and short term physical effects.

Chapter 5 – Overall summary and future work

The objectives of the research presented in this thesis are:

i. To examine the relationship between the isotopic compositions of C, H and O in timber cellulose and differences contributing to the growth conditions and meteorological influences upon trees.

ii. To investigate the link between the trace element profiles of the underlying lithology of the trees' growing environment with that of the timber samples.

iii. To investigate whether multivariate statistical treatment of stable isotope ratio and trace element data enables discrimination of the geographical origin of timber.

The stable isotope ratios of cellulose and multi element profiles of timber from different geographical origins were determined by isotope ratio mass spectrometry (IRMS) and inductively coupled plasma mass spectrometry (ICP-MS). Timber samples originating from Ghana, Cameroon, DRC, The Congo and Madagascar were all differentiated from one another by applying the multivariate statistical technique of canonical discriminant analysis (CDA) to the stable isotope ratio and multi element data. The twelve elemental variables (Mo, Zn, Ca, As, $\delta^{13}C$, $\delta^{18}O$, Sb, Mn, Pb, Cu, La, Ba) were identified by the statistical software in the discriminant analysis as having the greatest variation enabling differentiation of the geographical origin of timber. Statistical analysis of the data from the combined trace element and stable isotope methodologies meets the main objective of this research, proving discrimination of geographical origin of tropical timber samples by multi-element and stable isotope analysis is possible.

A multivariate model derived only from the stable isotope ratios of hydrogen, carbon and oxygen of timber cellulose was shown to produce a near complete separation of Madagascan, Congolese and Cameroon from the Ghanaian sample group, as well as a high degree of separation of DRC from the Congolese, Cameroon and Madagascan sample groups. There was significant overlap between the Congolese, Cameroon and Madagascan sample groups, reducing the precision of the multivariate

model in determining geographical origin. Hydrogen isotope ratios did not appear to vary significantly between the respective countries in this study; hence, hydrogen did not play a significant role in the multivariate model. Improvements to the preparation processes for the hydrogen isotope analysis, such as nitration, equilibration, or analysis of non-exchangeable components (Keppler *et al*., 2007) may improve the classification rates of the multivariate model, as would calibration of δ^2H against suitable matrix matched standards within the natural abundance range of the samples. No common individual climatic variable was shown to influence the stable isotope profiles of the trees. Instead, a variety of factors such as humidity, rainfall, temperature and altitude were shown to influence the stable isotope profiles of the timber cellulose, making it difficult to decipher the individual meteorological and biological conditions influencing cellulose biosynthesis.

This study sought to investigate the link between the trace element profiles of the underlying lithology of the trees growing environment with that of the timber samples, and the selection of a number of the trace elements by the canonical discriminant analysis added depth to the understanding of the impacts of the soil on the trace element profile of the timber sustained on it. No individual trace element variable was found to provide geographical discrimination. Instead, a number of trace element variables in combination were shown to provide a significant level of discrimination among the timber samples, and in the final multivariate model, the classification rate of 85% was further improved by inclusion of stable isotope ratio data.

The analysis of timber cores with uniform dimensions may improve the determination of a robust isotopic and trace element mean by incorporating data from several growth rings. Notably however, the factors controlling annual variations in the trace element concentrations of individual tree rings is not well understood. Future work could involve assessment of the mobilisation of trace elements within a tree species, and of the radial and vertical trans-location of individual trace elements throughout the tree. Multi element dendrochronological analysis could allow for sampling protocols to be modified accordingly, and would reveal which trace element concentrations remain stable over several years of growth. Another approach could involve analysis and comparison of the stable isotope and trace element profiles in multiple timber cores from a within a single tree. This is of

particular importance for enforcement of EU FLEGT due diligence. Thus, timber suspected to have been illegally harvested may be derived from younger wood than the authentic samples in the reference database. Any temporal variations in the concentrations of the trace elements used in the multivariate model would reduce the precision of the model, in turn increasing the potential for origin misclassification.

Additional future work could also assess the impact of timber preparation and storage on the stable isotope and trace element profiles. The problem of timber laundering through 3rd party countries means that many illegally harvested species of timber are finished into products before export to consumers. Genetic analysis may struggle to resolve the issue, as preparation and processing steps associated with seasoning and manufacturing complicates DNA extraction. Trace elements and stable isotopes may prove more resilient and remain preserved during the manufacturing processes, potentially allowing for origin determination to be carried out on finished products. An additional test of the robustness of the database would be to challenge it with samples of known origin. Participation in timber proficiency testing schemes would allow for inter laboratory measurement precision and repeatability to be assessed.

Chapter 6 – Experimental

6.1 Sources of timber samples

Seventy-five timber core samples of Sapele (*Entandrophragma cylindricum*) and (*Entandrophragma angolense*), were collected from old growth forests by the International Tropical Timber Organisation from across Cameroon, Ghana, Congo, and the Democratic Republic of Congo. Twelve core samples (Fig 6.1) of Ebony (*Diospyros)* and 13 core samples of Rosewood (*Dalbergia*) were collected from Madagascar by representatives of Kew Botanic Gardens during January, 2013 (Fig. 6.1).

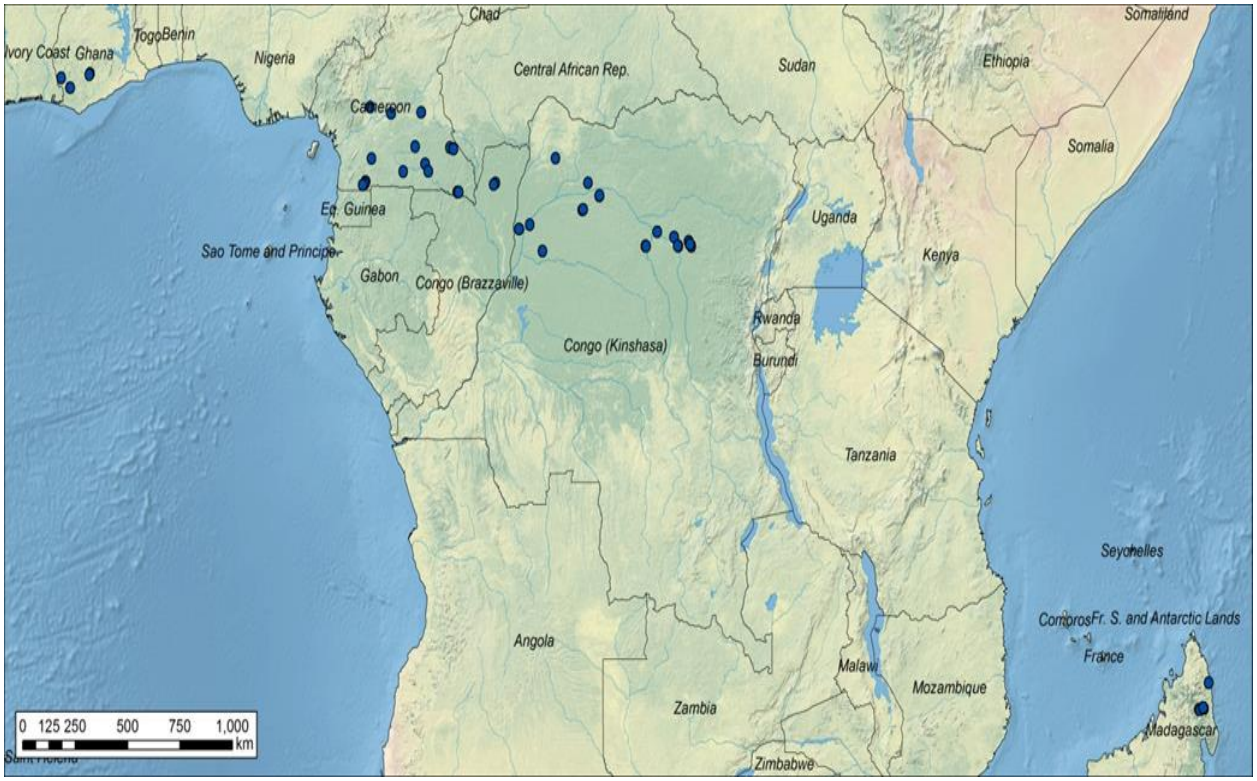

Fig. 6.1 West African and Madagascan sampling locations.

6.1.1 Collection of timber samples

In order to standardise measurements, core samples measuring 0.5 cm diameter x10 cm length, were taken from trees using increment borers (Fig 6.2), approximately 1 metre up the trunk of the tree from the forest floor. Global positioning system information co-ordinates as well as altitude information were recorded for each sample location (see appendix 2).

Fig. 6.2 Increment borer. Taken from Forestry-suppliers.com

6.2 Preparation of timber samples

Upon receipt at FERA, samples were logged into the laboratory information management system (LIMS) and each assigned a unique identifier. Freeze drying of the timber cores was carried out in order to remove any excess moisture and to aid breaking the samples into smaller pieces.

6.2.1 Preparation of in house wood reference material

Pine shavings (50 g) were gradually transferred to a Retsch centrifugal mill (Fig 6.3) and ground to a fine powder with a particle size of 0.2 µm. The powder was homogenised in a sealed bag after which 10 g was taken as a procedural quality control.

Fig. 6.3 Retsch centrifugal mill. Photo taken at FERA, Sand Hutton. UK.

6.2.2 Pulverisation of timber samples by ball mill.

Following freeze drying, core samples (Fig 6.4)were broken into small pieces enabling transfer in small amounts to a Retsch mixer mill MM400 (Fig 6.5) where they were pulverised to a fine powder.

Fig. 6.4 Madagascan Ebony core. Photo taken at FERA, Sand Hutton. UK.

Fig. 6.5 Retsch ball mill, MM400. Taken from www.coleparmer.co.uk

6.3 Isotope ratio analysis

6.3.1 Preparation of timber samples for IRMS analysis

Different species of tree vary slightly in their morphological makeup; some species have a greater portion of lignin and hemicellulose relative to alpha cellulose (Sjostrom, 1993). In addition, the lignin:cellulose ratio of secondary xylem can vary between early wood and late wood (Wilson & Grinsted, 1977). The pathway of fractionation for these components varies, introducing a source of measurement uncertainty in isotopic measurements on bulk wood (Mazany *et al.*, 1980; Marshall & Monserud, 1996).

In order to standardise measurement practices and overcome the source of uncertainty introduced through bulk measurement of timber, it was agreed with international partners involved in stable isotope analysis of timber that the cellulose purification method by Brendel *et al*. (2000) be applied to the powdered timber samples. The Brendel method has the advantage of utilising only small sample mass (less than 100 mg), produces alpha cellulose of greater than 99% purity, and up to 56 samples can be prepared within an 8 hour period. This contrasts with other labour intensive methods; e.g. Brooks *et al. (*1998), where samples have to be continuously extracted in large volumes of

toluene/ethanol, allowing preparation of only a small number of samples per batch , or restricting the analysis to only one isotope (Brenninkmeijer, 1983; Sheu & Chiu, 1995; Loader *et al*., 1997; Brooks & Gregg, 2002; Kepler *et al.*, 2007).

The Brendel method outlined in Fig. 6.6 achieves simultaneous delignification and removal of non-cellulosic polysaccharides using an acetic acid : nitric acid mixture (Crampton & Maynard, 1938). In order to monitor the repeatability of the Brendel method (Fig. 6.6), powdered timber shavings of wood in house reference material (WIHRM) were extracted and analysed along with each batch of samples.

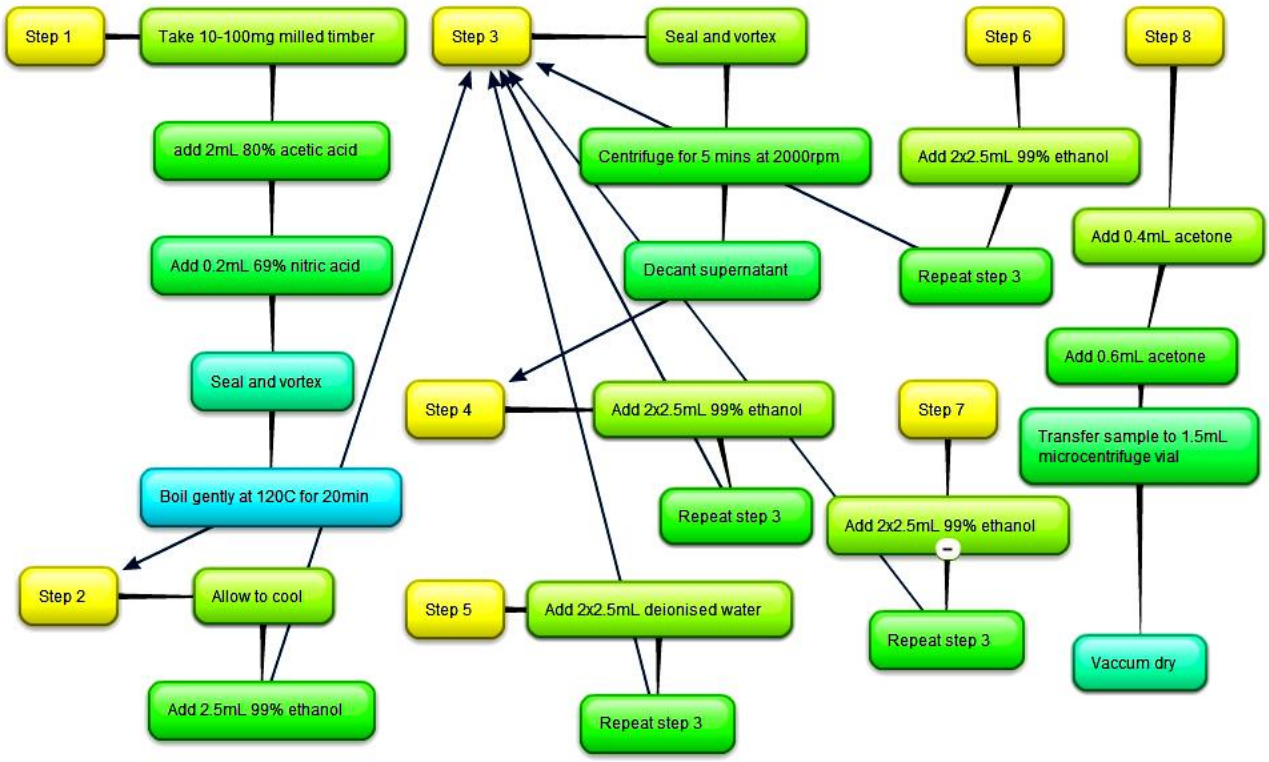

Fig. 6.6 The protocol for purification of cellulose from microsamples of plant cell wall material using acetic acid : nitric acid for simultaneous delignification and removal of non-cellulose polysaccharides. Adapted from Brendel *et al.* (2000).

6.3.2 Selection of stable isotope standards and reference materials

The stable isotope standards used in this study for calibration and quality control were selected based on their availability, closest matrix match to the samples, and where possible, certified or reputable

consensus delta value. Standards were also selected based on how close their assigned values were to the values measured in the cellulose samples. For example, correcting samples in the -12 per mil range to standards in the -30 range can reduce the precision of the data through scale compression.

6.3.2.1 Materials with known carbon isotopic composition

Two laboratory reference materials with certified $\delta^{13}C‰$ values (IAEA CH3 cellulose, $\delta^{13}C‰$ -24.72, IAEA CH6 Sucrose, $\delta^{13}C‰$ -10.45), versus the Pee Dee Belemnite (PDB) scale, were used to calibrate the $\delta^{13}C$ measurements of the cellulose samples by flash combustion EA-IRMS.

For the purposes of quality control, a cane sugar reference material (JRC sucrose), issued as part of a joint research commission project, was routinely monitored in the batches. The JRC sucrose has an inter-laboratory consensus $\delta\ ^{13}C‰$ value of -11.3 (EU joint research commission) enabling the effective monitoring of the stretch correction between the aforementioned IAEA certified calibration standards. For an additional QC check, IAEA CH3 cellulose (IAEA, Vienna), was also routinely monitored.

6.3.2.2 Materials with known oxygen isotopic compositions

Two certified benzoic acid standard reference materials (IAEA 601, $\delta^{18}O‰$ +23.3, IAEA 602, $\delta^{18}O‰$ +71.4) versus the Vienna standard mean ocean water (VSMOW) scale were used to calibrate the $\delta^{18}O$ measurements of the cellulose samples by pyrolysis EA-IRMS. Quality control monitoring was carried out by analysing IAEA CH3 with each batch of samples. The IAEA CH3 standard has only a certified $\delta^{13}C$ reference value, therefore a $\delta^{18}O$ value adopted for this reference material was obtained from research carried out by Loader & Buhay (1999).

6.3.2.3 Materials with known hydrogen isotopic compositions

A lack of suitable matrix and δ matched certified reference standards posed a significant challenge for validating the hydrogen measurements. Polyethylene certified reference material (IAEA CH7, $\delta^{2}H‰$ -103.2 versus VSMOW, deemed the closest certified matrix match to the expected range of $\delta^{2}H‰$ in the cellulose samples), was used to perform a single point calibration of the cellulose samples by pyrolysis EA-IRMS. Quality control monitoring was carried out by analysing IAEA CH3 cellulose

with each batch of samples. There is currently no official method to overcome the problems encountered when attempting measurement of compounds containing a significant molecular fraction of exchangeable hydrogen. As a consequence, consensus values for δ^2H in IAEA CH3 vary somewhat between different approaches used, such as nitration or equilibration (Filot *et al.*, 2006; Schimmelmann, 1991). Hence, monitoring of δ^2H was carried out without an assigned value, and a retrospective robust mean was calculated following the analysis of all of the batches of samples.

6.3.3 Measurement by IRMS

For ^{13}C combustion measurements, 1 mg of IAEA sucrose or purified cellulose was weighed in duplicate into tin capsules (3.5 x 5 mm, obtained from Elemental Microanalysis, Okehampton, UK). Capsules were sealed before transferring to a 96 position well plate which was stored in a desiccator prior to analysis. For ^{2}H and ^{18}O pyrolysis measurements, 1 mg of IAEA certified reference material or purified cellulose was weighed in quadruplicate into tin capsules (3.5 x 5 mm). Capsules were sealed before transferring to a 96 position well plate which was stored in a desiccator prior to analysis.

6.3.3.1 δ^{13}C analysis

Sealed tin capsules containing the purified cellulose and standards were placed in the autosampler of the elemental analyser (Fisons, Milan, Italy) and purged with helium, before dropping into a vertical quartz tube maintained at a temperature of 1020 °C (Kelly *et al.*, 2006). The carrier gas stream was temporarily enriched with oxygen and the sample and tin capsule oxidised in a 'flash' combustion reaction. Quantitative combustion was achieved by passing the gas mixture over two catalyst layers of chromium oxide and silvered copper or cobaltous oxide (Isoprime, Cheadle, UK). The combustion gases were passed first over elemental copper at a temperature of 650 °C to remove residual oxygen and second through a chromatographic column (Porapak PQS, SS, 2 m, 6 x 5 mm) heated at 35 °C to remove CO_2 and water. Residual Water was removed from the gas stream before entering the IRMS by a trap containing anhydrous magnesium perchlorate. During the measurement a portion of the effluent from the elemental analyser (ca. 0.5 ml/min) was transferred into the IRMS (Isoprime,

Cheadle, UK) using helium carrier gas (ca. 85 mL/min). The signal from ions at *m/z* 44, *m/z* 45 and *m/z* 46 for CO_2 were monitored.

6.3.3.2 δ^2H and $\delta^{18}O$ analysis

Sealed tin capsules containing purified cellulose and standards were placed in the autosampler of a Pyrocube elemental analyser (Elementar, Hanau, Germany), purged with helium, and dropped into a vertical glassy carbon tube with quartz liner maintained at a temperature of 1450°C. The products of thermal decomposition (gaseous H_2 and CO) were passed through a water trap containing sodium hydroxide/phosphorus pentoxide to remove residual moisture. A a carbon monoxide trap retained CO while enabling free transfer of H_2 into the IRMS for measurement. Following H_2 analysis the CO trap was heated rapidly, transferring desorbed CO into the IRMS for measurement. Application of a CO heating trap enables separation of H_2 and CO, as does use of the unique helium backflush capability of the pyrocube in eliminating isobaric interference from nitrogen (N_2) and nitrogen monoxide (NO_2) for ion beams *m/z* 28 and *m/z* 30, respectively (Sieper *et al*, 2010).

6.3.4 Corrections applied to the instrumental result data

A number of corrections were applied automatically to data acquired by the mass spectrometer software. Algorithm corrections were applied for dealing with electronic noise, blank corrections and the contribution of the ^{17}O gas species which is known to have an effect on $\delta^{13}C$ and $\delta^{18}O$ determinations (FIRMS Good Practice Guide for Isotope Ratio Mass Spectrometry, 2011).

6.3.4.1 Correction for drift

Changes in the behaviour of the ion source and ref gas composition during an analytical sequence can sometimes produce a gradual offset to the measured isotope delta values**.** To account for drift during measurement of analytical batches, calibration standards were placed at regular intervals within each batch of samples so instrumental drift could be monitored. Unknown samples were drift corrected using the formula specified in Chapter 1 (Jamin & Martin, 2004). Some manufacturer's instrument

software applies automatic drift corrections and normalisation of sample data is performed during analysis. The data produced from this study was drift corrected off-line using Microsoft Excel.

6.3.4.2 Correction for delta linearity

Stretch correction, also known as stretch-shift correction, applies a two point calibration for the normalisation of the data. This is particularly useful when measuring a range of delta values within a sample batch and increases the accuracy of the data (Carter & Fry, 2013). Stretch correction was applied to all of the drift corrected results for the $\delta^{13}C$ and $\delta^{18}O$ measurements, except in the case of $\delta^{2}H$ where application of only one certified reference material made a stretch correction impossible.

6.3.4.3 H_3^+ correction

Following protonation in the ion source, formation of H_3^+ ions occurs increasingly with increasing gas pressure. In order to account for this and reduce the unwanted isobaric interferences when attempting measurements of both H_2 and H_2^+, a correction factor was calculated for H_3^+ and applied by the instrument software for each sample acquisition. The correction was performed by including a small and large hydrogen reference gas pulse at the start of each sample acquisition. The calculated H_3^+ correction factor for each sample acquisition was monitored at the start of each batch acquisition, the guideline for this recognising that the H_3^+ correction should not exceed 10 ppm/na and should not deviate more than 0.2 across an analytical batch (FIRMS Good Practice Guide for Isotope Ratio Mass Spectrometry, 2011).

6.4 Multi-element analysis

For all timber samples, sixty-six elements were measured simultaneously by inductively coupled plasma-mass spectrometry (ICP-MS), (Agilent Technologies, Berkshire, UK).

6.4.1 Preparation of timber samples for acid digestion

Coarse timber chips (0.2 g, not sieved) were weighed into digestion vessels and a concentrated nitric and hydrochloric acid mixture (4:1, 5 mL; Fisher Scientific, Loughborough, UK) was added. The vessels were capped and the contents digested under high temperature and a pressure of 75 bar using a microwave digestion system (Multiwave, Anton Paar, UK). The microwave digestion system parameters used in this study are detailed in Table 6.1.

Table 6.1 Sample digestion parameters for timber samples.

Step	Heating power (W)	Time (min)	Fan
1	0-500	2:00	1
2	500	5:00	1
3	500-1000	2:00	1
4	1000	20:00	1
4	0	15:00	3
Total		44:00	

6.4.2 Selection of multi-element standards and reference materials

A number of single and multi-element standards (Table 6.2) were prepared and analysed at differing concentrations in order to span and calibrate the variable range of trace elements concentrations present in the timber samples. Certified reference materials Oriental Basma tobacco leaves, OBTL-5 (LGC, UK) and Spinach powder, ZC73013 (China National Analysis Centre for Iron and Steel, Beijing, China) were selected as quality controls in the ICP-MS analysis.

Table 6.2 List of elemental standards used in the ICP-MS analysis.

Elemental standards used in the ICP-MS analysis	
Standard type	**Element**
Multi-element solution 1	(Ce, Dy, Er, Eu, Gd, Ho, La, Lu, Nd, Pr, Sc, Sm, Tb, Th, Tm, Y, Yb)
Multi-element solution 2a	(Ag, Al, As, Ba, Be, Ca, Cd, Co, Cr, Cs, Cu, Fe, Ga, K, Li, Mg, Mn, Na, Ni, Pb, Rb, Se, Sr, Tl, U, V, Zn)
Multi-element solution 3	(Au, Hf, Ir, Pd, Pt, Rh, Ru, Sb, Sn, Te)
Multi-element solution 4	(B, Ge, Mo, Nb, P, Re, S, Si, Ta, Ti, W, Zr)
Single standard solutions	Aluminium
	Antimony
	Bismuth
	Calcium
	Copper
	Indium
	Iron
	Magnesium
	Manganese
	Mercury
	Osmium
	Potassium
	Scandium
	Sodium
	Tellurium
	Tin
	Zinc

6.4.3 Measurement by ICP-MS

The digest solutions for the simultaneous quantitative determination of 66 elements, together with a set of standards covering the expected concentration range, were internally standardised with indium and rhodium in dilute nitric acid (1% v/v) prior to analysis by the ICP-MS. Approximately 25% of the timber samples were randomly selected for duplicate analysis as part of the quality control procedure. Measurements were made using an Agilent 7700 x ICP-MS with collision cell.

To minimize background contribution, deionized water (18.2 MΩ cm), metal analysis grade reagents and acid cleaned plastic-ware were used throughout. A method was set up to give optimum resolution settings for each element taking into consideration spectral interferences and expected analyte concentrations. Typically the settings were 400 resolutions for ultra trace levels where maximum signal is required, then between 2,000 and 10,000 resolutions depending on the severity of interference, thus ensuring an accurate analyte signal. In total, a 66 element list (Li, Be, B, Na, Mg, Al, K, Ca, Sc, Ti, V, Cr, Mn, Fe, Co, Ni, Cu, Zn, Ga, Ge, As, Se, Rb, Sr, Y, Zr, Nb, Mo, Ru, Rh, Pd, Ag, Cd, Sn, Sb, Te, Cs, Ba, La, Ce, Pr, Nd, Sm, Eu, Gd, Tb, Dy, Ho, Er, Tm, Yb, Lu, Hf, Ta, W, Re, Os, Ir, Pt, Au, Hg, Tl, Pb, Bi, Th, U) was acquired by the by ICP-MS). Reagent blanks, certified reference materials and a blank reagent spiked with multi element solutions 1 and 2a were also taken through the procedure. The volume of multi-element solutions 1 and 2a, added to the reagent blank, was adjusted accordingly so those element concentrations were at a similar level to the concentration of the majority of the same elements in the timber samples. The resulting solutions were transferred to pre-marked acid-washed plastic test tubes and diluted to 10 mL with high purity deionised water (Millipore, Massachusetts, USA).

6.4.3.1 Quality control acceptance criteria

The calibration linearity for standard metal solutions was assessed and criteria specified that the data correlation coefficient had to be better than 0.99. Instrument drift had to be less than ±20% across the analytical run. The limit of detection was based on three standard deviations of the analytical blank variation, corrected for dilution and sample weight. The limit of quantification was based on 10 times the standard deviations of the analytical blank variation, corrected for dilution and sample weight. The recovery of added analyte had to be within 60 to 140% for all accepted elements whilst the majority of the (75%) should be within 80 to 120%. Agreement with certified CRM values had to be within ±20% of the target value and between -50 to 100% for indicative values.

Appendices

Appendix I Summary of the elemental analysis parameters, LoD and quality control results for ICP-MS

				ZC73013 (Spinach)													
					Recovery (%)												
Element	Selected mass	Mode of ORS	LoD (ng/g)	Certified value (ng/g)	20-Sep-13	22-Sep-13	02-Oct-13	15-Oct-13	17-Oct-13	27-Oct-13	30-Oct-13	02-Oct-13	04-Oct-13	06-Oct-13	08-Oct-13	12-Oct-14	18-Oct-13	25-Oct-13
Li	7	Standard	2.8	1460	86	85	91	86	83	82	84	85	84	81	87	88	87	82
Be	9	Standard	1.2	17	67	71	51	84	125	95	120	96	51	66	108	88	104	95
B	11	Standard	362.3	25000	119	102	118	100	102	92	98	106	102	98	108	115	104	105
Na	23	Standard	5654.2	15000000	89	88	88	90	90	90	93	86	89	88	93	98	94	93
Mg	24	Standard	611.7	5520000	101	104	100	89	91	97	92	95	94	96	104	109	99	97
Al	27	Standard	1925	610000	52	65	48	50	66	51	62	44	54	58	64	71	63	66
K	39	Standard	18736.1	24900000	98	100	103	101	101	100	101	99	119	115	115	119	115	113
Ca	44	Standard	11558.7	6600000	96	96	82	101	98	80	92	92	95	97	98	106	102	98
Sc	45	Standard	11	93	56	47	48	86	85	109	98	27	84	125	127	74	124	80
Ti	47	Helium	449	28000	52	59	54	43	57	51	73	35	53	50	71	58	68	57
V	51	Helium	11.4	870	67	66	66	68	68	65	66	60	66	63	64	71	73	71
Cr	52	Helium	220.3	1400	85	77	63	74	78	90	79	71	66	73	69	73	74	71
Mn	55	Standard	67.4	41000	82	83	86	82	78	87	81	81	79	78	82	88	81	81
Fe	56	Helium	1215.5	540000	91	91	92	85	86	86	84	92	94	93	94	98	90	95
Co	59	Standard	17.1	220	82	78	79	75	78	73	82	72	65	71	75	87	72	76
Ni	60	Helium	658.2	920	97	71	80	65	74	80	70	67	62	73	73	67	66	38
Cu	63	Helium	150.2	8900	76	78	80	78	79	77	78	74	75	92	81	82	78	83
Zn	66	Helium	504.6	35300	91	91	94	89	88	91	86	90	88	90	92	92	90	97
Ga	71	Helium	8.4	0	-	-	-	-	-	-	-	-	-	-	-	-	-	-
Ge	72	Helium	19.8	20	227	193	88	116	56	103	139	216	147	175	369	138	537	179
As	75	Helium	4.3	230	82	90	91	89	99	90	85	77	96	87	91	84	93	94
Se	78	H_2	8.6	92	62	73	64	72	69	93	64	79	73	77	68	74	73	87
Rb	85	Standard	6.8	30000	85	85	84	86	83	81	77	84	85	85	85	87	87	87
Sr	88	Standard	22.3	87000	78	82	76	77	78	72	77	89	82	81	86	86	79	79
Y	89	Standard	0.3	200	74	76	70	69	79	77	78	72	73	74	88	88	89	87
Zr	90	Standard	2.7	0	-	-	-	-	-	-	-	-	-	-	-	-	-	-
Nb	93	Standard	24.9	60	72	76	66	69	88	93	90	63	70	65	96	89	81	93
Mo	95	Standard	47.6	470	89	88	92	88	78	88	92	86	84	91	84	92	88	90
Ru	101	Standard	49.5	0	-	-	-	-	-	-	-	-	-	-	-	-	-	-
Rh	103	Standard	19.8	0	-	-	-	-	-	-	-	-	-	-	-	-	-	-
Pd	105	Standard	0.8	0	-	-	-	-	-	-	-	-	-	-	-	-	-	-
Ag	107	Standard	16.5	0	-	-	-	-	-	-	-	-	-	-	-	-	-	-
Cd	111	Standard	2	150	111	116	115	112	114	107	109	107	105	109	103	109	107	113

Appendix I continued Summary of the elemental analysis parameters, LoD and quality control results for ICP-MS.

				ZC73013 (Spinach)														
				Certified value (ng/g)	Recovery (%)													
Element	Selected mass	Mode of ORS	LoD (ng/g)		20-Sep-13	22-Sep-13	02-Oct-13	15-Oct-13	17-Oct-13	27-Oct-13	30-Oct-13	02-Oct-13	04-Oct-13	06-Oct-13	08-Oct-13	12-Oct-14	18-Oct-13	25-Oct-13
Sn	118	Standard	26.9	0	-	-	-	-	-	-	-	-	-	-	-	-	-	-
Sb	121	Standard	14.5	43	66	72	77	74	65	63	62	71	65	72	70	79	65	66
Te	125	Standard	6.6	0	-	-	-	-	-	-	-	-	-	-	-	-	-	-
Cs	133	Standard	0.3	130	77	78	75	75	73	82	79	75	76	77	77	76	75	76
Ba	137	Standard	23.7	9000	76	92	77	74	83	88	80	77	73	78	86	81	78	79
La	139	Standard	0.4	350	79	79	74	73	79	77	82	81	72	84	82	79	74	81
Ce	140	Standard	0.6	660	87	79	77	77	85	77	82	81	77	87	84	87	77	84
Pr	141	Standard	0.2	75	86	82	77	78	82	80	85	91	78	90	85	88	77	91
Nd	146	Standard	0.8	280	86	80	80	79	82	79	89	90	76	88	80	90	77	83
Sm	147	Standard	0.7	56	72	77	77	74	72	79	74	81	82	85	80	84	88	88
Eu	153	Standard	0.2	11	76	71	90	83	92	92	101	81	77	89	72	90	75	77
Gd	157	Standard	0.7	54	75	78	74	75	77	54	84	63	64	86	76	80	83	88
Tb	159	Standard	0.1	7	71	73	78	71	82	51	75	82	70	79	92	89	81	95
Dy	163	Standard	0.5	41	78	80	67	72	83	79	81	79	78	68	79	75	79	80
Ho	165	Standard	0.1	8	78	77	70	70	79	76	79	62	64	68	68	99	88	75
Er	166	Standard	0.4	17	84	98	88	74	106	96	118	94	99	85	99	105	98	117
Tm	169	Standard	0.1	3	63	70	61	77	66	59	64	61	64	51	97	79	56	84
Yb	172	Standard	0.5	19	72	67	66	59	89	71	84	67	57	70	86	65	69	82
Lu	175	Standard	0.1	3	73	68	52	55	63	86	68	59	54	64	43	77	67	75
Hf	178	Standard	0.4	40	20	18	16	17	26	28	28	12	15	18	17	30	19	31
Ta	181	Standard	26.3	0	-	-	-	-	-	-	-	-	-	-	-	-	-	-
W	182	Standard	2.5	0	-	-	-	-	-	-	-	-	-	-	-	-	-	-
Re	185	Standard	0	0	-	-	-	-	-	-	-	-	-	-	-	-	-	-
Os	189	Standard	4.8	0	-	-	-	-	-	-	-	-	-	-	-	-	-	-
Ir	193	Standard	0.7	0	-	-	-	-	-	-	-	-	-	-	-	-	-	-
Pt	195	Standard	1.1	0	-	-	-	-	-	-	-	-	-	-	-	-	-	-
Au	197	Standard	4.1	0	-	-	-	-	-	-	-	-	-	-	-	-	-	-
Hg	201	Standard	16.2	20	109	127	98	94	214	143	92	105	119	99	126	170	101	92
Tl	205	Standard	5.3	49	71	69	74	75	62	74	65	78	63	74	67	74	59	76
Pb	208	Standard	6.7	11100	93	93	94	91	89	96	90	93	89	92	92	91	89	88
Bi	209	Standard	0.3	14	63	64	68	68	61	75	68	65	66	75	69	67	72	66
Th	232	Standard	0.3	114	77	80	79	74	83	80	75	87	75	74	94	92	67	96
U	238	Standard	0.2	89	81	79	80	79	83	80	82	77	82	79	84	88	74	78

Appendix I continued Summary of the elemental analysis parameters, LoD and quality control results for ICP-MS.

				OBTL-5 (Tobacco leaves)														
				Certified	Recovery (%)													
Element	Selected mass	Mode of ORS	LoD (ng/g)	value (ng/g)	20-Sep-13	22-Sep-13	02-Oct-13	15-Oct-13	17-Oct-13	27-Oct-13	30-Oct-13	02-Oct-13	04-Oct-13	06-Oct-13	08-Oct-13	12-Oct-14	18-Oct-13	25-Oct-13
Li	7	Standard	2.8	19300	116	115	113	108	115	118	114	115	117	116	115	107	108	111
Be	9	Standard	1.2	81.2	83	85	78	70	89	74	92	71	85	69	81	67	72	82
B	11	Standard	362.3	33600	108	117	103	107	99	110	97	104	111	105	102	104	104	102
Na	23	Standard	5654.2	435000	45	46	43	48	44	56	53	53	46	47	44	48	45	46
Mg	24	Standard	611.7	8530000	109	111	117	115	93	102	103	98	117	112	105	114	107	107
Al	27	Standard	1925	1980000	74	72	88	71	68	84	62	76	67	79	83	79	85	77
K	39	Standard	18736.1	22710000	103	100	103	112	96	104	97	97	107	126	115	115	111	111
Ca	44	Standard	11558.7	39960000	79	96	98	88	96	98	81	89	102	102	94	104	98	97
Sc	45	Standard	11	640	60	65	86	67	77	68	68	84	90	67	60	96	63	71
Ti	47	Helium	449	80700	102	89	118	110	84	97	94	118	97	112	96	117	118	123
V	51	Helium	11.4	4012	81	85	80	88	79	96	79	87	86	91	81	88	86	88
Cr	52	Helium	220.3	6300	64	81	90	89	67	87	78	83	101	71	63	81	79	81
Mn	55	Standard	67.4	180000	92	89	92	98	83	87	92	87	94	91	84	91	87	85
Fe	56	Helium	1215.5	1490000	101	105	109	111	97	107	104	102	116	115	105	112	105	107
Co	59	Standard	17.1	981	78	84	89	87	78	78	78	78	90	78	77	84	76	75
Ni	60	Helium	658.2	8500	80	111	135	126	81	83	80	82	148	82	80	85	84	79
Cu	63	Helium	150.2	10100	85	84	88	96	82	90	83	84	93	87	84	90	84	84
Zn	66	Helium	504.6	52400	93	94	96	100	93	96	91	89	100	96	91	103	93	94
Ga	71	Helium	8.4	0	-	-	-	-	-	-	-	-	-	-	-	-	-	-
Ge	72	Helium	19.8	0	-	-	-	-	-	-	-	-	-	-	-	-	-	-
As	75	Helium	4.3	668	95	100	96	105	93	103	97	104	106	110	103	100	97	96
Se	78	H_2	8.6	0	-	-	-	-	-	-	-	-	-	-	-	-	-	-
Rb	85	Standard	6.8	19100	84	86	82	84	84	85	80	78	77	78	77	83	84	82
Sr	88	Standard	22.3	105000	82	87	89	84	84	87	77	87	99	89	86	94	93	85
Y	89	Standard	0.3	963	105	100	102	97	94	106	102	103	99	95	98	102	102	102
Zr	90	Standard	2.7	0	-	-	-	-	-	-	-	-	-	-	-	-	-	-
Nb	93	Standard	24.9	0	-	-	-	-	-	-	-	-	-	-	-	-	-	-
Mo	95	Standard	47.6	414	79	119	169	212	87	77	79	76	390	81	80	84	111	77
Ru	101	Standard	49.5	0	-	-	-	-	-	-	-	-	-	-	-	-	-	-
Rh	103	Standard	19.8	0	-	-	-	-	-	-	-	-	-	-	-	-	-	-
Pd	105	Standard	0.8	0	-	-	-	-	-	-	-	-	-	-	-	-	-	-
Ag	107	Standard	16.5	53	87	89	96	89	192	82	82	81	89	95	84	100	86	82
Cd	111	Standard	2	2640	93	95	94	92	93	97	88	93	94	93	92	92	96	94

Appendix I continued Summary of the elemental analysis parameters, LoD and quality control results for ICP-MS.

				OBTL-5 (Tobacco leaves)													
				Certified value (ng/g)	Recovery (%)												
Element	Selected mass	Mode of ORS	LoD (ng/g)		20-Sep-13	22-Sep-13	02-Oct-13	15-Oct-13	17-Oct-13	27-Oct-13	30-Oct-13	02-Oct-13	04-Oct-13	06-Oct-13	08-Oct-13	12-Oct-14	18-Oct-13	25-Oct-13
Sn	118	Standard	26.9	0	-	-	-	-	-	-	-	-	-	-	-	-	-	-
Sb	121	Standard	14.5	75.5	81	76	75	64	69	60	69	79	75	68	64	88	68	67
Te	125	Standard	6.6	0	-	-	-	-	-	-	-	-	-	-	-	-	-	-
Cs	133	Standard	0.3	288	79	77	77.11251	79	77	78	79	79	78	76	74	77	80	78
Ba	137	Standard	23.7	67400	82	88	84.75733	88	81	83	87	86	87	83	82	85	87	86
La	139	Standard	0.4	1690	93	87	88.07535	85	81	89	84	85	85	81	86	83	81	82
Ce	140	Standard	0.6	2990	94	89	86.98926	85	85	90	85	83	82	82	84	85	83	82
Pr	141	Standard	0.2	321	106	97	99.07829	93	92	99	98	97	98	93	95	99	98	95
Nd	146	Standard	0.8	1330	96	92	90.75054	86	89	93	87	91	90	83	90	85	87	89
Sm	147	Standard	0.7	264	100	90	89.75208	84	81	93	87	84	85	80	90	81	84	82
Eu	153	Standard	0.2	60.2	90	85	87.53293	81	82	84	81	100	88	76	82	89	88	85
Gd	157	Standard	0.7	243	96	93	93.85913	94	88	88	91	97	90	80	90	89	97	90
Tb	159	Standard	0.1	34.7	97	86	93.31156	92	87	90	81	91	91	86	89	91	93	91
Dy	163	Standard	0.5	184	104	100	99.92962	95	95	96	85	95	95	98	98	108	95	95
Ho	165	Standard	0.1	34.5	103	95	100.9945	94	94	109	102	103	100	95	95	104	100	112
Er	166	Standard	0.4	101	101	99	94.63653	91	96	100	92	90	98	97	93	96	98	103
Tm	169	Standard	0.1	13.6	96	101	95.27112	92	92	97	92	103	94	91	99	92	102	105
Yb	172	Standard	0.5	115	72	71	69.54517	68	69	79	73	79	73	70	68	73	66	76
Lu	175	Standard	0.1	16.7	71	67	65.99941	68	68	71	73	76	67	57	69	60	75	70
Hf	178	Standard	0.4	291	5	6	5.04801	6	4.990375	6	6	7	5	4	5	5	9	7
Ta	181	Standard	26.3	41.7	2	1	1.414798	0.534089	0.895402	-12	-69	-49	1	24	4	-73	6	-20
W	182	Standard	2.5	0	-	-	-	-	-	-	-	-	-	-	-	-	-	-
Re	185	Standard	0	0	-	-	-	-	-	-	-	-	-	-	-	-	-	-
Os	189	Standard	4.8	0	-	-	-	-	-	-	-	-	-	-	-	-	-	-
Ir	193	Standard	0.7	0	-	-	-	-	-	-	-	-	-	-	-	-	-	-
Pt	195	Standard	1.1	0	-	-	-	-	-	-	-	-	-	-	-	-	-	-
Au	197	Standard	4.1	3	100	67	60.882	111.8549	88.59714	-25	272	47	103	114	66	59	-13	48
Hg	201	Standard	16.2	20.9	91	83	81.04938	92.87407	79.14395	67	64	56	82	72	84	71	63	68
Tl	205	Standard	5.3	51.3	86	89	90.08246	87.67752	90.80737	88	91	85	91	80	87	89	84	86
Pb	208	Standard	6.7	2010	83	85	78.80277	77.13021	113.5881	90	79	82	81	79	77	79	82	79
Bi	209	Standard	0.3	0	-	-	-	-	-	-	-	-	-	-	-	-	-	-
Th	232	Standard	0.3	503	85	80	82.68268	72.56052	74.86498	81	78	79	77	75	76	81	76	77
U	238	Standard	0.2	113	66	66	67.43501	62.66415	65.67825	75	65	65	66	63	63	73	64	62

Appendix I continued Summary of the elemental analysis parameters, LoD and quality control results for ICP-MS.

				Blank spike														
				Spiked quantitiy (ng)	Recovery (%)													
Element	Selected mass	Mode of ORS	LoD (ng/g)		20-Sep-13	22-Sep-13	02-Oct-13	15-Oct-13	17-Oct-13	27-Oct-13	30-Oct-13	02-Oct-13	04-Oct-13	06-Oct-13	08-Oct-13	12-Oct-14	18-Oct-13	25-Oct-13
Li	7	Standard	2.8	50	107	114	107	102	106	112	110	108	104	110	93	95	97	100
Be	9	Standard	1.2	50	102	105	102	97	101	105	106	103	102	106	95	92	92	98
B	11	Standard	362.3	50	93	110	93	108	175	112	107	104	101	113	85	87	93	93
Na	23	Standard	5654.2	1000	117	111	118	114	111	122	119	116	109	116	107	105	101	102
Mg	24	Standard	611.7	100000	108	100	107	117	109	112	125	107	106	112	96	95	99	99
Al	27	Standard	1925	1000	79	86	188	211	102	127	434	49	29	258	52	70	79	90
K	39	Standard	18736.1	100000	111	104	103	106	111	117	114	102	98	105	101	100	98	98
Ca	44	Standard	11558.7	10000	95	69	884	148	128	110	137	103	101	107	93	93	94	98
Sc	45	Standard	11	50	98	89	105	107	89	144	104	102	99	96	79	104	91	97
Ti	47	Helium	449	50	82	95	89	88	129	80	87	70	64	102	100	72	80	100
V	51	Helium	11.4	50	108	104	106	107	103	113	109	109	99	103	103	99	95	100
Cr	52	Helium	220.3	50	107	99	108	107	100	112	113	109	101	111	104	98	94	98
Mn	55	Standard	67.4	10000	104	99	95	108	163	101	111	103	100	109	99	94	98	95
Fe	56	Helium	1215.5	1000	105	99	106	108	102	108	111	102	97	103	101	97	94	95
Co	59	Standard	17.1	50	110	104	114	109	105	112	113	111	104	110	106	102	100	101
Ni	60	Helium	658.2	50	108	98	104	112	107	119	120	108	107	110	104	98	101	99
Cu	63	Helium	150.2	1000	115	107	110	115	106	116	117	112	107	111	106	102	101	97
Zn	66	Helium	504.6	10000	108	103	106	106	102	110	110	107	104	110	103	100	101	98
Ga	71	Helium	8.4	50	110	91	100	111	103	104	113	101	98	111	102	102	100	97
Ge	72	Helium	19.8	50	101	102	97	113	96	109	113	107	101	100	100	99	101	103
As	75	Helium	4.3	50	104	101	102	101	96	108	107	101	95	101	101	103	96	95
Se	78	H_2	8.6	50	99	97	96	94	93	98	96	98	98	97	99	98	98	93
Rb	85	Standard	6.8	50	101	99	98	99	98	105	103	104	101	102	100	97	97	97
Sr	88	Standard	22.3	50	100	95	99	121	173	113	118	93	97	134	87	87	91	93
Y	89	Standard	0.3	1	100	94	99	101	96	103	102	96	99	97	103	97	99	97
Zr	90	Standard	2.7	50	96	97	96	97	96	102	99	98	98	98	98	93	95	85
Nb	93	Standard	24.9	50	94	90	93	96	93	98	92	95	97	93	94	89	89	86
Mo	95	Standard	47.6	50	97	99	96	99	95	102	98	100	99	98	99	95	96	95
Ru	101	Standard	49.5	1	91	103	98	105	103	105	104	100	115	-67	102	99	103	93
Rh	103	Standard	19.8	1	94	102	101	104	105	107	105	102	102	106	100	102	104	95
Pd	105	Standard	0.8	1	87	101	104	104	107	105	101	104	102	107	101	105	102	94
Ag	107	Standard	16.5	50	103	99	102	101	99	104	103	104	100	101	106	100	100	101
Cd	111	Standard	2	50	101	98	101	98	97	101	101	102	99	99	101	97	98	98

Appendix I continued Summary of the element analysis parameters, LoD and quality control results for ICP-MS.

				Blank spike													
				Spiked	Recovery (%)												
Element	Selected mass	Mode of ORS	LoD (ng/g)	quantitiy (ng)	YFB	YFC	YFD	YFE	YFF	YFG	YFH	YFI	YFJ	YFK	YFL	YFM	YFN	YFO
Sn	118	Standard	26.9	50	100	102	103	100	98	105	101	101	101	100	106	101	102	97
Sb	121	Standard	14.5	50	89	100	103	131	102	103	97	96	100	107	97	102	103	91
Te	125	Standard	6.6	50	84	96	94	99	103	98	100	107	88	97	96	99	105	103
Cs	133	Standard	0.3	50	91	89	92	94	86	95	91	93	93	91	95	91	91	89
Ba	137	Standard	23.7	50	100	97	97	103	102	99	101	97	98	98	102	97	97	96
La	139	Standard	0.4	5	99	93	100	99	97	105	103	97	101	94	106	101	101	98
Ce	140	Standard	0.6	50	97	96	101	98	96	105	106	103	99	98	106	100	101	97
Pr	141	Standard	0.2	50	99	95	105	100	99	104	102	98	99	99	106	100	101	98
Nd	146	Standard	0.8	1	95	94	103	95	97	104	98	98	101	97	107	100	101	96
Sm	147	Standard	0.7	1	98	95	104	100	93	106	102	97	102	94	107	100	100	97
Eu	153	Standard	0.2	1	99	94	102	101	97	104	99	99	102	99	104	99	100	96
Gd	157	Standard	0.7	1	101	93	102	99	95	109	99	97	101	97	103	94	101	103
Tb	159	Standard	0.1	1	98	95	102	97	96	102	100	98	98	96	106	99	101	95
Dy	163	Standard	0.5	1	98	94	103	98	94	105	103	99	98	94	104	96	104	96
Ho	165	Standard	0.1	1	98	93	102	102	97	101	100	99	98	96	107	99	101	97
Er	166	Standard	0.4	1	100	95	103	100	97	105	102	97	96	94	105	99	101	98
Tm	169	Standard	0.1	1	99	94	104	101	96	105	101	97	99	94	107	98	101	98
Yb	172	Standard	0.5	1	98	99	102	101	92	105	105	101	98	98	106	99	101	98
Lu	175	Standard	0.1	1	98	96	105	100	96	105	100	99	99	97	108	98	100	97
Hf	178	Standard	0.4	1	91	104	102	101	100	106	101	100	101	103	97	97	105	80
Ta	181	Standard	26.3	50	41	35	36	29	30	27	23	31	27	32	26	38	32	35
W	182	Standard	2.5	50	96	99	103	97	95	99	95	98	96	97	103	93	99	98
Re	185	Standard	0	50	98	99	103	99	96	101	100	99	97	98	103	93	100	99
Os	189	Standard	4.8	50	0	49	36	34	21	21	26	44	104	74	18	24	9	26
Ir	193	Standard	0.7	1	91	104	111	106	102	102	104	102	101	103	105	101	104	97
Pt	195	Standard	1.1	1	89	103	105	102	96	105	104	100	101	102	101	101	105	98
Au	197	Standard	4.1	1	80	97	101	87	90	91	92	90	89	92	83	82	87	91
Hg	201	Standard	16.2	50	96	98	99	92	91	97	92	98	97	94	101	92	100	97
Tl	205	Standard	5.3	50	93	94	98	90	89	93	91	94	92	89	99	91	95	95
Pb	208	Standard	6.7	50	99	100	107	100	98	102	101	100	98	98	105	97	102	101
Bi	209	Standard	0.3	50	0	0	0	0	0	0	0	0	0	0	0	0	0	0
Th	232	Standard	0.3	1	96	94	105	98	96	101	98	99	98	95	104	96	103	95
U	238	Standard	0.2	50	95	96	103	98	89	100	97	84	88	87	99	91	98	99

Appendix II List of sample information

FERA sample identifier	External sample identifier	Timber species	Country of origin	Region	Altitude (m)	Latitude	Longtitude
S13-055204	C-04-ENTC-03	*Entandrophragma cylindricum*	Cameroon	Forêt secondaire, près de Mandjan	571	3.0099	13.8258
S13-055222	C-09-ENTC-41	*Entandrophragma cylindricum*	Cameroon	Forêt Nyiemeyong	664	3.1895	11.3742
S13-055217	C-08-ENTC-06	*Entandrophragma cylindricum*	Cameroon	Forêt secondaire, Mayang(près de Mindourou)	717	3.5705	13.3797
S13-055206	C-04-ENTC-14	*Entandrophragma cylindricum*	Cameroon	Forêt secondaire, Mbalam I	569	2.7708	13.9690
S13-055212	C-06-ENTC-07	*Entandrophragma cylindricum*	Cameroon	FBR, Medoumo	568	3.4819	15.1295
S13-055197	C-02-ENTC-31	*Entandrophragma cylindricum*	Cameroon	FBR, Minkan	609	2.4558	11.0921
S13-055218	C-08-ENTC-07	*Entandrophragma cylindricum*	Cameroon	Forêt secondaire, Mayang	724	3.5691	13.3820
S13-055198	C-02-ENTC-32	*Entandrophragma cylindricum*	Cameroon	FBR, Minkan	600	2.3887	11.0524
S13-055207	C-05-ENTC-06	*Entandrophragma cylindricum*	Cameroon	Forêt secondaire, Bangohé	379	2.0902	15.3020
S13-055211	C-06-ENTC-05	*Entandrophragma cylindricum*	Cameroon	Forêt secondaire, Modoumo	562	3.5001	15.1218
S13-055208	C-05-ENTC-10	*Entandrophragma cylindricum*	Cameroon	FBR, Ngoli	390	2.0938	15.3633
S13-055205	C-04-ENTC-12	*Entandrophragma cylindricum*	Cameroon	Vieille jachère, Mbalam I	585	2.7745	13.9727
S13-055199	C-02-ENTC-33	*Entandrophragma cylindricum*	Cameroon	Forêt secondaire, Nnezan	542	2.3381	10.9611
S13-055210	C-06-ENTC-01	*Entandrophragma cylindricum*	Cameroon	FBR, Nbol 9	567	3.5243	14.9749
S13-055226	C-13-ENTC-03	*Entandrophragma angolense*	Cameroon	Egona II foret secondaire	450	4.8453	11.3170
S13-055200	C-03-ENTC-23	*Entandrophragma cylindricum*	Cameroon	Mpacko, foret exploitee	600	2.7629	12.8249
S13-055227	C-14-ENTC-08	*Entandrophragma cylindricum*	Cameroon	Akak foret secondaire	607	4.6412	12.2785
S13-055228	C-14-ENTC-09	*Entandrophragma cylindricum*	Cameroon	Akak foret secondaire	610	4.6419	12.2790
S13-055229	C-14-ENTC-10	*Entandrophragma cylindricum*	Cameroon	Akak foret secondaire	611	4.6420	12.2789
S13-055231	C-15-ENTC-11	*Entandrophragma angolense*	Cameroon	Goume-Goffi foret secondaire	699	4.6663	13.6557
S13-055233	C-15-ENTC-13	*Entandrophragma angolense*	Cameroon	Goume-Goffi foret secondaire	701	4.6661	13.6548
S13-055232	C-15-ENTC-12	*Entandrophragma angolense*	Cameroon	Goume-Goffi foret secondaire	718	4.6667	13.6554
S13-055235	CB-02-ENTC-13	*Entandrophragma cylindricum*	Congo	UFA Loundougou	450	2.3798	17.0609
S13-055236	CB-02-ENTC-14	*Entandrophragma cylindricum*	Congo	Forêt dense, UFA Loundougou	450	2.3840	17.0628
S13-055237	CB-02-ENTC-15	*Entandrophragma cylindricum*	Congo	Forêts mixtes, UFA Loundougou	450	2.3840	17.0628

Appendix II continued. List of sample information

FERA sample identifier	External sample identifier	Timber species	Country of origin	Region	Altitude (m)	Latitude	Longtitude
S13-055238	CB-02-ENTC-17	*Entandrophragma cylindricum*	Congo	Ancien camp forestier (jeune forêt secondaire), UFA Loundougou	390	2.3215	16.9703
S13-055258	DRC-04-ENTC-03	*Entandrophragma cylindricum*	DRC	Bloc Ubundu	428	0.3289	25.4560
S13-055265	DRC-05-ENTC-05	*Entandrophragma cylindricum*	DRC	Bloc Lubutu	503	0.3251	26.0462
S13-055263	DRC-05-ENTC-03	*Entandrophragma cylindricum*	DRC	Bloc Lubutu	505	0.3271	26.0430
S13-055268	DRC-06-ENTC-03	*Entandrophragma cylindricum*	DRC	Bloc Kisangani-Est	525	0.4864	25.9294
S13-055264	DRC-05-ENTC-04	*Entandrophragma cylindricum*	DRC	Bloc Lubutu	513	0.3270	26.0430
S13-055260	DRC-04-ENTC-05	*Entandrophragma cylindricum*	DRC	Bloc Ubundu	435	0.3377	25.4234
S13-055269	DRC-06-ENTC-04	*Entandrophragma cylindricum*	DRC	Bloc Kisangani-Est	487	0.3947	25.9758
S13-055261	DRC-05-ENTC-01	*Entandrophragma cylindricum*	DRC	Bloc Lubutu	493	0.3494	26.0339
S13-055270	DRC-06-ENTC-05	*Entandrophragma cylindricum*	DRC	Bloc Kisangani-Est	483	0.3901	25.9845
S13-055257	DRC-04-ENTC-02	*Entandrophragma cylindricum*	DRC	Bloc Ubundu	431	0.3356	25.4533
S13-055256	DRC-04-ENTC-01	*Entandrophragma cylindricum*	DRC	Bloc Ubundu	446	0.3387	25.4512
S13-055293	DRC-29-ENTC-11	*Entandrophragma cylindricum*	DRC	Bloc Bumba	NA	1.9576	21.8260
S13-055262	DRC-05-ENTC-02	*Entandrophragma cylindricum*	DRC	Bloc Lubutu	483	0.3422	26.0353
S13-055246	DRC-02-ENTC-03	*Entandrophragma cylindricum*	DRC	Bloc Yangambi	445	0.7842	24.4868
S13-055295	DRC-29-ENTC-18	*Entandrophragma cylindricum*	DRC	Bloc Bumba	NA	1.9591	21.8316
S13-055294	DRC-29-ENTC-14	*Entandrophragma cylindricum*	DRC	Bloc Bumba	NA	1.9586	21.8303
S13-055286	DRC-15-ENTC-06	*Entandrophragma cylindricum*	DRC	Bloc Bongadanga	NA	1.5125	21.0810
S13-055252	DRC-03-ENTC-04	*Entandrophragma cylindricum*	DRC	Bloc Lomami	428	0.3428	23.9418
S13-055267	DRC-06-ENTC-02	*Entandrophragma cylindricum*	DRC	Bloc Kisangani-Est	501	0.4864	25.9293
S13-055250	DRC-03-ENTC-01	*Entandrophragma cylindricum*	DRC	Bloc Lomami	415	0.3236	23.9483
S13-055292	DRC-29-ENTC-10	*Entandrophragma cylindricum*	DRC	Bloc Bumba	NA	1.9575	21.8274
S13-055271	DRC-07-ENTC-13	*Entandrophragma cylindricum*	DRC	Bloc Mabali	316	0.8816	18.1409
S13-055274	DRC-07-ENTC-16	*Entandrophragma cylindricum*	DRC	Bloc Mabali	310	0.8824	18.1316
S13-055282	DRC-13-ENTC-05	*Entandrophragma cylindricum*	DRC	Bloc Embondo	NA	0.1804	19.2112

Appendix II continued. List of sample information

FERA sample identifier	External sample identifier	Timber species	Country of origin	Region	Altitude (m)	Latitude	Longtitude
S13-055248	DRC-02-ENTC-05	*Entandrophragma cylindricum*	DRC	Bloc Yangambi	445	0.7815	24.4872
S13-055296	DRC-29-ENTC-19	*Entandrophragma cylindricum*	DRC	Bloc Bumba	NA	1.9597	21.8323
S13-055273	DRC-07-ENTC-15	*Entandrophragma cylindricum*	DRC	Bloc Mabali	320	0.8859	18.1267
S13-055290	DRC-16-ENTC-14	*Entandrophragma cylindricum*	DRC	Bloc Lisala	NA	2.3653	21.3053
S13-055259	DRC-04-ENTC-04	*Entandrophragma cylindricum*	DRC	Bloc Ubundu	444	0.3379	25.4233
S13-055251	DRC-03-ENTC-02	*Entandrophragma cylindricum*	DRC	Bloc Lomami	407	0.3426	23.9417
S13-055253	DRC-03-ENTC-05	*Entandrophragma cylindricum*	DRC	Bloc Lomami	413	0.3299	23.9724
S13-055275	DRC-08-ENTC-01	*Entandrophragma cylindricum*	DRC	Bloc Mbala	342	1.0295	18.6281
S13-055242	DRC-01-ENTC-04	*Entandrophragma cylindricum*	DRC	Kisangani	424	0.6164	25.2598
S13-055291	DRC-16-ENTC-16	*Entandrophragma cylindricum*	DRC	Bloc Lisala	NA	2.3669	21.3044
S13-055284	DRC-15-ENTC-02	*Entandrophragma cylindricum*	DRC	Bloc Bongadanga	NA	1.4920	21.0432
S13-055239	DRC-01-ENTC-01	*Entandrophragma cylindricum*	DRC	Kisangani	428	0.6163	25.2590
S13-055285	DRC-15-ENTC-05	*Entandrophragma cylindricum*	DRC	Bloc Bongadanga	NA	1.5083	21.0786
S13-055240	DRC-01-ENTC-02	*Entandrophragma cylindricum*	DRC	Kisangani	430	0.6167	25.2589
S13-055301	DRC-30-ENTC-08	*Entandrophragma cylindricum*	DRC	Bloc Gemena	NA	3.1724	19.8129
S13-055283	DRC-13-ENTC-06	*Entandrophragma cylindricum*	DRC	Bloc Embondo	NA	0.1792	19.2107
S13-055281	DRC-13-ENTC-04	*Entandrophragma cylindricum*	DRC	Bloc Embondo	NA	0.1808	19.2113
S13-055309	GH-03-ENTC-13	*Entandrophragma cylindricum*	Ghana	Fure Headwaters F.R.	79	5.5887	-2.4427
S13-055304	GH-03-ENTC-02	*Entandrophragma cylindricum*	Ghana	Nkrabia	132	6.0380	1.5243
S13-055305	GH-03-ENTC-03	*Entandrophragma cylindricum*	Ghana	Nkrabia	136	6.0386	1.5244
S13-055310	GH-03-ENTC-14	*Entandrophragma cylindricum*	Ghana	Fure Headwaters F.R.	118	5.5883	-2.4349
S13-055308	GH-03-ENTC-07	*Entandrophragma cylindricum*	Ghana	Nkrabia	128	6.0084	1.5530
S13-055307	GH-03-ENTC-05	*Entandrophragma cylindricum*	Ghana	Nkrabia	150	6.0407	1.5235
S13-055306	GH-03-ENTC-04	*Entandrophragma cylindricum*	Ghana	Nkrabia	141	6.0402	1.5246
S13-055303	GH-02-ENTC-01	*Entandrophragma cylindricum*	Ghana	Yoyo Forest Reserve	143	5.9174	2.8402

Appendix II continued. List of sample information

FERA sample identifier	External sample identifier	Timber species	Country of origin	Region	Altitude (m)	Latitude	Longtitude
S13-055336	6 A	*Dalbergia bathiei*	Madagascar	Marojejy	NA	-14.2661	49.45571
S13-055338	8 A	*Dalbergia bathiei*	Madagascar	Marojejy	NA	-14.2673	49.45524
S13-055366	36 A	*Dalbergia monticola*	Madagascar	Marojejy	NA	-14.2948	49.36381
S13-055357	27 A	*Dalbergia monticola*	Madagascar	Marojejy	NA	-14.2995	49.34290
S13-055361	31 A	*Dalbergia monticola*	Madagascar	Marojejy	NA	-14.2951	49.36558
S13-055376	46 A	*Dalbergia bathiei*	Madagascar	Marojejy	NA	-14.2603	49.45304
S13-055377	47 A	*Dalbergia bathiei*	Madagascar	Marojejy	NA	-14.2605	49.45256
S13-055362	32 A	*Dalbergia bathiei*	Madagascar	Marojejy	NA	-14.2951	49.36558
S13-055337	7 A	*Dalbergia bathiei*	Madagascar	Marojejy	NA	-14.2661	49.45554
S13-055375	45 A	*Diospyros mangabensis*	Madagascar	Marojejy	NA	-14.2603	49.45304
S13-055373	43 A	*Dalbergia bathiei*	Madagascar	Marojejy	NA	-14.2604	49.45310
S13-055363	33 A	*Dalbergia monticola*	Madagascar	Marojejy	NA	-14.2951	49.36558
S13-055334	4 A	*Dalbergia bathiei*	Madagascar	Marojejy	NA	-14.2677	49.46650
S13-055339	9 A	*Dalbergia bathiei*	Madagascar	Marojejy	NA	-14.2613	49.46323
S13-055365	35 A	*Diospyros*	Madagascar	Marojejy	NA	-14.2953	49.36373
S13-055358	28 A	*Diospyros masoalensis*	Madagascar	Marojejy	NA	-14.2957	49.36454
S13-055356	26 A	*Diospyros*	Madagascar	Marojejy	NA	-14.2995	49.34290
S13-055367	37 A	*Diospros*	Madagascar	Marojejy	NA	-14.2953	49.36382
S13-055360	30 A	*Diospyros masoalensis*	Madagascar	Marojejy	NA	-14.2957	49.36451
S13-055359	29 A	*Disopsros*	Madagascar	Marojejy	NA	-14.2957	49.36451
S13-055368	38 A	*Disopyros*	Madagascar	Marojejy	NA	-13.3754	50.01990
S13-055369	39 A	*Diopyros sp*	Madagascar	Marojejy	NA	-14.2716	49.47331
S13-055372	42 A	*Diospyros*	Madagascar	Marojejy	NA	-14.2721	49.47235
S13-055340	10 A	*Diospyros velutipes*	Madagascar	Marojejy	NA	-14.2613	49.46327
S13-055344	14 A	*Diospyros lokohensis*	Madagascar	Marojejy	NA	-14.2613	49.46313

List of abbreviations and units

‰	Per mil
3-PGA	3-phosphoglycerate
ATP	Adenosine triphosphate
BSIA	Bulk stable isotope analysis
ca.	Circa
CDA	Canonical discriminant analysis
CDT	Cañon Diabolo Troilite
CITES	Convention on international trade in endangered species
DHAP	Dihydroxyacetone phosphate
DRC	Democratic Republic of Congo
DNA	Deoxyribonucleic acid
EA	Elemental analyser
EC	European Council
EU	European Union
FERA	Food and Environment Research Agency
FOE	Friends of the Earth
FSC	Forestry stewardship council
PTS	Proficiency Testing Scheme
FLEGT	Forest law enforcement governance and trade
G-3-P	Glyceraldehyde phosphate
GC	Gas chromatography
HPLC	High performance liquid chromatography
Hz	Hertz
i.d.	Internal diameter
IAEA	International Atomic Energy Agency

ICP-MS	Inductively coupled plasma mass spectrometry
IRMS	Isotope ratio mass spectrometry
ITTO	International tropical timber organisation
LEAF	Law enforcement assistance for forests
LOD	limit of detection
m/z	Mass-to-charge ratio
GMWL	Global meteoric water line
N.A.	Not applicable
NADPH	Nicotinamide adenine dinucleotide phosphate
NBS	National Bureau of Standards
NIST	National Institute for Standards and Technology
ORS	Octopole reaction system
PCA	Principal component analysis
PDB	Pee Dee Belemnite
PPM	Parts per million
RUBISCO	Ribulose-1,5-bisphosphate carboxylase/oxygenase
RuBP	Ribulose-1,5-bisphosphate
rf	Radio frequency
S.D.	Standard deviation
SSR	Simple sequence repeats
SMOW	Standard Mean Ocean Water
UK	United Kingdom
VPDB	Vienna Pee Dee Belemnite
VSMOW	Vienna Standard Mean Ocean Water
WIHRM	Wood in house reference material

List of references

Albrigo, L. G., Szafranck, R. C.and Childers, N. F. (1966), The Role of Molybdenum in Plants and Soils, *Climax Molybdenum Co., Supplemental volume*, 1966. Available at http://www.imoa.info/HSE/environmental_data/biology/plants_soils.php. Accessed 26 July 2013.

Amali, O., Iwar, I. M., & Oboshi, I. M. (2013). Ecological effect of timber expraction in Ohimini LGA of Benue State, Nigeria. *Journal of Research in Forestry, Wildlife and Environment*, *4*(2), 64-72.

Anderson, K. A., & Smith, B. W. (2005). Use of chemical profiling to differentiate geographic growing origin of raw pistachios. *Journal of Agricultural and Food Chemistry*, *53*(2), 410-418.

Anthoni, P. M., Law, B. E., Unsworth, M. H., & Vong, R. J. (2000). Variation of net radiation over heterogeneous surfaces: measurements and simulation in a juniper–sagebrush ecosystem. *Agricultural and Forest Meteorology*, *102*(4), 275-286.

Ariyama, K., Aoyama, Y., Mochizuki, A., Homura, Y., Kadokura, M., & Yasui, A. (2007). Determination of the geographic origin of onions between three main production areas in Japan and other countries by mineral composition. *Journal of agricultural and food chemistry*, *55*(2), 347-354.

Armstrong, A. H., Shugart, H. H., & Fatoyinbo, T. E. (2011). Characterization of community composition and forest structure in a Madagascar lowland rainforest. *Trop. Conserv. Sci*, *4*, 428-444.

Baes, C. F., & McLaughlin, S. B. (1984). Trace elements in tree rings: evidence of recent and historical air pollution. *Science*, *224*(4648), 494-497.

Barber, S. A. (1995). Soil nutrient bioavailability: a mechanistic approach. John Wiley & Sons.

Begoude, B. A. D., Slippers, B., Wingfield, M. J., & Roux, J. (2011). The pathogenic potential of endophytic Botryosphaeriaceous fungi on Terminalia species in Cameroon. *Forest Pathology*, *41*(4), 281-292.

Berry, S. C., Varney, G. T., & Flanagan, L. B. (1997). Leaf δ13C in Pinus resinosa trees and understory plants: variation associated with light and CO2 gradients. *Oecologia*, *109*(4), 499-506.

Barker, V. A. Y Pilbeam JD (2007). *Handbook of Plant Nutrition. Taylor y Francis*, 28.

Bajracharya, D. (1983). Deforestation in the food/fuel context: historical and political perspectives from Nepal. *Mountain Research and Development*, 227-240.

Bearhop, S., Furness, R. W., Hilton, G. M., Votier, S. C., & Waldron, S. (2003). A forensic approach to understanding diet and habitat use from stable isotope analysis of (avian) claw material. *Functional Ecology*, *17*(2), 270-275.

Boner, M., & Förstel, H. (2004). Stable isotope variation as a tool to trace the authenticity of beef. *Analytical and bioanalytical chemistry*, *378*(2), 301-310.

Bowen, G. J., & Revenaugh, J. (2003). Interpolating the isotopic composition of modern meteoric precipitation. *Water Resources Research*, *39*(10).

Branch, S., Burke, S., Evans, P., Fairman, B., & Briche, C. S. W. (2003). A preliminary study in determining the geographical origin of wheat using isotope ratio inductively coupled plasma mass

spectrometry with ^{13}C, ^{15}N mass spectrometry. *Journal of analytical atomic spectrometry*, *18*(1), 17-22.
Brendel, O., Iannetta, P. M., & Stewart, D. (2000). A rapid and simple method to isolate pure alpha-cellulose. *Phytochemical Analysis*, *11*(1), 7-10.

Brenninkmeijer, C. A. M. (1983). Deuterium, oxygen-18 and carbon-13 in three rings and peat deposits in relation to climate.

Brooks, J. R., Flanagan, L. B., & Ehleringer, J. R. (1998). Responses of boreal conifers to climate fluctuations: indications from tree-ring widths and carbon isotope analyses. *Canadian Journal of Forest Research*, *28*(4), 524-533.

Brooks, J. R., Meinzer, F. C., Coulombe, R., & Gregg, J. (2002). Hydraulic redistribution of soil water during summer drought in two contrasting Pacific Northwest coniferous forests. *Tree Physiology*, *22*(15-16), 1107-1117.

Butler, T. (2005). Timber hungry China moves into Africa.

Callaghan, R. (2008). Zirconium and Hafnium Statistics and Information. US Geological Survey. Available at http://minerals.usgs.gov/minerals/pubs/commodity/zirconium/. Accessed November 2013.

Campbell, N. A., Reece, J. B., Urry, L. A., Cain, M. L., Wasserman, S. A., Minorsky, P. V., & Jackson, R. B. (2008). *AP Edition Biology*. Benjamin/Cummings.

Carter, J. F., & Fry, B. (2013). Ensuring the reliability of stable isotope ratio data—beyond the principle of identical treatment. *Analytical and bioanalytical chemistry*, *405*(9), 2799-2814.

Cheng, T. L., & Durst, P. B. (2000). *Development of national-level criteria and indicators for the sustainable management of dry forests in Asia: background papers. Bhopal, India, 30 November-3 December 1999* (No. 8). FAO Regional Office for Asia and the Pacific.

Clark, I. D., & Fritz, P. (1997). *Environmental isotopes in hydrogeology*. CRC press.

Coetzee, P. P., Steffens, F. E., Eiselen, R. J., Augustyn, O. P., Balcaen, L., & Vanhaecke, F. (2005). Multi-element analysis of South African wines by ICP-MS and their classification according to geographical origin. *Journal of Agricultural and Food Chemistry*, *53*(13), 5060-5066.

Coplen, T. B., & Kendall, C. (2000). *Stable hydrogen and oxygen isotope ratios for selected sites of the US Geological Survey's NASQAN and benchmark surface-water networks* (No. USGS-OFR-00-160).

Coplen, T. B., Brand, W. A., Gehre, M., Gröning, M., Meijer, H. A., Toman, B., & Verkouteren, R. M. (2006). New guidelines for δ 13C measurements. *Analytical Chemistry*, *78*(7), 2439-2441.

Clark, I. D., & Fritz, P. (1997). *Environmental isotopes in hydrogeology*. CRC press.

Craig, H. (1961). Isotopic variations in meteoric waters. *Science*, *133*(3465), 1702-1703.

Crampton, E. W., & Maynard, L. A. (1938). The relation of cellulose and lignin content to the nutritive value of animal feeds. *the Journal of Nutrition*, *15*(4), 383-395.

Crawford, R. L. (1981). *Lignin biodegradation and transformation* (p. 154). New York: Wiley.

Crowther, T. W., Maynard, D. S., Leff, J. W., Oldfield, E. E., McCulley, R. L., Fierer, N., & Bradford, M. A. (2014). Predicting the responsiveness of soil biodiversity to deforestation: a cross-biome study. *Global change biology*, *20*(9), 2983-2994.

Cullen, W. R., & Reimer, K. J. (1989). Arsenic speciation in the environment. *Chemical Reviews*, *89*(4), 713-764.

Dansgaard, W. (1964). Stable isotopes in precipitation. *Tellus A*, *16*(4).

Dass C. (2007). *Fundamentals of contemporary mass spectrometry*. New Jersey: John Wiley & Sons, Inc., (7).

Dawson, T. E., & Ehleringer, J. R. (1991). Streamside trees that do not use stream water. *Nature*, *350*(6316), 335-337.

Dawson, T. E., & Ehleringer, J. R. (1993). Isotopic enrichment of water in the "woody" tissues of plants: implications for plant water source, water uptake, and other studies which use the stable isotopic composition of cellulose. *Geochimica et Cosmochimica Acta*, *57*(14), 3487-3492.

Dawson, T. E., Mambelli, S., Plamboeck, A. H., Templer, P. H., & Tu, K. P. (2002). Stable isotopes in plant ecology. *Annual review of ecology and systematics*, 507-559.

Debroux, L., Topa, G., Kaimowitz, D., Karsenty, A., Hart, T., Abdon, A., & Yambayamba, N. (2007). Forests in post-conflict Democratic Republic of Congo: Analysis of a priority agenda. *Selected Books*, *1*. Available at http://www.cifor.org/publications/pdf_files/Books/BCIFOR0701.pdf. Accessed May 2013.

Demura, T., & Fukuda, H. (2007). Transcriptional regulation in wood formation. *Trends in plant science*, *12*(2), 64-70.

Dooley, K., & Ozinga, S. (2011). Building on forest governance reforms through FLEGT: the best way of controlling forests' contribution to climate change? *Review of European Community & International Environmental Law*, *20*(2), 163-170.

Doucet, A., Savard, M. M., Bégin, C., Marion, J., Smirnoff, A., & Ouarda, T. B. (2012). Combining tree-ring metal concentrations and lead, carbon and oxygen isotopes to reconstruct peri-urban atmospheric pollution. *Tellus B*, *64*.

Eckstein, D., & Bauch, J. (1974). Dendrochronologie und Kunstgeschichte--dargestellt an Gemalden hollandischer und altdeutscher Malerei. *Mitteilungen der Deutschen Dendrologischen Gesellschaft*.

Emsley, J. (2001). Manganese. Nature's Building Blocks: An AZ Guide to the Elements.

Enamorado-Báez, S. M., Abril, J. M., & Gómez-Guzmán, J. M. (2013). Determination of 25 trace element concentrations in biological reference materials by icp-ms following different microwave-assisted acid digestion methods based on scaling masses of digested samples. *ISRN Analytical Chemistry*, *2013*.

Epstein, S., Yapp, C. J., & Hall, J. H. (1976). The determination of the D/H ratio of non-exchangeable hydrogen in cellulose extracted from aquatic and land plants. *Earth and Planetary Science Letters*, *30*(2), 241-251.

Epstein, S., Krishnamurthy, R. V., Oeschger, H., Eddy, J. A., & Pecker, J. C. (1990). Environmental information in the isotopic record in trees [and discussion]. *Philosophical Transactions of the Royal Society of London A: Mathematical, Physical and Engineering Sciences*, *330* (1615), 427-439.

Fay L. B., & Kussmann M. (2010). Mass spectrometry technologies. In L. B. Fay & M. Kussmann (Eds.) *Mass spectrometry and nutrition research* (pp. 3-47) UK: The Royal Society of Chemistry.
Farquhar, G. D., & Sharkey, T. D. (1982). Stomatal conductance and photosynthesis. *Annual review of plant physiology*, *33*(1), 317-345.

Farquhar, G. D., Ehleringer, J. R., & Hubick, K. T. (1989). Carbon isotope discrimination and photosynthesis. *Annual review of plant biology*, *40*(1), 503-537.

Fearnside, P. M., & Laurance, W. F. (2004). Tropical deforestation and greenhouse-gas emissions. *Ecological Applications*, *14*(4), 982-986.

Feldmann, J., Krupp, E. M., Glindemann, D., Hirner, A. V., & Cullen, W. R. (1999). Methylated bismuth in the environment. *Applied organometallic chemistry*, *13*(10), 739-748.

Ferrio, J. P., Voltas, J., & Araus, J. L. (2003). Use of carbon isotope composition in monitoring environmental changes. *Management of Environmental Quality: An International Journal*, *14*(1), 82-98.

Filot, M. S., Leuenberger, M., Pazdur, A., & Boettger, T. (2006). Rapid online equilibration method to determine the D/H ratios of non-exchangeable hydrogen in cellulose. *Rapid communications in mass spectrometry*, *20*(22), 3337-3344.

Francey, R. J. (1985). Cape Grim isotope measurements - a preliminary assessment. *Journal of atmospheric chemistry*, *3*(2), 247-260.

Francey, R. J., Gifford, R. M., Sharkey, T. D., & Weir, B. (1985). Physiological influences on carbon isotope discrimination in huon pine (Lagarostrobos franklinii). *Oecologia*, *66*(2), 211-218.

Friedman, I., Redfield, A. C., Schoen, B., & Harris, J. (1964). The variation of the deuterium content of natural waters in the hydrologic cycle. *Reviews of Geophysics*, *2*(1), 177-224.

Gat, J. R. (1980). The isotopes of hydrogen and oxygen in precipitation. In *Handbook of environmental isotope geochemistry. Vol. 1*.

Geiger, D. R., & Servaites, J. C. (1994). Diurnal regulation of photosynthetic carbon metabolism in C3 plants. *Annual review of plant biology*, *45*(1), 235-256.

Ghuman, B. S., & Lal, R. (1987). Effects of partial clearing on microclimate in a humid tropical forest. *Agricultural and Forest Meteorology*, *40*(1), 17-29.

Gillespie, J. E., Wicklund, R. E., & Miller, M. H. (1968). soils of Leeds County. *Ontario Soil Survey Report*.

Gohil, H. L., Correll, M. J., & Sinclair, T. (2011). Predicting the effects of gas diffusivity on photosynthesis and transpiration of plants grown under hypobaria. *Advances in Space Research*, *47*(1), 49-54.

Gomez-Ariza, J. L., Garcia-Barrera, T., & Lorenzo, F. (2005). Optimisation of a two-dimensional on-line coupling for the determination of anisoles in wine using ECD and ICP-MS after SPME-GC separation. *Journal of Analytical Atomic Spectrometry*, *20*(9), 883-888.

Goodland, R. J. A., & Irwin, H. S. (1974). An ecological discussion of the environmental impact of the highway construction program in the Amazon Basin. *Landscape planning*, *1*, 123-254.

Gori, Y. U. R. I., Wehrens, R., Greule, M., Keppler, F., Ziller, L., La Porta, N., & Camin, F. (2013). Carbon, hydrogen and oxygen stable isotope ratios of whole wood, cellulose and lignin methoxyl groups of Picea abies as climate proxies. *Rapid Communications in Mass Spectrometry*, *27*(1), 265-275.

Gray, A. L., & Date, A. R. (1983). Inductively coupled plasma source mass spectrometry using continuum flow ion extraction. *Analyst*, *108*(1290), 1033-1050.

Gray, J., & Thompson, P. (1977). Climatic information from 18O/16O analysis of cellulose, lignin and whole wood from tree rings.

Gremaud, G., & Hilkert, A. (2008). Isotopic-spectroscopic technique: Stable isotope ratio mass spectrometry (IRMS). *Modern Techniques for Food Authentication, Elsevier, London, UK*, 269-320.

Ha, M. A., Apperley, D. C., Evans, B. W., Huxham, I. M., Jardine, W. G., Viëtor, R. J., & Jarvis, M. C. (1998). Fine structure in cellulose microfibrils: NMR evidence from onion and quince. *The Plant Journal*, *16*(2), 183-190.

Hammond, C. R. (2000). The elements. *Handbook of chemistry and physics*, *81*.

Harper, G. J., Steininger, M. K., Tucker, C. J., Juhn, D., & Hawkins, F. (2007). Fifty years of deforestation and forest fragmentation in Madagascar. *Environmental Conservation*, *34*(04), 325-333.

Heaton, K., Kelly, S. D., Hoogewerff, J., & Woolfe, M. (2008). Verifying the geographical origin of beef: The application of multi-element isotope and trace element analysis. *Food Chemistry*, *107*(1), 506-515.

Hemming, D. L., Switsur, V. R., Waterhouse, J. S., Heaton, T. H. E., & Carter, A. H. C. (1998). Climate variation and the stable carbon isotope composition of tree ring cellulose: an intercomparison of Quercus robur, Fagus sylvatica and Pinus silvestris. *Tellus B*, *50*(1), 25-33.

Hobson, K. A. (1990). Stable isotope analysis of marbled murrelets: evidence for freshwater feeding and determination of trophic level. *Condor*, 897-903.

Hoefs J. (2009). *Stable isotope geochemistry*. (6th ed.). Berlin: Springer, (Chapter 1).

Horacek, M., Jakusch, M., & Krehan, H. (2009). Control of origin of larch wood: discrimination between European (Austrian) and Siberian origin by stable isotope analysis. *Rapid Communications in Mass Spectrometry*, *23*(23), 3688-3692.

Hudson, N. (1995). *Soil conservation* (No. 3. ed.). BT Batsford.

Igamberdiev, A. U., Mikkelsen, T. N., Ambus, P., Bauwe, H., Lea, P. J., & Gardeström, P. (2004). Photorespiration contributes to stomatal regulation and carbon isotope fractionation: a study with barley, potato and Arabidopsis plants deficient in glycine decarboxylase. *Photosynthesis Research*, *81*(2), 139-152.

Iglesias, M., Besalú, E., & Anticó, E. (2007). Internal standardization-atomic spectrometry and geographical pattern recognition techniques for the multielement analysis and classification of Catalonian red wines. *Journal of agricultural and food chemistry*, *55*(2), 219-225.

Jacobs, C. M. J., & De Bruin, H. A. R. (1992). The sensitivity of regional transpiration to land-surface characteristics: significance of feedback. *Journal of Climate*, *5*(7), 683-698.

Jacobs, M. R. (1954). The effect of wind sway on the form and development of Pinus radiata D. Don. *Australian Journal of Botany*, *2*(1), 35-51.

Jacobson. M. (2013). Extent of Agroforestry Extension Programs in the United States. *Journal of extension*, August 2013, Volume 51, Number 4, Research In Brief, 4RIB4. Available at http://www.joe.org/joe/2013august/rb4.php. Accessed October 2014.

Jakubowski, N., Brandt, R., Stuewer, D., Eschnauer, H. R., & Görtges, S. (1999). Analysis of wines by ICP-MS: Is the pattern of the rare earth elements a reliable fingerprint for the provenance?. *Fresenius' journal of analytical chemistry*, *364*(5), 424-428.

Jamin, E., Gonzalez, J., Remaud, G., Naulet, N., & Martin, G. G. (1997). Detection of exogenous sugars or organic acids addition in pineapple juices and concentrates by 13C IRMS analysis. *Journal of Agricultural and Food Chemistry*, *45*(10), 3961-3967.

Jamin E., Martin F., & Martin G. G. (2004). Determination of the $^{13}C/^{12}C$ ratio of ethanol derived from fruit juices and maple syrup by isotope ratio mass spectrometry: collaborative study. *Journal of AOAC International*, *87*, 621-631.

Joshi, U. M., & Balasubramanian, R. (2010). Characteristics and environmental mobility of trace elements in urban runoff. *Chemosphere*, *80*(3), 310-318.

Jungk, A., & Claassen, N. (1997). Ion diffusion in the soil-root system. *Advances in agronomy (USA)*.

Kabata-Pendias, A. (2004). Soil–plant transfer of trace elements—an environmental issue. *Geoderma*, *122*(2), 143-149.

Kagawa, A., Abe, H., Fujii, T., & Itoh, Y. (2008, December). Stable isotopes and inorganic elements as potential indicators of timber geographic origin. *AGU Fall Meeting Abstracts* (Vol. 1, p. 02).

Kagawa, A., & Leavitt, S. W. (2010). Stable carbon isotopes of tree rings as a tool to pinpoint the geographic origin of timber. *Journal of wood science*, *56*(3), 175-183.

Kahmen, A., Sachse, D., Arndt, S. K., Tu, K. P., Farrington, H., Vitousek, P. M., & Dawson, T. E. (2011). Cellulose δ18O is an index of leaf-to-air vapor pressure difference (VPD) in tropical plants. *Proceedings of the National Academy of Sciences*, *108*(5), 1981-1986.

Kanel, K. R., & Shrestha, K. (2001). Tropical secondary forests in Nepal and their importance to local people. *Journal of Tropical Forest Science*, *13*(4).

Kärkönen, A., & Koutaniemi, S. (2010). Lignin biosynthesis studies in plant tissue cultures. *Journal of integrative plant biology*, *52*(2), 176-185.

Kelly, S.D. (2010). The British Beef Origin Project (BBOP – Q01123), *4*(1), 11-13.

Kelly, S., Baxter, M., Chapman, S., Rhodes, C., Dennis, J., & Brereton, P. (2002). The application of isotopic and elemental analysis to determine the geographical origin of premium long grain rice. *European Food Research and Technology*, *214*(1), 72-78.

Kelly, S. D. (2003). Using stable isotope ratio mass spectrometry (IRMS) in food authentication and traceability. *Food authenticity and traceability*, *156*.

Khan, A. (2001). *Plant anatomy and physiology*. Gyan Publishing House.

Kim, K. W., & Thornton, I. (1993). Influence of uraniferous black shales on cadmium, molybdenum and selenium in soils and crop plants in the Deog-Pyoun-g area of Korea. *Environmental Geochemistry and Health*, *15*(2-3), 119-133.

King, D. A. (1990). The adaptive significance of tree height. *American Naturalist*, 809-828.

King, E. E., & Barclay, D. (2003). Microwave Based Extraction. *Sample Preparation for Trace Element Analysis, 1st edition, eds. Z. Mester, RE Sturgeon, Elsevier, Amsterdam*, 257-300.

King, L. D. (1988). Retention of metals by several soils of the southeastern United States. *Journal of Environmental Quality*, *17*(2), 239-246.

Kingston, H. M., & Walter, P. J. (1997). The art and science of microwave sample preparations for trace and ultratrace elemental analysis. *Inductively Coupled Mass Spectrometry, A. Montaser, Wiley-VCH.*

Kitata, R. B., & Chandravanshi, B. S. (2012). Concentration levels of major and trace metals in onion (Allium cepa L.) and irrigation water around Meki Town and Lake Ziway, Ethiopia. *Bulletin of the Chemical Society of Ethiopia*, *26*(1).

Kiyosu, Y., & Kidoguchi, M. (2000). Variations in the stable carbon isotope ratios of Zelkova serrata leaves from roadside trees in Toyama City, Japan. *Geochemical Journal*, *34*(5), 379-382.

Klecka, W. R. (1980). *Discriminant analysis* (No. 19). Sage.

Klemm, D., Heublein, B., Fink, H. P., & Bohn, A. (2005). Cellulose: fascinating biopolymer and sustainable raw material. *Angewandte Chemie International Edition*, *44*(22), 3358-3393.

Kou, D., & Mitra, S. (2003). Extraction of semivolatile organic compounds from solid matrices. *Sample preparation techniques in analytical chemistry*, 139.

Kovacs, M., Nyary, I., & Toth, L. (1984). The microelement content of some submerged and floating aquatic plants. *Acta Botanica Hungarica*.

Laurance, W. F. (1999). Reflections on the tropical deforestation crisis. *Biological Conservation*, *91*(2), 109-117.

Lawrence, D., D'Odorico, P., Diekmann, L., DeLonge, M., Das, R., & Eaton, J. (2007). Ecological feedbacks following deforestation create the potential for a catastrophic ecosystem shift in tropical dry forest. *Proceedings of the National Academy of Sciences*, *104*(52), 20696-20701.

Leisola, M., Pastinen, O., & Axe, D. D. (2012). Lignin--Designed Randomness. *Bio-Complexity*, *2012*.

Li, A., Keely, B., Chan, S. H., Baxter, M., Rees, G., & Kelly, S. (2014). Verifying the provenance of rice using stable isotope ratio and multi-element analyses: a feasibility study. *Quality Assurance and Safety of Crops & Foods*, *7*(3), 343-354.

Li, X., & Chapple, C. (2010). Understanding lignification: challenges beyond monolignol biosynthesis. *Plant physiology*, *154*(2), 449-452.

Li, X., Wu, H. X., & Southerton, S. G. (2010). Seasonal reorganization of the xylem transcriptome at different tree ages reveals novel insights into wood formation in Pinus radiata. *New Phytologist*, *187*(3), 764-776.

Loader, N. J., Robertson, I., Barker, A. C., Switsur, V. R., & Waterhouse, J. S. (1997). An improved technique for the batch processing of small wholewood samples to α-cellulose. *Chemical Geology*, *136*(3), 313-317.

Loader, N. J., & Buhay, W. M. (1999). Rapid catalytic oxidation of CO to CO2–On the development of a new approach to on-line oxygen isotope analysis of organic matter. *Rapid communications in mass spectrometry*, *13*(18), 1828-1832.

Lombardozzi D., (2003). The Effects of Deforestation on nutrient concentrations in tributaries of Lake Tanganyika. Available at http://www.geo.arizona.edu/nyanza/pdf/Burce.pdf. Accessed June 2013.

Map of Life - "Reversion from xylem vessels to tracheids" http://www.mapoflife.org/topics/topic_451_reversion-from-xylem-vessels-to-tracheids/. Accessed November, 2013.

Marfo, E., Danso, E., & Nketiah, S. K. (2013). *Analysis of linkages and opportunities for synergies between FLEGT, REDD and national forest programme in Ghana*. Wageningen, the Netherlands: Tropenbos International Ghana.

Marschner, H. (1983). General introduction to the mineral nutrition of plants. *Inorganic plant nutrition*. Springer Berlin Heidelberg, 5-60.

Marschner, H. (1995). Functions of mineral nutrients: macronutrients. *Mineral nutrition of higher plants*, *2*, 379-396.

Marshall, J. D., & Monserud, R. A. (1996). Homeostatic gas-exchange parameters inferred from 13C/12C in tree rings of conifers. *Oecologia*, *105*(1), 13-21.

Marshall, J. D., Brooks, J. R., & Lajtha, K. (2007). Sources of variation in the stable isotopic composition of plants. *Stable isotopes in ecology and environmental science*, 22-60.

Mazany, T., Lerman, J. C., & Long, A. (1980). Carbon-13 in tree-ring cellulose as an indicator of past climates.

McGuire, K., & McDonnell, J. (2007). Stable isotope tracers in watershed hydrology. *Stable isotopes in ecology and environmental science*, 334.

McMurtrey, J. E., Jr., and W. O. Rob- inson. (1938). Neglected soil constituents that affect plant and animal development, in soils and man. *USDA Yearbook of Agriculture*. 807-829.

Medina, E., & Minchin, P. (1980). Stratification of δ13C values of leaves in Amazonian rain forests. *Oecologia*, *45*(3), 377-378.

Medina, E., Montes, G., Cuevas, E., & Rokzandic, Z. (1986). Profiles of CO 2 concentration and δ 13 C values in tropical rain forests of the upper Rio Negro Basin, Venezuela. *Journal of Tropical Ecology*, *2*(03), 207-217.

Meier-Augenstein, W. (2010). Stable Isotope Forensics.

Meinzer, F. C., Andrade, J. L., Goldstein, G., Holbrook, N. M., Cavelier, J., & Wright, S. J. (1999). Partitioning of soil water among canopy trees in a seasonally dry tropical forest. *Oecologia*, *121*(3), 293-301.

Michener, R., & Lajtha, K. (Eds.). (2008). *Stable isotopes in ecology and environmental science*. John Wiley & Sons.

Mizutani, H., Fukuda, M., Kabaya, Y., & Wada, E. (1990). Carbon isotope ratio of feathers reveals feeding behaviour of cormorants. *The auk*, 400-403.

Moreda-Pineiro, A., Fisher, A., & Hill, S. J. (2003). The classification of tea according to region of origin using pattern recognition techniques and trace metal data. *Journal of Food Composition and Analysis*, *16*(2), 195-211.

Műnch, E. (1930). Die Stoffbewegungen in der Pflanze. *Jena. G. Fischer*, 234-238.

Muntean, D. (2005). Boron, the overlooked essential element. *Bellevue: Soil and Plant Laboratory Inc*. Available at http://www.soilandplantlaboratory.com/pdf/articles/BoronOverlookedEssential.pdf. Accessed May 2013.

Muschler, R. G. (2001). Shade improves coffee quality in a sub-optimal coffee-zone of Costa Rica. *Agroforestry systems*, *51*(2), 131-139.

Nier, A. O. (1940). A mass spectrometer for routine isotope abundance measurements. *Review of Scientific Instruments*, *11*(7), 212-216.

O'Connor G., & Evans E. H. (1999). Fundamental aspects of ICP-MS. In S. J. Hill (Ed.), *Inductively coupled plasma mass spectrometry and its applications* (pp. 119-144). UK: Sheffield Academic Press.

Olander, L. P., Bustamante, M. M., Asner, G. P., Telles, E., Prado, Z., & Camargo, P. B. (2005). Surface soil changes following selective logging in an eastern Amazon forest. *Earth Interactions*, *9*(4), 1-19.

O'Leary, M. H. (1981). Carbon isotope fractionation in plants. *Phytochemistry*, *20*(4), 553-567.

Paula, F. S., Rodrigues, J. L., Zhou, J., Wu, L., Mueller, R. C., Mirza, B. S., & Pellizari, V. H. (2014). Land use change alters functional gene diversity, composition and abundance in Amazon forest soil microbial communities. *Molecular ecology*, *23*(12), 2988-2999.

Pawelczyk, S., & Pazdur, A. (2004). Carbon isotopic composition of tree rings as a tool for biomonitoring CO (sub 2) level. *Radiocarbon*, *46*(2), 701-719.

Peterson, D. L., & Anderson, D. R. (1990). Content of chemical elements in tree rings of lodgepole pine and whitebark pine from a subalpine Sierra Nevada forest. *Research Paper-Pacific Southwest Research Station, USDA Forest Service*, 198-200.

Petit, R. J., & Hampe, A. (2006). Some evolutionary consequences of being a tree. *Annual review of ecology, evolution, and systematics*, 187-214.

Pfahl, S., & Sodemann, H. (2014). What controls deuterium excess in global precipitation?. *Climate of the Past*, *10*(2), 771-781.

Pilcher, J. R., Baillie, M. G., Schmidt, B., & Becker, B. (1984). A 7,272-year tree-ring chronology for Western Europe. *Nature*, *312*(5990), 150-152.

Pilgrim, T. S., Watling, R. J., & Grice, K. (2010). Application of trace element and stable isotope signatures to determine the provenance of tea (Camelliasinensis) samples. *Food Chemistry*, *118*(4), 921-926.

Plomion, C., Leprovost, G., & Stokes, A. (2001). Wood formation in trees. *Plant physiology*, *127*(4), 1513-1523.

Pojar, J. (1991). Ecosystems of British Columbia. In *Special Report Series No. 6. British Columbia Ministry of Forests*.

Pourrut, B., Shahid, M., Dumat, C., Winterton, P., & Pinelli, E. (2011). Lead uptake, toxicity, and detoxification in plants. *Reviews of Environmental Contamination and Toxicology, Volume 213* (113-136).

Rachmayanti, Y., Leinemann, L., Gailing, O., & Finkeldey, R. (2009). DNA from processed and unprocessed wood: factors influencing the isolation success. *Forensic Science International: Genetics*, *3*(3), 185-192.

Raines, C. A. (2003). The Calvin cycle revisited. *Photosynthesis research*, *75*(1), 1-10.

Rhodes, C. N., Lofthouse, J. H., Hird, S., Rose, P., Reece, P., Christy, J., ... & Brereton, P. A. (2010). The use of stable carbon isotopes to authenticate claims that poultry have been corn-fed. *Food chemistry*, *118*(4), 927-932.

Roßmann, A., Schmidt, H. L., Reniero, F., Versini, G., Moussa, I., & Merle, M. H. (1996). Stable carbon isotope content in ethanol of EC data bank wines from Italy, France and Germany. *Zeitschrift für Lebensmittel-Untersuchung und Forschung*, *203*(3), 293-301.

Roden, J. S., & Ehleringer, J. R. (1999). Hydrogen and oxygen isotope ratios of tree-ring cellulose for riparian trees grown long-term under hydroponically controlled environments. *Oecologia*, *121*(4), 467-477.

Rowell, R. (1984). The chemistry of solid wood. *The chemistry of solid wood handbook.*

Rozanski, K., Araguás-Araguás, L., & Gonfiantini, R. (1993). Isotopic patterns in modern global precipitation. *Climate change in continental isotopic records*, 1-36.

Ryan, M. G., & Asao, S. (2014). Phloem transport in trees. *Tree physiology*, 34(1), 1-4.

Saurer, M., Aellen, K. A. S. R., & Siegwolf, R. (1997). Correlating δ13C and δ18O in cellulose of trees. *Plant, Cell & Environment*, *20*(12), 1543-1550.

Sauer, N. (2007). Molecular physiology of higher plant sucrose transporters. *FEBS letters*, *581*(12), 2309-2317.

Schimmelmann, A. (1991). Determination of the concentration and stable isotopic composition of nonexchangeable hydrogen in organic matter. *Analytical chemistry*, *63*(21), 2456-2459.

Schulte, E. E., & Kelling, K. A. (1999). Understanding plant nutrients: Soil and applied copper. *Univ. Wisconsin Ext. Publ. A*, *2527*.

Schroeder, H. A., & Balassa, J. J. (1966). Abnormal trace metals in man: zirconium. *Journal of chronic diseases*, *19*(5), 573-586.

Sedjo, R., & Sohngen, B. (2012). Carbon sequestration in forests and soils. *Annu. Rev. Resour. Econ.*, *4*(1), 127-144.

Sheu, D. D., & Chiu, C. H. (1995). Evaluation of cellulose extraction procedures for stable carbon isotope measurement in tree ring research. *International Journal of Environmental Analytical Chemistry*, *59*(1), 59-67.

Siegenthaler, U., & Oeschger, H. (1980). Correlation of 18O in precipitation with temperature and altitude.

Sieper, H. P., Kupka, H. J., Lange, L., Roßmann, A., Tanz, N., & Schmidt, H. L. (2010). Essential methodological improvements in the oxygen isotope ratio analysis of N-containing organic compounds. *Rapid Communications in Mass Spectrometry*, *24*(19), 2849-2858.

Singh, N., Ma, L. Q., Srivastava, M., & Rathinasabapathi, B. (2006). Metabolic adaptations to arsenic-induced oxidative stress in Pterisvittata L and Pterisensiformis L. *Plant Science*, *170*(2), 274-282.

Sizer, N., & Plouvier, D. (2000). Increased investment and trade by transnational logging companies in Africa, the Caribbean and the Pacific: *Implications for the sustainable management and conservation of tropical forests*. WWF.

Smith, I. C., & Carson, B. L. (1977). Trace metals in the environment.

Sjostrom, E. (1993). *Wood chemistry*. Elsevier Science.

Soylak, M., Tuzen, M., Narin, I., & Sari, H. (2004). Comparison of microwave, dry and wet digestion procedures for the determination of trace metal contents in spice samples produced in Turkey. *Journal of Food and Drug Analysis*, *12*(3), 254-258.

State of the Environment and Policy Retrospective: (1972–2002). *Biodiversity*, page 120. Available at http://www.grida.no/geo/geo3/english/pdfs/chapter2-4_biodiversity.pdf. Accessed April 2013.

Sternberg, L., Pinzon, M. C., Anderson, W. T., & Jahren, A. (2006). Variation in oxygen isotope fractionation during cellulose synthesis: intramolecular and biosynthetic effects. *Plant, Cell & Environment*, *29*(10), 1881-1889.

Stürup, S. (2004). The use of ICPMS for stable isotope tracer studies in humans: a review. *Analytical and bioanalytical chemistry*, *378*(2), 273-282.

Sulzman, E.W. (2008). Stable Isotope Chemistry and Measurement: A Primer. *Stable isotopes in ecology and environmental science*, second edition. (1), 1 –21.

Switsur, R., & Waterhouse, J. (1998). Stable isotopes in tree ring cellulose. *Stable Isotopes*, 303-321.

Tangahu, B. V., Sheikh Abdullah, S. R., Basri, H., Idris, M., Anuar, N., & Mukhlisin, M. (2011). A review on heavy metals (As, Pb, and Hg) uptake by plants through phytoremediation. *International Journal of Chemical Engineering*, *2011*.

Toman, B., & Verkouteren, R. M. (2006). Guest Editorial After two decades a second anchor for the VPDB d 13 C scale y. *Rapid Commun. Mass Spectrom*, *20*, 3165-3166.

Thomas, F., & Jamin, E. (2009). 2 H NMR and 13 C-IRMS analyses of acetic acid from vinegar, 18 O-IRMS analysis of water in vinegar: International collaborative study report. *Analytica chimica acta*, *649*(1), 98-105.

Thorburn, P. J., & Ehleringer, J. R. (1995). Root water uptake of field-growing plants indicated by measurements of natural-abundance deuterium. *Plant and Soil*, 177(2), 225-233.

Timber, G. (2006). China-illegal imports and exports. *Retrieved February*, *20*, 2008.

Treydte, K., Frank, D., Esper, J., Andreu, L., Bednarz, Z., Berninger, F., ... & Schleser, G. H. (2007). Signal strength and climate calibration of a European tree-ring isotope network. Geophysical Research Letters, 34(24).

United Nations Office on Drugs and Crime, (2013). Transnational Organized Crime in East Asia and the Pacific: A Threat Assessment. Available at http://www.unodc.org/documents/data-and analysis/Studies/TOCTA_EAP_web.pdf. Accessed on November 2013.

Vanholme, R., Demedts, B., Morreel, K., Ralph, J., & Boerjan, W. (2010). Lignin biosynthesis and structure. *Plant Physiology*, *153*(3), 895-905.

Van Solinge, T. B. (2008). *Eco-crime: the tropical timber trade* (pp. 97-111). Springer New York.

Vogel, J. C., Grootes, P. M., & Mook, W. G. (1970). Isotopic fractionation between gaseous and dissolved carbon dioxide. *Zeitschrift für Physik*, *230*(3), 225-238.

Vogel, J. C. (1978). Recycling of carbon in a forest environment. *Oecologia Plantarum*, *13*(1), 89-94.

Vogel, J. C. (1980). Fractionation of the carbon isotopes during photosynthesis, 5-29.

Warneke, T., Croudace, I. W., Warwick, P. E., & Taylor, R. N. (2002). A new ground-level fallout record of uranium and plutonium isotopes for northern temperate latitudes. *Earth and Planetary Science Letters*, *203*(3), 1047-1057.

Watmough, S. A., & Hutchinson, T. C. (2003). Uptake of 207 Pb and 111 Cd through bark of mature sugar maple, white ash and white pine: a field experiment. *Environmental Pollution*, *121*(1), 39-48.

Whitehead, D. C. (2000). *Nutrient elements in grassland: soil-plant-animal relationships*. *Cambridge university Press.*

Whitmore, T. C. (1982). On pattern and process in forests. *Special publications series of the British Ecological Society*. *Cambridge Univ. Press*, 639-655.

Wilson, A. T. & Grinstead, M. J., (1977). $^{12}C/^{13}C$ in cellulose and lignin as palaeothermometers. *Nature* 265,133-135.

Winkler, F. J. (1984). Application of natural abundance stable isotope mass spectrometry in food control. In *Analytical chemistry symposia series*.

Woodrow, I. E., & Berry, J. A. (1988). Enzymatic regulation of photosynthetic CO2, fixation in C3 plants. *Annual Review of Plant Physiology and Plant Molecular Biology*, *39*(1), 533-594.

Wooster, M. J., Perry, G. L. W., & Zoumas, A. (2012). Fire, drought and El Nino relationships on Borneo (Southeast Asia) in the pre-MODIS era (1980–2000). *Biogeosciences*, *9*(1), 317-340.

Yakir, D., & da SL Sternberg, L. (2000). The use of stable isotopes to study ecosystem gas exchange. Oecologia, 123(3), 297-311.

Yapp, C. J., & Epstein, S. (1982). A reexamination of cellulose carbon-bound hydrogen δD measurements and some factors affecting plant-water D/H relationships. *Geochimica et Cosmochimica Acta*, *46*(6), 955-965.